UNIVERSITY OF CAPE TOWN

DEPARTMENT OF CIVIL ENGINEERING

Optimizing the content and gradation of recycled tyre rubber particles to improve cracking resistance of concrete mortars

Prepared by	:	Tsoana Donald Molefe
Supervisor	:	A/Prof Hans Beushausen
Co-Supervisor	:	Prof. Mark Alexander
Date	:	20th May 2015

A dissertation submitted to the Department of Civil Engineering, University of Cape Town on the 20th May 2015 in partial fulfillment of the requirements for the Degree of Master of Science in Engineering.

CoMSIRU

The author wish to acknowledge with gratitude the financial assistance from the Concrete Materials and Structural Integrity Research Integrity (CoMSIRU) towards this research. Opinions expressed and conclusions arrived at, are those of the author and are not necessarily to be attributed to CoMSIRU.

PLAGIARISM DECLARATION

1. I know the meaning of plagiarism and declare that all the work in this document, save for that which is properly acknowledged, is my own.

2. This dissertation is submitted to the Department of Civil Engineering, University of Cape Town in partial fulfillment of the requirements for the Degree of Master of Science in Civil Engineering. It has not been submitted for any other degree or examination at any other university.

3. I have used the Harvard convention for citation and referencing. Each contribution to, and quotation in this dissertation from the work(s) of other people has been attributed, and has been cited and referenced.

4. This dissertation is my own work.

5. I have not allowed, and will not allow anyone to copy my work with the intention of passing it off as his or her own work.

Molefe Donald Tsoana
20th May 2015
Signature: _____

ABSTRACT

Concrete structures are designed to be sustained for a specific service life time. When some of these structures age, they undergo deterioration due to their exposure to harsh environmental conditions and thus their structural and aesthetic functionalities get compromised. In order to restore such functionalities, concrete structures can be rehabilitated or repaired using concrete mortars as overlays (Vaysburd *et al*., 2012). On application, the concrete mortars usually experience substantial differential shrinkage that causes the build-up of internal tensile stress. Shrinkage cracking often happens if the concrete mortar does not exhibit sufficient tensile strength to sustain these stresses. The ingress of aggressive agents that may cause further deterioration on structure becomes easier (Shazali *et al*., 2012). The cracking resistance of concrete mortars has thus become a major concern in repair and rehabilitation of concrete structures.

The literature suggests that the performance of concrete mortars could be improved by enhancing the material properties that influence their cracking resistance. A large amount of research exists pertaining to the use of rubber particles in concrete mixes to improve their cracking resistance. However, no research was found regarding the influence of optimizing recycled tyre rubber particle grading and content in concrete mortar mixes in particular. This research investigated the influence of optimizing recycled tyre rubber particle grading and content in various concrete mortar mixes to improve their cracking resistance.

The initial experimental phase involved testing concrete mortars with water to binder (w/b) ratios of 0.45 and 0.60, incorporating rubber particle contents of 0%, 5%, 10% and 20% from 3 different particle gradations (0.42-0.84) mm, (1.00-2.50) mm and (0.42-2.50) mm. The concrete mortar mixes with the best cracking resistance (optimum mixes) were determined and adopted for testing in the main experimental phase. The optimum mortars were then subjected to various tests including; ring test, free shrinkage, elastic modulus, tensile strength, tensile relaxation, compressive strength and durability, in the main experimental phase.

An existing material properties' analytical model (used by Masuku (2009)) based on the measurable material properties was used to predict the cracking age of the rubberized concrete mortar mixes. The predicted cracking age results were compared to the experimental cracking age results from the ring tests to assess the prediction efficiency of this model on rubberized concrete mortars. It was observed from the results that model also predicted longer age of

cracking for rubberized mortars as observed experimentally. It was however found that the model underestimates the age of cracking for rubberized mortars, while a very small difference in predicted and observed age of cracking was observed.

The results of this research indicated that the optimization of rubber particle content and grading had a positive influence on prolonging age of cracking (ring test), reducing elastic modulus and increasing tensile relaxation more especially in mixes with a higher w/b ratio. However, the results also indicated that an increase in rubber particle content resulted in reduction of strength development and increased free shrinkage. The observations on age of cracking from both the ring test results and the modelling results, show that incorporation of rubber particles has a potential to improve cracking resistance of concrete mortars, despite the reduced tensile strength and increased shrinkage in rubberized concrete mortars. On the other hand, it was found that incorporation of rubber particles reduced the oxygen permeability index (OPI) and increased the sorptivity index of concrete mortars. These OPI and sorptivity results imply that the resistance of ingress of aggressive agents into concrete mortars is reduced when rubber particles are incorporated, hence reduced durability performance.

ACKNOWLEDGEMENTS

I would like to thank God for giving me strength in undertaking this research until this far.

My sincere gratitude to my supervisor A/Prof. Hans Beushausen for guiding me through the research; I am grateful for his continuous and timely review of my research work. I would also like to thank Prof. Mark Alexander and Prof. Pilate Moyo for their insightful review and constructive criticism in certain aspects of the research. Dr. Björn Höhlig, Dr Thabiso Mokotjomela and Mr Molefi Matsutsu who provided me with useful review and guidance in the data analysis of this research as well as compiling this dissertation are also acknowledged.

I wish to acknowledge with gratitude the financial support over the period of this work (2013-2014) received from: The University of Cape Town, the erstwhile Cement and Concrete Institute (C&CI), The National Research Foundation (NRF), Sika (SA) Pty Ltd, PPC Ltd, Afrisam, The Tertiary Education Support Programme (TESP) of ESKOM, Water Research Commission (WRC), and Concrete Society of Southern Africa (CSSA).

A special note of thanks is also given to a number of individuals for providing support to different aspects of this research:

- Justin van Heerden from SA Tyre Recyclers for producing and providing all the requested rubber particle samples used in this research study, free of charge
- Mr. Noor Hassen and the rest of technical laboratory assistants for providing invaluable guidance, time, and assistance throughout the experimental investigation.
- My family, Bokoro, Malepekola, Semonkana and Lent'sa Tsoana, for all their love, support and encouragement throughout my studies
- Miss Babalwa Ndlebe for her support and encouragement throughout my University career.
- My CoMSIRU colleagues and friends for their advices and assistance in peer reviewing my research work.
- Elly Yelverton for her warm and tremendous help throughout my engagement with CoMSIRU.

TABLE OF CONTENTS

PLAGIARISM DECLARATION I

ABSTRACT II

ACKNOWLEDGEMENTS IV

TABLE OF CONTENTS V

LIST OF FIGURES VIII

LIST OF TABLES X

1. INTRODUCTION 1

1.1. BACKGROUND AND PROBLEM STATEMENT 1

1.2. MOTIVATION FOR RESEARCH 3

1.3. RESEARCH KEY QUESTIONS AND OBJECTIVES 4

1.4. HYPOTHESIS 4

1.5. RESEARCH SCOPE 5

1.6. RESEARCH OUTLINE 5

2. LITERATURE REVIEW 9

2.1. INTRODUCTION 9

2.2. GENERAL OVERVIEW ON APPLICATIONS OF BONDED CONCRETE OVERLAYS 9

2.3. FACTOR INFLUENCING PERFORMANCE OF BONDED CONCRETE OVERLAYS 10

2.3.1. Restrained shrinkage strains and stresses 11

2.3.2. Creep and relaxation 15

2.3.3. Debonding 17

2.3.4. Free Shrinkage strains 18

2.4. PARAMETERS AFFECTING RESTRAINED SHRINKAGE CRACKING 22

2.4.1. Content and type of mix constituents 22

2.4.2. Water to binder ratio 23

2.4.3. Curing method 24

2.4.4. Size of a concrete member 25

2.4.5. Environmental conditions 25

2.5. REVIEW OF RECYCLED TYRE RUBBER PARTICLE USAGE IN MORTARS 26

2.5.1. General review 26

2.5.2. Production of tyre rubber particles 27
2.5.3. The use of tyre rubber particles in concrete mortars 30
2.5.4. The influence of tyre rubber particles in concrete mortars properties 31
2.6. DURABILITY INDEXES OF RUBBERIZED CEMENT BASED MATERIALS 38
2.7. CHAPTER SUMMARY 38
3. EXPERIMENTAL METHODOLOGY 40
3.1. EXPERIMENTAL APPROACH 40
3.1.1. Trial mixing phase 40
3.1.2. Initial experimental phase 41
3.1.3. Main experimental phase 50
3.2. INITIAL EXPERIMENTAL TESTING 52
3.2.1. Testing for restrained shrinkage 53
3.2.2. Testing for splitting tensile strength 55
3.2.3. Testing for compressive strength 56
3.3. MAIN EXPERIMENTAL TESTING 56
3.3.1. Testing for restrained shrinkage 57
3.3.2. Testing for free shrinkage 57
3.3.3. Testing for tensile strength 58
3.3.4. Testing for tensile relaxation 60
3.3.5. Testing for compressive strength 60
3.3.6. Testing for elastic modulus 60
3.3.7. Testing for durability indexes 62
3.4. ANALYTICAL MODELING OF RESULTS 66
3.5. CHAPTER SUMMARY 66
4. EXPERIMENTAL RESULTS AND DISCUSSIONS 68
4.1. INTRODUCTION 68
4.2. INITIAL EXPERIMENTAL TEST RESULTS 68
4.2.1. Ring test 68
4.2.2. Strength development 75
4.3. MAIN EXPERIMENTAL TEST RESULTS 79
4.3.1. Compressive strength 79
4.3.2. Tensile strength 81
4.3.3. Ring test 83

4.3.4. Free shrinkage 84
4.3.5. Tensile relaxation 86
4.3.6. Elastic modulus 89
4.4. ANALYTICAL MODELING OF RESULTS 91
4.4.1. Overview 91
4.4.2. Main assumptions about material properties inputs 96
4.4.3. Modeling the age of cracking for mortar mixes 97
4.4.4. Summary of predicted age of cracking compared to experimental age of cracking 100
4.5. DURABILITY INDEX RESULTS 101
4.5.1. Oxygen Permeability Index (OPI) 102
4.5.2. Water Sorptivity Index (WSI) 103
4.5.3. Porosity 103
4.6. CHAPTER SUMMARY 104
5. CONCLUSIONS AND RECOMMENDATIONS 106
5.1. INTRODUCTION 106
5.2. GENERAL CONCLUSIONS 107
5.2.1. Initial experimental phase conclusions 107
5.2.2. Main experimental phase conclusions 108
5.2.3. Analytical modeling conclusions 108
5.3. GENERAL RECOMMENDATIONS 108
REFERENCES 110
APPENDICES 118
APPENDIX A: AVERAGE TEMPERATURES AND RELATIVE HUMIDITY FOR OPEN LABORATORY SECTION 118
APPENDIX B: TABLES OF LABORATORY TEST RESULTS FROM INITIAL TESTING PHASE 119
APPENDIX C: TABLES OF LABORATORY TEST RESULTS FROM MAIN TESTING PHASE 121
APPENDIX D: MATERIAL PROPERTIES REGRESSION GRAPHS 124

LIST OF FIGURES

Figure 1-1: Demonstration of patch repair method (Meadows, 2014). 1
Figure 1-2: Plan of research experiment. 8
Figure 2-1: Concrete overlay used to repair a bridge deck (http://www.wildcatcompanies.com/concrete.html) 10
Figure 2-2: Idealized schematic of restrained shrinkage strains and stresses in a thin overlay composite section (Beushausen (2005)). 11
Figure 2-3: Schematics of strain and stress distribution in bonded concrete overlays (Beushausen (2005)). 13
Figure 2-4: Time dependent increase in strain under constant stress (Alexander & Beushausen. 2009). 16
Figure 2-5: Time depended decrease in stress under constant imposed strain (Alexander & Beushausen. 2009). 16
Figure 2-6: Debonding and edge lifting of concrete overlays. 17
Figure 2-7: Mechanism of capillary tension in cement paste (Mindess *et al*., 2003). 20
Figure 2-8: Mechanism of surface tension in cement paste (Mindess *et al*., 2003). 21
Figure 2-9: Mechanism of swelling pressure in cement paste (Mindess *et al*., 2003).....21
Figure 2-10: Effect of w/b ratio on restrained drying shrinkage (Mehta & Monteiro, 2006a). 24
Figure 2-11: Influence of relative humidity on shrinkage of concrete (Alexander & Beushausen. 2009). 26
Figure 2-12: A typical process diagram for the mechanical processing of waste tyres (Gadkar, 2013). 28
Figure 2-13: A typical process diagram for the cryogenic processing of waste tyres (Gadkar, 2013). 29
Figure 2-14: Comparison of the compositions of passenger car tyres and truck tyres (Ali *et al*., 1993). 29
Figure 2-15: The model of the compressive failure mode of rubberized mortar specimens (Eldin & Senouci, 1993). 32
Figure 2-16: Influence of rubber particle content on tensile and compressive strength (Ho & Turatsinze, 2009).....33
Figure 2-17: Effects of rubber particle content on the modulus of elasticity (Ho & Turatsinze, 2009). 34
Figure 3-1: Apparatus for mechanical sieve analysis.....43

Figure 3-2: Illustration of slump test of fresh concrete mortar. 45
Figure 3-3 : Grading curves of 3 rubber particle gradations and Klipheuwel sand. 47
Figure 3-4: Illustration of wet curing using hessian blanket and clip wrap sheets. 48
Figure 3-5: A data logger used to record temperature and RH readings in the laboratory 50
Figure 3-6: Dimensions and preparation of ring specimen mould. 53
Figure 3-7: A ring specimen showing crack width measuring points and a hand microscope. ...54
Figure 3-8: Illustration of the crack length measurement using a woolen thread....55
Figure 3-9: A cube specimen under splitting tensile strength test. 56
Figure 3-10: Dimensions of a prismatic specimen and an illustration of shrinkage strain measurement. 58
Figure 3-11: Dimensions of a notched dog bone shaped specimen and a ZwickRoell Z020 machine used testing tensile strength. 59
Figure 3-12: Failure modes on notched dog bone shaped specimens under tensile strength testing. 59
Figure 3-13: Dimensions for cylindrical specimen and a ZwickRoell Z100 machine used to test elastic modulus. 61
Figure 3-14: (i). Illustration for elastic modulus test set up and a cylindrical specimen showing spikey rubber particles on its ground test surface. 62
Figure 3-15: (i). A schematic diagram of OPI apparatus (Alexander and Mackechnie, 2001) and pressure cells used for the testing. 65
Figure 3-16: (i). A schematic diagram of sorptivity apparatus (Alexander and Mackechnie, 2001). (ii). Sorptivity test apparatus 66
Figure 4-1: Crack ages for rubberized concrete mortars of 0.45 w/b ratio. 69
Figure 4-2: Crack ages for rubberized concrete mortars of 0.60 w/b ratio. 70
Figure 4-3: Total crack areas for rubberized concrete mortars of 0.45 w/b ratio. 70
Figure 4-4: Total crack areas for rubberized concrete mortars of 0.60 w/b ratio. 71
Figure 4-5 (a-c): Cracking area growth for the 0.45 w/b rubberized mortar mixes. 72
Figure 4-6 (a-c): Cracking area growth for the 0.60 w/b rubberized mortar mixes. 73
Figure 4-7: Compressive strength of 0.45 w/b rubberized mortar mixes. 76
Figure 4-8: Compressive strength of 0.60 w/b rubberized mortar mixes. 76
Figure 4-9: Splitting tensile strength of 0.45 w/b rubberized mixes. 78
Figure 4-10: Splitting tensile strength of 0.60 w/b rubberized mixes. 78
Figure 4-11: Compressive strength development of main rubberized mixes. 80
Figure 4-12: Failure modes for cube specimens tested under compressive test. 81

Figure 4-13: Tensile strength development of main rubberized mixes 81
Figure 4-14 (a-c): Free shrinkage results of main experimental phase mixes 86
Figure 4-15: Typical relaxation curves for 0.80R:20G3 across all test ages. 87
Figure 4-16: Tensile relaxation results for main experimental phase test specimens 88
Figure 4-17: Elastic modulus results for main experimental phase test specimens. 90
Figure 4-18: Schematic of cracking delay of mortars due to the effect of relaxation (Masuku, 2009). 91
Figure 4-19: Regression curves of; (a) Tensile strength, (b) Elastic modulus and (c) Tensile relaxation for 0.80:R20G3 mix 94
Figure 4-20: Time varying strain history due to shrinkage. 94
Figure 4-21: Tensile strength and tensile stress development for 0.80:R0 mix. 98
Figure 4-22: Tensile strength and tensile stress development for 0.80:R20G3 mix. 98
Figure 4-23: Tensile strength and tensile stress development for 0.60:R0 mix. 99
Figure 4-24: Tensile strength and tensile stress development for 0.60:R20G3 mix. 99
Figure 4-25: Tensile strength and tensile stress development for CRM:R0 mix. 100
Figure 4-26: Tensile strength and tensile stress development for CRM:R20G3 mix. 100
Figure 4-27: OPI results of the main mortar mixes. 102
Figure 4-28: Sorptivity results of the main mortar mixes. 103
Figure 4-29: Porosity results of the main mortar mixes. 104

LIST OF TABLES

Table 3-1: Mix proportions of initial control concrete mortars 41
Table 3-2: Typical physical properties of CEM III/ 42.5N from PPC (PPC, 2014). 46
Table 3-3: Mix proportions of main experimental phase control mortar mixes. 51
Table 3-4: Mix proportions of control CRM mix. 52
Table 3-5: Suggested range for durability classification using DI values (Alexander and Mackechnie, 2001) 63
Table 4-1: Ring test results for main experimental phase mixes. 83
Table 4-2: Tensile relaxation results for main experimental phase test specimens. 88
Table 4-3: Comparison of experimental age of cracking and modeling age of cracking 101

CHAPTER ONE

INTRODUCTION

1.1. Background and problem statement

In design of most of the reinforced concrete structures, the focus is put on using concrete with high compressive strength to safely sustain the expected loading. In spite of its high strength, under harsh environment conditions, reinforced concrete elements experience defects that compromise their functionality. This is commonly due to corrosion of reinforcement inside concrete elements (Ho & Turatsinze, 2009). To extend the service life of these deteriorated structural elements, rehabilitation and repair using concrete mortars are usually preferred. In most instances, the patch repair or overlay method are opted for.

The patch repair method is required where steel reinforcement has corroded. This method involves chipping away old damaged concrete to expose and clean reinforcing bars and casting a new layer of concrete mortar over the existing sound concrete (substrate) to protect exposed reinforcing bars. However, the economic implications of poorly conducted concrete mortar can be as high as those incurred in rehabilitating the whole structural element in some instances (Meadows, 2014). Figure 1-1 below demonstrates the application of the patch repair method.

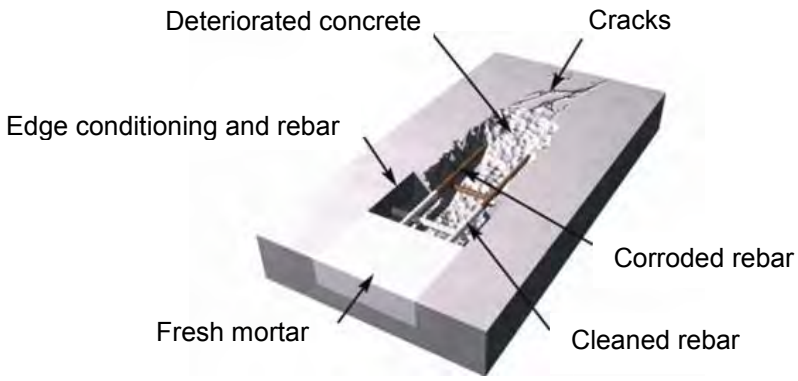

Figure 1-1: Demonstration of patch repair method (Meadows, 2014).

The overlays casting rehabilitation may be applied on deteriorated concrete substrate in order to increase the structure's service-life, for substrate surface protection and to improve its aesthetic appearance. The substrate surface is prepared to enhance the adhesion and bond strength development with the concrete overlay. The most common failure mechanisms that are usually experienced by concrete overlays in place are debonding and cracking.

Debonding develops between the new overlay and old substrate concrete due to differential shrinkage that happens within overlays. The overlay to substrate bond provides restraint to these differential shrinkage strains thus causing tensile stress built-up within the new overlay. If these stresses exceed the bond strength debonding happens. The cracking of overlays occurs if there is sufficient bond strength to withstand the tensile stresses but the tensile strength of the overlay is lower than the developed stresses (Turatsinze *et al*., 2007).

All cement based concrete mortars usually have low strain capacity and tensile strength that make them highly sensitive to cracking. One problem with cracking pathology is that; the points of crack initiation, crack propagation and capacity of cracking within the concrete mortar are unpredictable (Turatsinze *et al*., 2007). The cracking of concrete mortars is considered as a repair failure because it compromises aesthetics of a structure as well as the protection against steel corrosion that may be caused by the ingress of aggressive environmental agents (Carlswärd, 2006).

Literature from studies by Beushausen (2005), Masuku (2009) and Chilwesa (2012) suggests that the most efficient solution to reduce these detrimental cracking defects is by designing the concrete mortar with increased tensile strength, increased tensile relaxation, reduced shrinkage and/or reduced elastic modulus to lengthen the time of cracks development. From experimental tests conducted by various researchers (Ho & Turatsinze (2009); Turatsinze *et al*. (2003); Turatsinze *et al*. (2005); Turatsinze *et al*. (2007)), results indicated that though mechanical properties such as compressive and tensile strengths of concrete mortars reduce when rubber particles are incorporated, their strain capacity significantly increases. Such strain capacity improvements include reduction of elastic modulus and an increase of margin of tensile relaxation. From the study conducted by Ho *et al* (2009) it was also suggested that the incorporation of rubber particles in concrete mortars improves their strain capacity before the occurrence of micro-crack localization. In the other research conducted by Ho *et al* (2012), it was stated that, where crack resistance due to shrinkage deformation is a priority, the rubber particles could be used to improve cracking resistance of concrete mortars. It was also stated that the success of incorporating of rubber particles in

concrete mortars is likely to help in waste tyre management. In this research ground recycled tyre rubber particles were variously graded and used to partially replace fine natural aggregates with different contents to investigate their influence on cracking resistance of concrete mortars.

1.2. Motivation for research

The balanced trade-off of strain capacity gain against strength loss in the rubberized concrete mortars has not been successfully achieved since the technology of incorporating rubber particles in cement based materials was established. In the research conducted by Ganjian *et al*. (2009), it was observed that compressive strength and tensile strength were reduced by about 10% at the test age of 28 days with the incorporation of only 5% ground rubber replacement in concrete mix. However, there were no noticeable changes observed in elastic modulus reduction and shrinkage strains. The compressive and tensile strength were detrimentally decreased by approximately 40% and the elastic modulus was reduced by about 17% when the ground rubber particles incorporation was increased to 10%. In this research, the optimum grading and content of ground rubber particles that can be incorporated in concrete mortar to offer optimum cracking resistance was investigated. The optimization of gradation and content was aimed at narrowing down the divergence of the strain capacity gain and strength loss.

There are contrasting views regarding the minimum rubber particle content that could affect the cracking resistance of rubberized concrete mortars. As assessed from drying shrinkage results Turatsinze *et al*. (2003) stated that 5% incorporation of rubber particles causes measurable shrinkage strains. On the other, Toumi *et al*. (2013) stated that the shrinkage strains observed when less than 5% rubber particles is incorporated, are merely due to curing regime conditions and have less to do with incorporated rubber particle content and size. In this research, not only the minimum and maximum contents of rubber particle incorporation were investigated but the optimum content as well as gradation were determined.

Limited research studies were found on the influence of rubber particles on other important concrete overlay properties such as bond strength, direct tensile strength and tensile relaxation. It is also not conclusive whether incorporation of rubber particles could improve or reduce durability of concrete mortars. Therefore the direct tensile strength, tensile relaxation and durability tests were undertaken. The durability of rubberized concrete mortars was tested in the South African durability context using the Durability Index test method. The research also serves as an important contribution towards

efforts aimed at assessing the efficiency of analytical model to predict cracking age of concrete mortars.

1.3. Research key questions and objectives

The main objective of this research is to determine an optimum concrete mortar mix design that could be utilized in improving service life of deteriorated reinforced concrete structures using recycled tyre rubber particles. This is aimed to be achieved through an establishment of optimum rubber particle content and grading of rubber particles to improve material properties that affect cracking resistance of concrete mortars. In order to assess the influence of optimum rubber particle content and grading, ring test, tensile strength, free shrinkage, tensile relaxation and elastic modulus were tested and analyzed.

From these experimental tests, observations and analysis were done in order to address the following research key questions;

- How can recycled tyre rubber particle grading be optimized in concrete mortars to improve the material properties that affect their cracking resistance?
- How can recycled tyre rubber particle content be optimized in concrete mortars to improve the material properties that affect their cracking resistance?
- How does rubber particle incorporation affect the durability of concrete mortars?
- How effective does the material properties analytical model predict the time of first crack on rubberized concrete mortars?

1.4. Hypothesis

The most sublime solution to improve cracking resistance of cement based mortars is through the design of a mixture that exhibits a high strain capacity before macro-crack localization and the tensile strength that is higher than the possible induced stresses. This research proposes that the partial replacement of fine natural aggregates by optimum recycled tyre rubber particles in the concrete mortars can potentially reduce the elastic modulus and increase in tensile relaxation. It is hypothesized that the optimization process of content and grading of rubber particles could provide the better trade-off between the possible improvements and draw-backs on properties that affect

cracking resistance of concrete mortars. These improvements in properties of concrete mortars will reduce the likelihood of concrete mortar cracking and will thus improve overlay performance.

1.5. Research scope

The initial phase of the research focused on 2 laboratory made mortar mixes of water to binder ratios (w/b) of 0.45 and 0.60. These w/b ratios were chosen because they are representative of the range of common w/b ratios. Three various gradations of rubber particles were prepared and used to partially replace fine natural aggregates with contents of 5%, 10% and 20%. An optimum rubber particle content and gradation were determined and used in the main experimental phase. The main experimental phase involved incorporation of an optimum content of the optimum gradation in 2 different laboratory made mortar mixes and 1 commercially available repair mortar. The testing was only concerned with durability properties and properties that affect cracking resistance of concrete mortars.

1.6. Research outline

Literature review on cracking resistance of concrete mortars and the use of rubber particles in concrete mortars were done. Experiments were then carried out systematically as laid in the experimental research plan shown in Figure 1-2 below. The “R” and “G” used for the mix identities represent percentage rubber content and gradation used, for example, the 0.60 w/b ratio mix incorporating 20% of gradation 3 rubber particles is denoted as 0.60:R20G3.

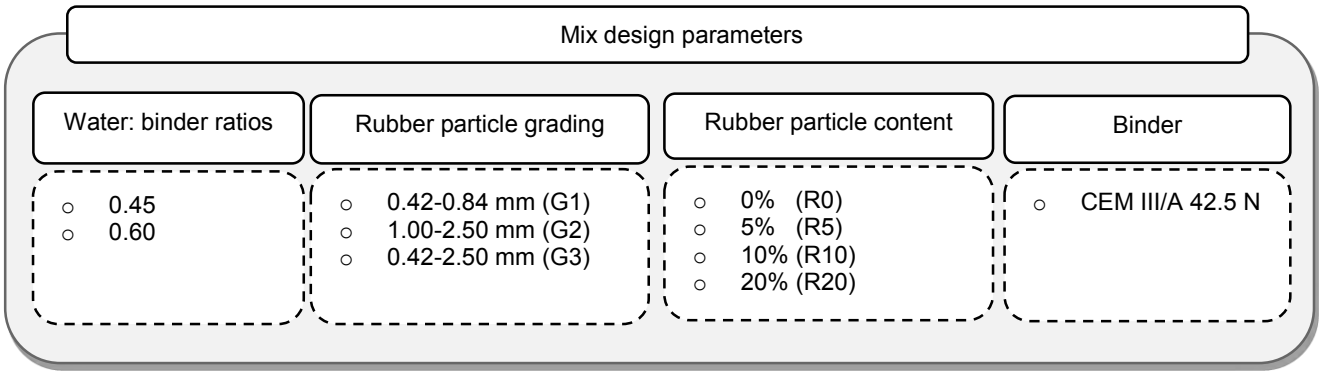

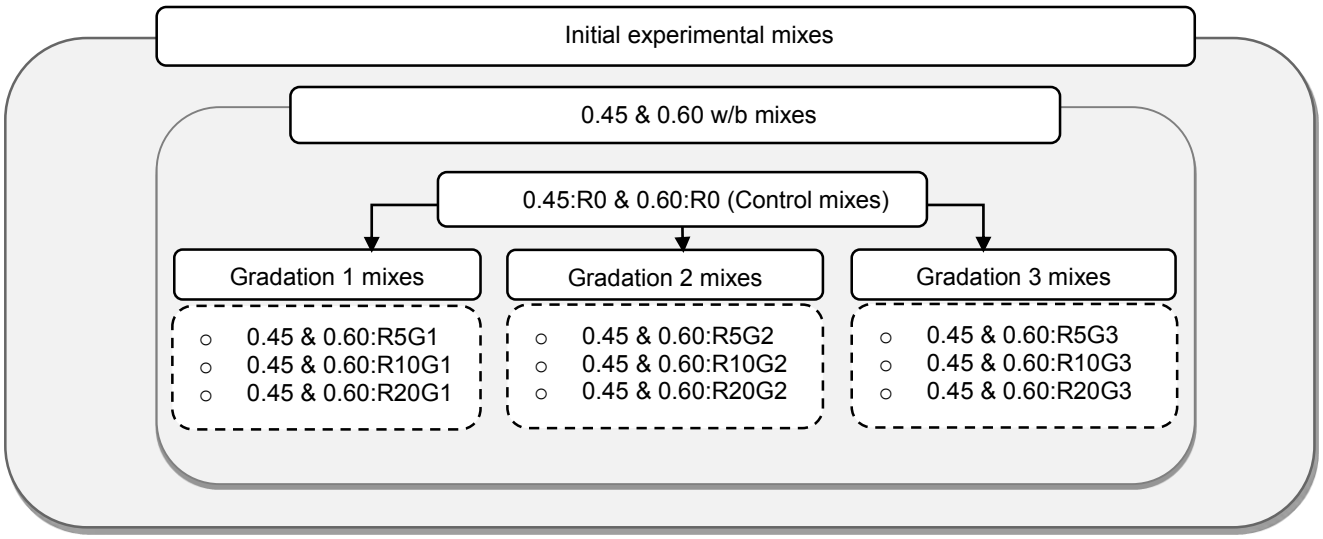
Initial experimental mixes
0.45 & 0.60 w/b mixes
0.45:R0 & 0.60:R0 (Control mixes)
Gradation 1 mixes
0.45 & 0.60:R5G1
0.45 & 0.60:R10G1
0.45 & 0.60:R20G1
Gradation 2 mixes
0.45 & 0.60:R5G2
0.45 & 0.60:R10G2
0.45 & 0.60:R20G2
Gradation 3 mixes
0.45 & 0.60:R5G3
0.45 & 0.60:R10G3
0.45 & 0.60:R20G3

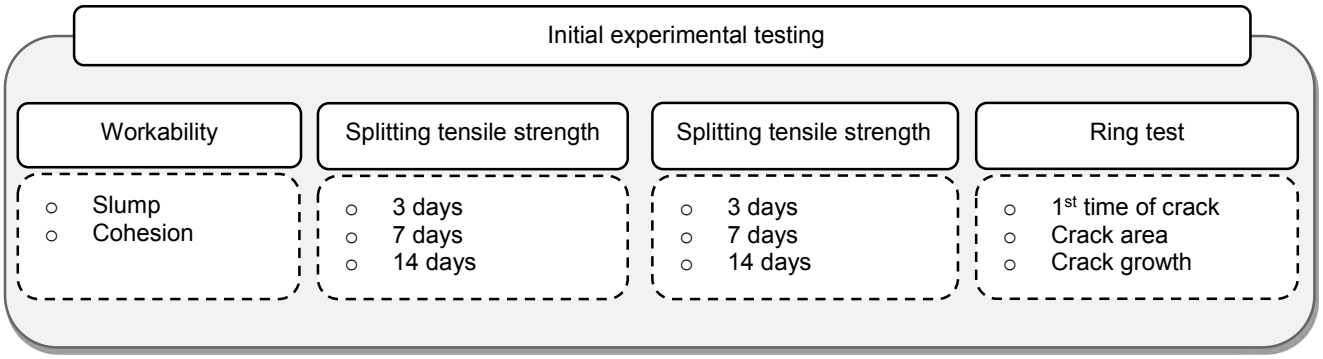
Initial experimental testing
Workability
Slump
Cohesion
Splitting tensile strength
3 days
7 days
14 days
Splitting tensile strength
3 days
7 days
14 days
Ring test
1st time of crack
Crack area
Crack growth

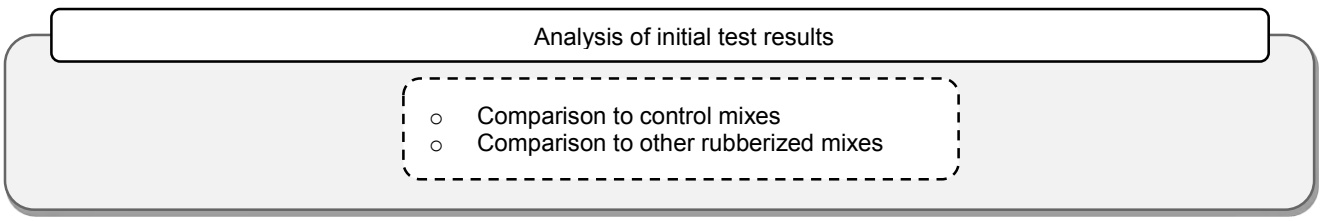
Analysis of initial test results
Comparison to control mixes
Comparison to other rubberized mixes

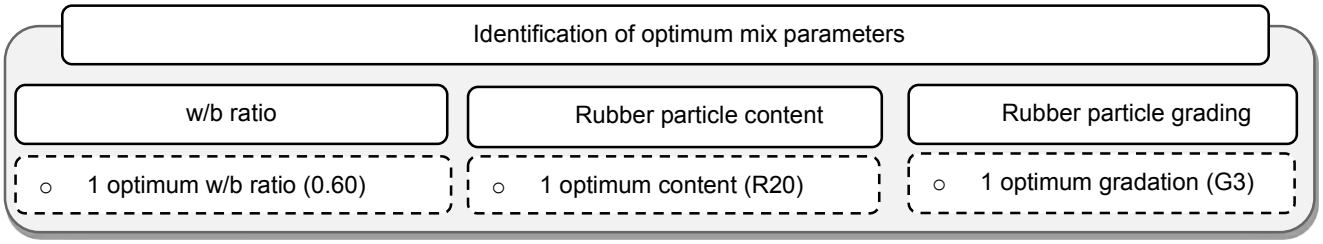
Identification of optimum mix parameters
w/b ratio
1 optimum w/b ratio (0.60)
Rubber particle content
1 optimum content (R20)
Rubber particle grading
1 optimum gradation (G3)

Main optimum concrete mortar mix

- 0.60:R20G3

Rationale for choice of the other main test mixes

- The optimum concrete mortar mix was adopted and used in the main experimental phase. One more laboratory made concrete mortar of w/b ratio of 0.80 and one commercially available repair mortar were prepared for further experimentation.
- These 2 mixes were chosen because they were identified to have the longer cracking age amongst all the mixes that were cured using the same curing method (wet hessian cloth) from the other research conducted in CoMSIRU by Bester, 2014. This experimental process was conducted on effort to investigate whether the incorporation of optimum rubber particles could further improve the cracking resistance of the other best performing (optimum) overlays.

Main experimental mixes

0.60 w/b mixes	0.80 w/b mixes	Commercial repair mortar (CRM)mixes
0.60:R0 (Control mix) 0.60:R20G3	0.80:R0 (Control mix) 0.80:R20G3	CRM:R0 (Control mix) CRM:R20G3

Main experimental

Material properties affecting cracking

Tensile strength	Free shrinkage	Elastic modulus	Tensile relaxation
3 days 7 days 14 days' 28 days	Daily, for the period of 56 days weeks.	7 days 14 days 28 days	3 days 7 days 14 days

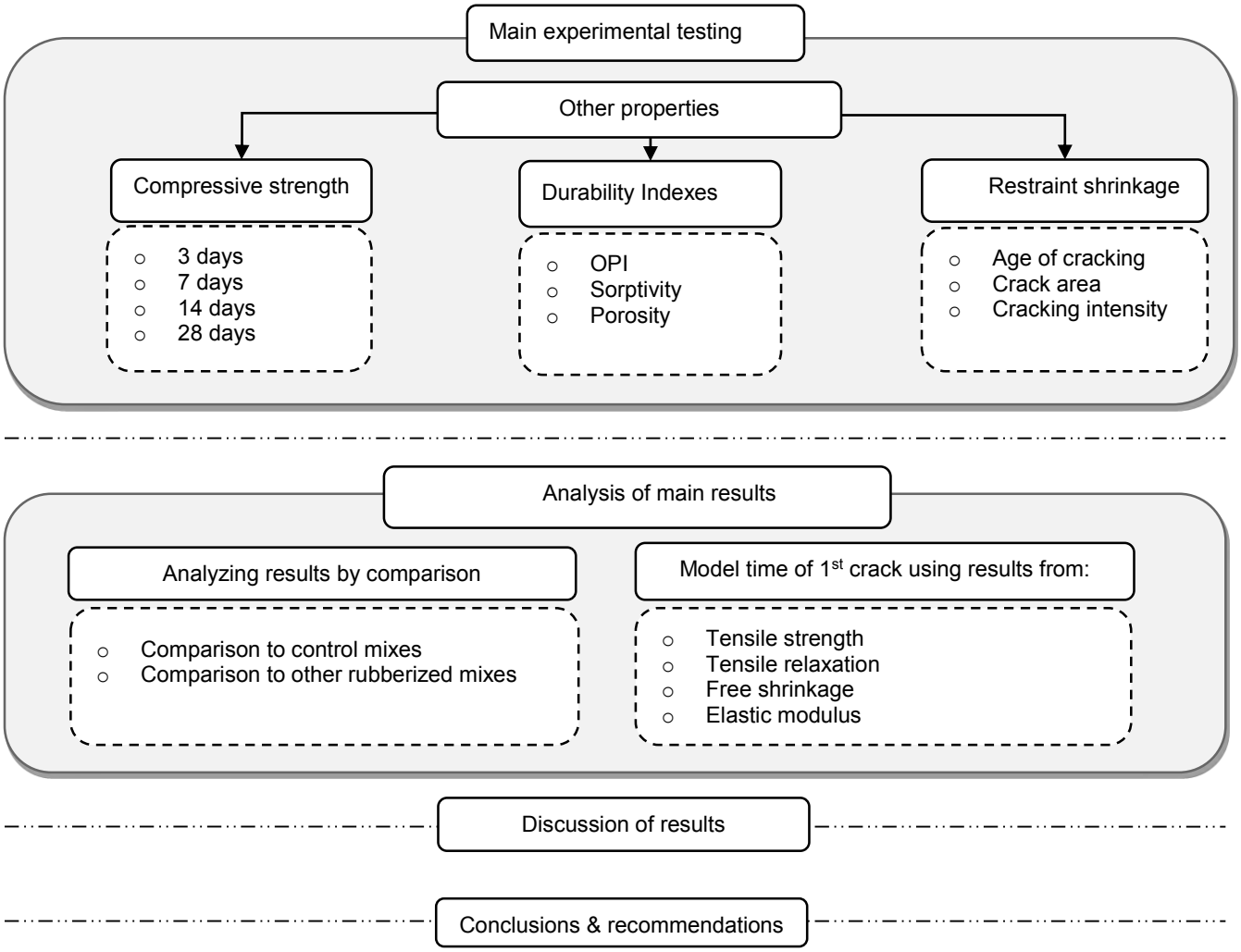

Figure 1-2: Plan of research experiment.

CHAPTER TWO

LITERATURE REVIEW

2.1. Introduction

This chapter comprises a detailed literature review on bonded concrete overlays/ mortars and the different factors that influence their performance. The main problems that are usually experienced in bonded concrete overlays, are cracking and debonding, and will be discussed in details in sections to follow. Discussion of the material properties that influence cracking performance of bonded concrete overlays is also presented. The literature review on the usage of recycled tyre rubber particles in concrete overlays is also presented. This chapter also provides detailed discussion of the production of recycled tyre rubber particles, which are used for the production of rubberized cement based materials. The influence of the material properties of the recycled tyre rubber particles on cracking of bonded concrete overlays is discussed also.

2.2. General overview on applications of bonded concrete overlays

A bonded concrete overlay is a layer of concrete or mortar, with a thickness less than 25 mm. It is placed on top of a deteriorated pre-existing concrete (substrate) surface to restore or improve the function of the structure (ACI, 1999). Bonded concrete overlays/ mortars can be used in different structural and/or non-structural applications (ACI, 1999). They are commonly used for restoration of structural integrity such as; to repair and strengthen concrete elements, to improve abrasion resistance of concrete surfaces and to improve durability of concrete elements. In some instances overlays are used to restore the performance level or to improve the appearance of the structure. Figure 2-1 shows concrete overlay being applied to repair a deteriorated concrete bridge deck.

The quality of overlays reduces with age after placement. The performance of concrete overlays is mainly affected by the environmental conditions and the method of placement used. The most common deterioration/failure modes that are experienced by overlays at an early age are shrinkage cracking and substrate-overlay interface debonding. In many instances both shrinkage cracking and

debonding are as a result of restrained shrinkage strains and restrained shrinkage stresses. This two factors are discussed in detail in Section 2.3.

Figure 2-1: Concrete overlay used to repair a bridge deck (http://www.wildcatcompanies.com/concrete.html)

2.3. Factor influencing performance of bonded concrete overlays

There are several factors that affect performance of concrete overlays, these include: interface properties of the substrate, properties of the concrete overlay, condition of the substrate, environmental conditions and reinforcing rebar preparation in the case of patch repair, (Beushausen & Alexander, 2009). All these factors need to be taken into consideration during the overlay placement in order to attain its good quality performance. The scope of this research is limited to the overlay cracking performance and material properties that can affect their performance. Therefore the focus will only be on material properties that are concerned with shrinkage cracking.

Almost all the modes of failure of the concrete overlays are due to the differential volume change of overlay cement paste that occurs in the early age after placement. Differential volume change is often quantified by drying shrinkage strains. The differential shrinkage result in the intrinsic tensile stresses within the overlay matrix or at the substrate-overlay interface (Beushausen & Alexander, 2006). If the intrinsic tensile stresses exceed the tensile strength of the overlay, shrinkage cracking initiates.

Likewise, if the intrinsic tensile stresses on the substrate-overlay interface exceed the interfacial bond strength between the substrate and the overlay, debonding occurs.

2.3.1. Restrained shrinkage strains and stresses

Concrete overlays shrink after placement and the shrinkage strains that they undergo daily are measurable. To bond concrete overlays onto old substrate, they are cast on top of them. Relative to the amount shrinkage experienced by the newly placed concrete overlays, the old substrate hardly shrinks. This differential shrinkage between the concrete overlays and the substrate is often results to shrinkage cracking and/or debonding. If the bond between the concrete overlay and the substrate is strong it provides a constraint for concrete overlay to shrink freely. Due to this restraint condition against shrinkage, shrinkage stresses are then generated. Beushausen (2005) studied the performance of bonded concrete overlays subjected to differential shrinkage, and Figure 2-2 shows the schematics of restrained shrinkage strains and stresses in a thin overlay composite section. Beushausen (2005).

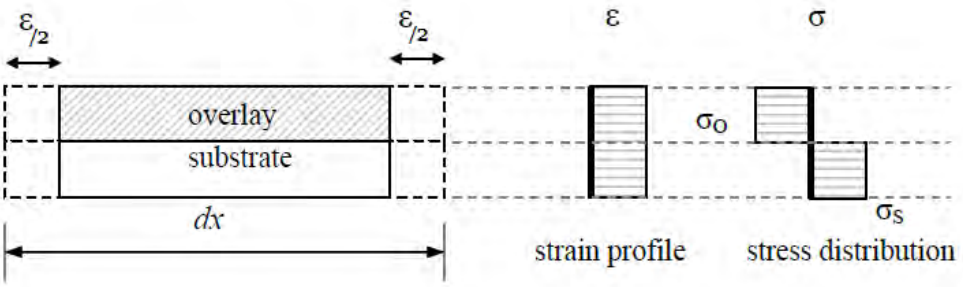

Where; ε = strain

σ = stress

σ_O = overlay stress

σ_S = substrate stress

Figure 2-2: Idealized schematic of restrained shrinkage strains and stresses in a thin overlay composite section (Beushausen (2005)).

It is shown in Figure 2-2 that, initially before shrinkage takes place, the length of the composite is dx. Due to shrinkage strains (ε) the composite total length reduces. In this schematic it is assumed that the bond between the substrate and the overlay is perfect, and there are no irregularities at the interface causing poor bonding. Therefore, both the substrate and the overlay are assumed to

undergo the same linear contraction. This assumption ignores the effects of curvature, bending moments, interface slip and strain gradients across both the overlay and the substrate because it is applied on small and thin sections. Since the substrate is old and hardly shrinks, the imposed strains lead to induced stresses (Beushausen, 2005). In sections with relatively low substrate stiffness, such as the `structural overlay on concrete slab, the bending moments due to differential shrinkage might cause considerable curvature. This results in compressive strain on the overlay.

The induced tensile strain in the overlay leads to tensile stress relief in the overlay. However, it is not simple to predict these stresses in bonded concrete overlays. This is because there are many factors influencing shrinkage induced stresses. Such factors include the rate at which the overlay shrinks, the restraint provided by the substrate, the degree to which the substrate creeps, direct stresses and bending stresses that are functions of overlay restraint and substrate stiffness. It is therefore simpler to consider the effects of direct stresses separately before considering effects of other stress mechanisms. The equations proposed by Beushausen (2005) for instantaneous elastic strain of the overlay and substrate strain at the interface are presented in Equation 2-1 and Equation 2-2 respectively. These formulations are valid only for a fully bonded overlay with consistent restraint along the interface.

$$\varepsilon_{rests.O,I} = \left(\varepsilon_{FSS} - \frac{\varepsilon_{FSS}}{1 + \frac{E_s}{E_0}.C_\varepsilon} \right) \quad [2\text{-}1]$$

$$\varepsilon_{S,I} = \left(\frac{\varepsilon_{FSS}}{1 + \frac{E_s}{E_0}.C_\varepsilon} \right) \quad [2\text{-}2]$$

Where; $\varepsilon_{rests.O,I}$ = restrained overlay strain at the interface

ε_I = strain at the interface

$\varepsilon_{S,I}$ = substrate strain at the interface

$\varepsilon_{O,I}$ = overlay strain at the interface, ($\varepsilon_{O,I} = \varepsilon_{S,I} = \varepsilon_I$)

ε_{FSS} = overlay free shrinkage strain

E_s = modulus of elasticity of substrate

E_0 = modulus of elasticity of overlay

C_ε = constant accounting for combined influence of relative member dimensions and strain profile characteristics.

The profile of shrinkage stress is determined using strain measurements. To analyze the stress profile of bonded concrete overlays, it is a reasonable assumption to take it that the top most part of the overlay shrinks easier compared to the part near the interface. Therefore, the shrinkage stress distribution on an overlay decreases from its interface with the substrate to its surface. Likewise, there are higher strains experienced by the substrate at its interface with the overlay because it is forced to shrink linearly with the shrinking overlay by the interfacial bond, this is shown in Figure 2-3 as presented by Beushausen (2005).

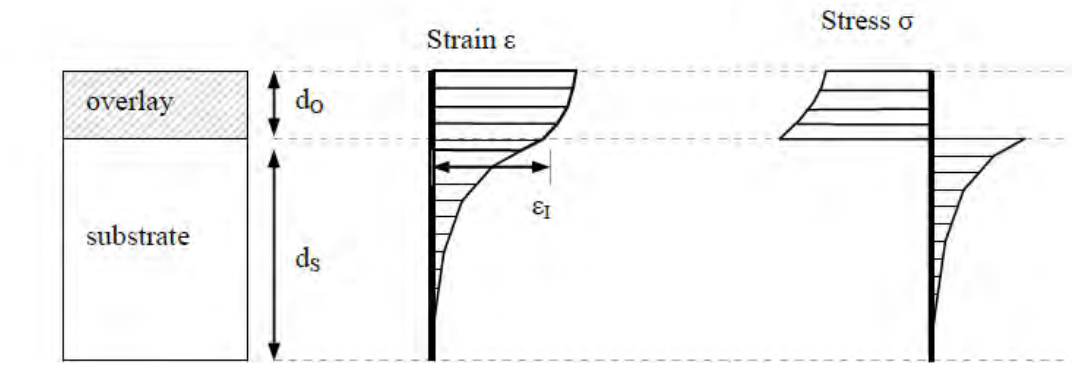

Where; ε_I = interface strain

d_0 = depth of overlay

d_S = depth of substrate

Figure 2-3: Schematics of strain and stress distribution in bonded concrete overlays (Beushausen (2005)).

Elastic strains also influence the performance of bonded concrete overlays. Restrained shrinkage strains at any time are proportional to overlay stresses, assumed from linear elastic theory. Beushausen, (2005) represented the direct elastic stresses due to the substrate and the overlay strains using Equation 2-3 and Equation 2-4, respectively.

$$\sigma_{O,I} = \left(\varepsilon_{FSS} - \frac{\varepsilon_{FSS}}{1 + \frac{E_s}{E_0}.C_\varepsilon} \right).E_0 \qquad \text{(tension)} \qquad [2\text{-}3]$$

$$\sigma_{S,I} = \left(\frac{\varepsilon_{FSS}}{1 + \frac{E_s}{E_0}.C_\varepsilon} \right).E_0 \qquad \text{(compression)} \qquad [2\text{-}4]$$

Where; $\sigma_{O,I}$ = direct elastic stress in an overlay

$\sigma_{S,I}$ = direct elastic stress in the substrate

Bonded concrete overlays are also influenced by the elastic stress. Beushausen, (2005) argued that direct elastic stresses do not remain constant in bonded concrete overlays. Direct elastic stresses change with respect to the degree of overlay tensile relaxation and the substrate creep. The creep in the substrate contributes to the stress relaxation by allowing more strains on an overlay. This leads to a reduction in restrained shrinkage. It should therefore be acknowledged that the resultant overlay stress is due to stress relaxed by substrate creep and stress relaxed due to tensile relaxation. These two mechanisms occur interdependently hence they cannot be dealt with independently. When including the effects of creep and relaxation the direct elastic stresses due to substrate and overlay strain are represented with Equation 2-5 and Equation 2-6, respectively (Beushausen, 2005).

$$\sigma_{S,I}(t) = \varepsilon_I(t).E_S = \frac{\Psi_O(t,t_o).\varepsilon_{FSS}(t)}{1 + \frac{E_s}{E_0(t)}.C_\varepsilon}.E_S \qquad [2\text{-}5]$$

$$\sigma_{O,I}(t) = (\Psi_O(t,t_o).\varepsilon_{FSS}(t) - \varepsilon_I(t)).E_O(t) \qquad \text{(tension)} \qquad [2\text{-}6]$$

$$= \left(\Psi_O(t,t_o).\varepsilon_{FSS}(t) - \frac{\Psi_O(t,t_o).\varepsilon_{FSS}(t)}{1 + \frac{E_s}{E_0(t)}.C_\varepsilon} \right).E_O(t)$$

$$= \Psi_O(t,t_o).\left(\varepsilon_{FSS}(t) - \frac{\varepsilon_{FSS}(t)}{1+\frac{E_s}{E_0(t)}.C_\varepsilon} \right).E_O(t)$$

Where; $\sigma_{S,I}(t)$ = direct stress in the substrate at the age t

$\sigma_{O,I}(t)$ = direct stress in an overlay at the age t

$\Psi_O(t,t_o)$ = relaxation function within the period of t and t_o

For; t= age at the time of testing

t_o= age at the time of loading

$\varepsilon_{FSS}(t)$ = free shrinkage strain of an overlay at the age t

$E_0(t)$ = modulus of elasticity of an overlay at the age t

There are also other mechanisms that are attributed to stress release of the concrete overlays. These include curvature displacement and interface slip. Curvature displacement is normally associated with overlays that are placed on relatively flexible substrates while interface slip is normally associated with poorly bonded overlays. In the present study these mechanisms are negligible because it is assumed that the overlays that are dealt with are properly bonded to the nonflexible concrete substrates

2.3.2. Creep and relaxation

Tensile creep is defined as the increase in strain due to an imposed constant tensile stress. Tensile relaxation is the reduction in stress due to a constant imposed strain. During the design of new concrete structures the tensile properties of concrete are generally disregarded (Bissonnette & Pigeon, 1995). This is usually a result of the difficulty in measuring tensile properties (tensile strength, tensile creep and tensile relaxation) of concrete. When concrete is loaded in constant tensile load for a period of time, it deforms in the direction of the applied load. As the loading period is prolonged, the increase in strain decays gradually. This effect is called tensile creep (Alexander & Beushausen, 2009). The creep phenomenon is shown diagrammatically in Figure 2-4 (i)-(ii).

When concrete is subjected to a constant tensile strain, it undergoes relaxation. Relaxation is defined as the decay of stress on a body when subjected to sustained strain. The sustained strain results in the built up of tensile stresses but these stresses decay gradually with time. This effect is called tensile relaxation (Alexander & Beushausen, 2009). In this research relaxation phenomenon will be used to express stress relaxation in concrete overlays. The relaxation phenomenon is shown diagrammatically in Figure 2-5 (i)-(ii).

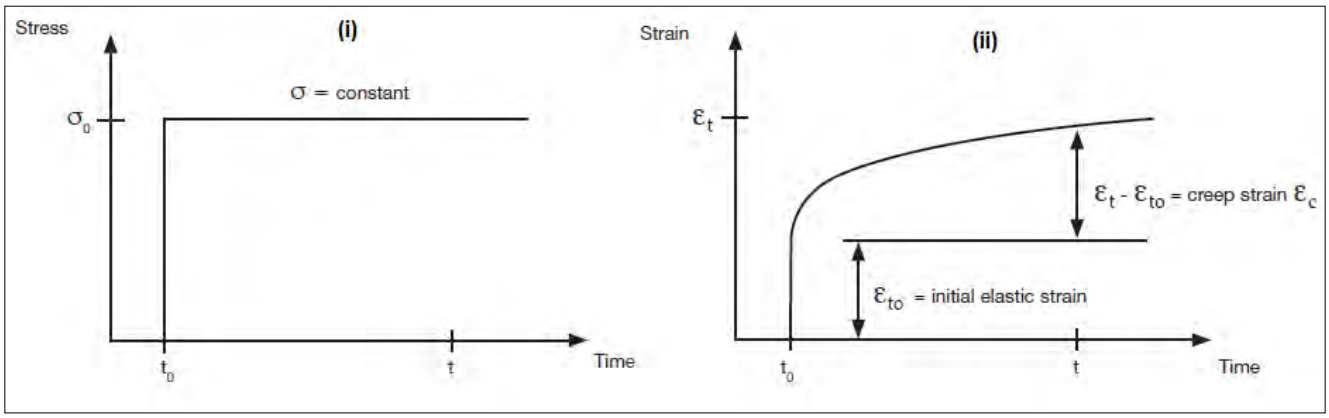

Figure 2-4: Time dependent increase in strain under constant stress (Alexander & Beushausen. 2009).

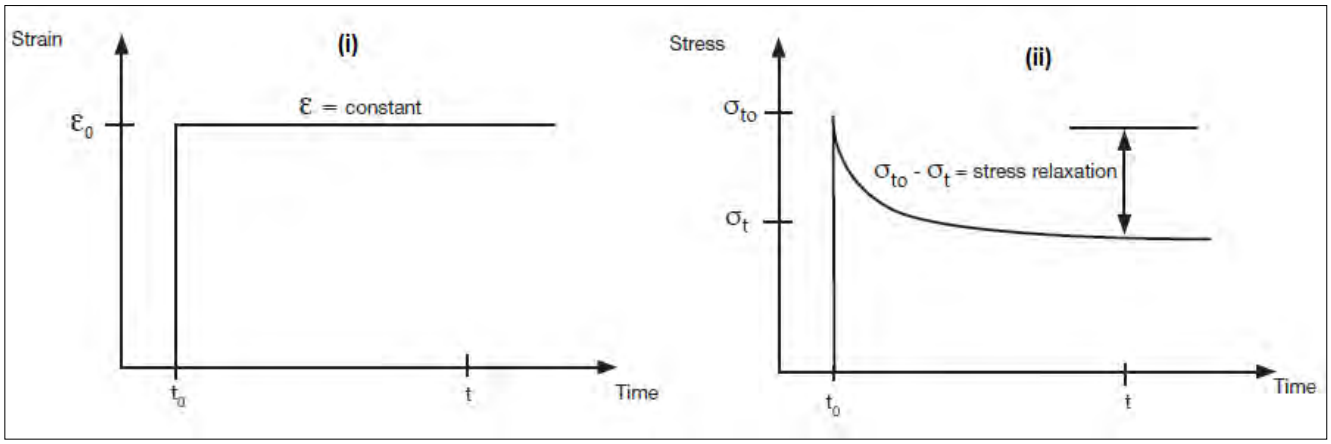

Figure 2-5: Time depended decrease in stress under constant imposed strain (Alexander & Beushausen. 2009).

Pigeon & Bissonnette (1999) used the viscous shear theory to define the mechanisms occurring in concrete experiencing tensile loading. Both creep and relaxation occur within cement paste and occur while the concrete is still in its visco-elastic behaviour (Pigeon & Bissonnette, 1999). Most researchers (Yokoyama, *et al*. (1994); Gutsch & Rostasy (1995); Beushausen & Alexander (2006)

and Masuku 2009)) report that the tensile relaxation degree in the concrete overlays is often as high as 60%.

The main importance of the tensile creep is to relieve tensile stresses within thin bonded concrete overlays (Pigeon & Bissonnette, 1999). This effect of stress relief is the one referred to as relaxation and it helps in reducing the occurrence of restrained shrinkage cracking. It is evident that the risk of shrinkage cracking in concrete overlays can be reduced by managing the relation between the tensile stress development and creep, and the relation between the strain development and relaxation. In the current study, recycled tyre rubber particles will be incorporated in concrete overlay mixes to study the effects of their grading and content on overlay relaxation behaviour.

2.3.3. Debonding

Debonding is defined as the detachment of the repair mortar/ overlay from the surface of the concrete substrate (Figure 2-6). For this failure mode, cleanliness and proper preparation of the substrate surfaces are very crucial since debonding depends mainly on the bond strength between the substrate and the overlay. It is also influenced by the amount of stresses caused by differential volume change on the substrate-mortar interface. The other factors such as the bond strength and overlay compressive strength play a large role on the substrate-overlay properties.

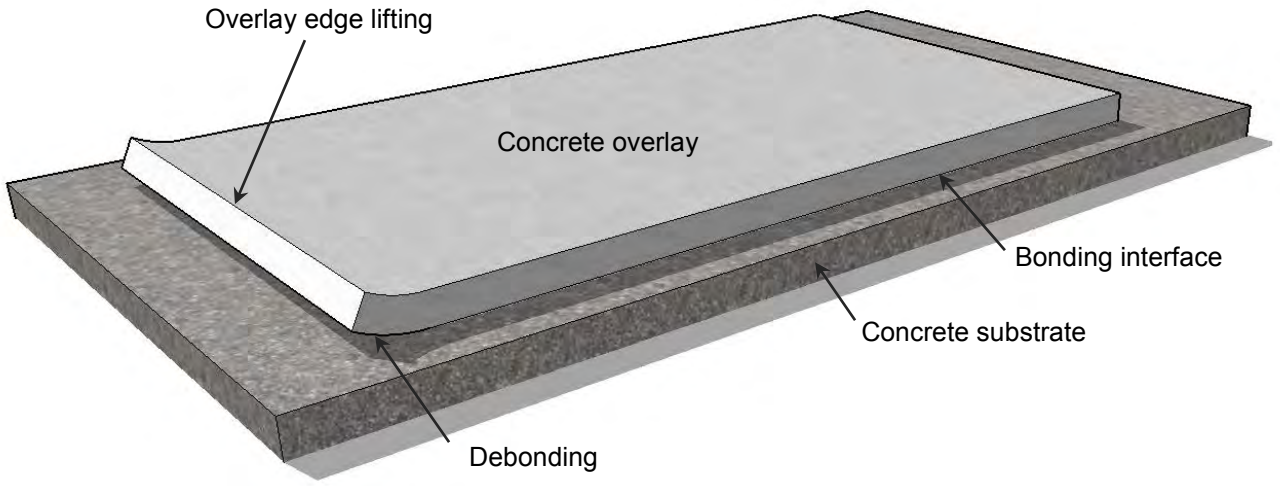

Figure 2-6: Debonding and edge lifting of concrete overlays.

Proper compaction is also considered important because it helps the overlay to achieve its homogeneity and thus avoid discontinuities that can become week zones for debonding to occur. Proper compaction also helps to release the air pockets on the interface of the substrate and the overlay. This ensures that uniform interfacial bond is achieved hence good bonding strength. To achieve good interlock and adhesion between substrate and overlay, substrate must be roughened and properly cleaned.

Preparation of the substrate surface for placement of overlay involves chipping away the old damaged concrete. This is done to expose and clean reinforcing bars if deterioration has gone through the entire concrete cover depth. The surface of the prepared substrate should consist of only strong and healthy concrete material to avoid week interfacial bond between the substrate and overlay. The new overlay is then cast over the existing sound substrate to protect the exposed reinforcing bars (Beushausen & Alexander, 2009), refer to Figure 1-1. The success of the overlay to overcome debonding is governed by proper cleaning and preparation of the surface of the substrate. Cleanliness of the substrate surface promotes its stronger bond strength with the overlay (Beushausen & Alexander, 2009).

2.3.4. Free Shrinkage strains

Shrinkage cracking of the concrete bonded overlays is a major concern in repair and service life extension of reinforced concrete structures. Most of the surface shrinkage cracks on concrete overlays develop as a result of the tensile stresses caused by differential shrinkage. Cracking happens at the point where these tensile stresses exceed the tensile strength of the overlay (Banthia & Gupta, 2008). Overlays undergo different shrinkage mechanisms throughout their setting and hardening time. These mechanisms are discussed below.

2.3.4.1. Plastic shrinkage

Plastic shrinkage is the volume reduction of the concrete mortar due to rapid loss of moisture through the surface at the early ages of an overlay casting, while the mortar is still plastic. It occurs within the first few hours after placement. Plastic shrinkage occurs when the rate of moisture loss to the surrounding exceeds the rate of bleeding of the concrete mortar. If excessive surface moisture loss occurs, a drop in the capillary pressure may lead to development of tensile strains. This happens because the inner cement paste and aggregates shrink at a slower rate compared to the outer

cement paste that shrinks relatively faster. If the concrete mortar is restrained, these restrained shrinkage strains may result in the development of surface cracks at the early age when sufficient tensile strength has still not developed (Banthia & Gupta, 2009). Shrinkage cracks are easily differentiated from other types of cracks. They are normally discontinuous, straight and closed spaced in a random pattern (Kellerman & Crosswell, 2009).

The plastic shrinkage cracking due to excessive moisture loss on concrete mortars is highly influenced by environmental conditions. Moisture could be lost through absorption by the dry substrate or evaporation facilitated by environmental conditions such as high wind velocity, high temperature and low relative humidity (Beushausen & Alexander, 2006). The concrete elements with a high surface to volume ratio like concrete overlays, are susceptible to higher rate of moisture loss hence are more susceptible to shrinkage cracking. However, it is recommended that where early age shrinkage resistance is a priority, a proper curing method should be practiced. A good curing method and duration prevents rapid and excessive moisture loss. In some instances, wind shields, bleed reducing admixtures and cement extenders are used in effort to reduce the moisture loss, hence the shrinkage cracking.

2.3.4.2. Autogenous shrinkage

Autogenous shrinkage also occurs during the early ages of overlays casting. It occurs few hours after the setting of the overlays (Alexander & Beushausen, 2009). Unlike plastic shrinkage, autogenous shrinkage is due to the consumption of water from the paste during the process of hydration. It is not associated with any moisture loss from the surface of the overlay. The absorption of pore water for hydration causes internal compressive stresses within the paste microstructure (Geiker *et al*., 2004). These stresses pull the paste into the pores in effort to fill up spaced left by the absorbed water. It is stated by Geiker *et al*. (2004) that the concrete with more and bigger pore sizes experiences higher induced compressive stresses within its microstructure. Therefore, it undergoes higher autogenous shrinkage strains. Geiker *et al*. (2004) also claimed that some of the autogenous shrinkage strains occur because the total volume of hydration products is effectively less than the total volume of hydration reactants.

It was also stated by Carlswärd, (2006) that autogenous shrinkage is normally prominent in high strength concretes with lower w/b ratios because of the high consumption of water in hydration process. The fact that autogenous shrinkage is chemically and internally initiated, proper curing

seemed to have negligible effect on degrees of autogenous shrinkage strains of concrete (Carlswärd, 2006).

2.3.4.3. Drying shrinkage

Drying shrinkage is the time-dependent reduction in volume of cement paste due to moisture loss to the environment. It is time dependent because the rate at which moisture is lost from the concrete mortar is fairly faster at the early age and becomes slower as the concrete mortar ages. Therefore, the shrinkage strain response also becomes time dependent. Moisture loss from capillary pores of concrete mortar causes differential reduction in the volume of concrete mortar (Alexander & Beushausen, 2009).

Drying shrinkage is prominent at the hardening stage of concrete and concrete mortars. Asad *et al*. (1997) stated that drying shrinkage in concrete mortars occurs because of the reduction in the volume of calcium silicate hydrate gel (C-S-H) during the hardening and drying stage. Alexander (2001) proposed that there are different mechanisms that are involved in drying shrinkage. These are capillary tension, surface tension, swelling pressure and movement of interlayer water theories.

Capillary tension

Capillary tension is caused by the loss of water from the capillary pores of the paste due to drying. A meniscus forms within cement paste during drying. The meniscus is under hydrostatic tension and places the cement paste in hydrostatic compression (Mindess *et al*., 2003). This compressive stress reduces the size of the capillary pores, and thus causes a reduction in the overall volume of the cement paste (Figure 2-7).

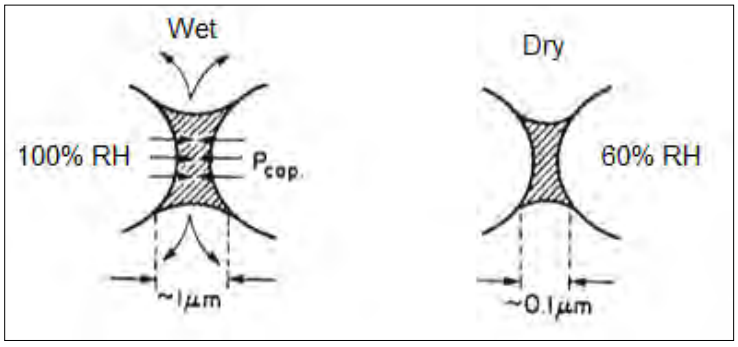

Figure 2-7: Mechanism of capillary tension in cement paste (Mindess *et al*., 2003).

Surface tension

Drying causes an increase in surface tension of the concrete. This surface tension induces compressive stresses inside solid particles and the cement gel (Mindess *et al*., 2003). The increase in induced compressive stresses causes shrinkage (Figure 2-8).

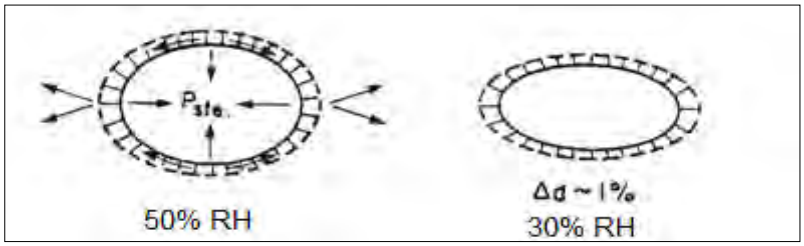

Figure 2-8: Mechanism of surface tension in cement paste (Mindess *et al*., 2003).

Swelling pressure

Swelling pressure, also referred to as disjoining pressure is the pressure caused by adsorbed water contained in the narrow spaces of the capillary pores. When the water is contained in the narrow pore space, it exerts pressure on the adjacent cement paste surfaces. The loss of this adsorbed water result in the drop in swelling pressure (Mindess *et al*., 2003). Due to pressure drop, the surrounding cement paste is drawn into pore spaces thus resulting in shrinkage (Figure 2-9).

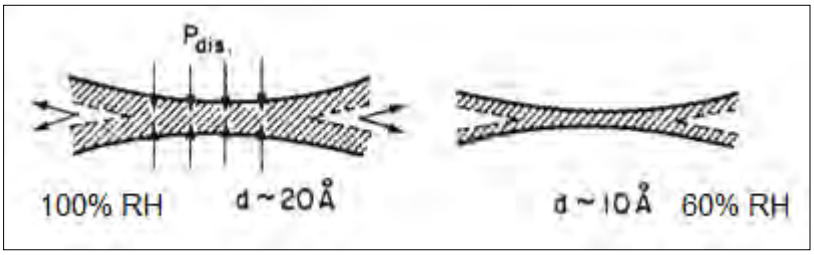

Figure 2-9: Mechanism of swelling pressure in cement paste (Mindess *et al*., 2003).

All these mechanisms occur at micro scale. They can be verified using special methods like spectroscopy as it is difficult to verify through conventional methods (Alexander, 2001). It is important to note that there are many factors/ parameters that directly affect the drying shrinkage of concrete. These include volume to surface area ratio, content of mix constituents, water/binder ratio, curing method and curing conditions. The effects caused by these factors on shrinkage are discussed in Section 2.4.

2.4. Parameters affecting restrained shrinkage cracking

The main parameters influencing shrinkage cracking can be factored into intrinsic factors such as mix constituents, content of mix constituents and water/binder ratio and material mechanical properties. There are also extrinsic factors such as curing method and environmental conditions. This section discusses briefly how these factors affect shrinkage cracking.

2.4.1. Content and type of mix constituents

Aggregate

The type and content of aggregate has an effect on the restrained shrinkage cracking of concrete overlays. Aggregates affect overlays by providing shrinkage restraint and diluting the paste (Alexander, 2001). Dilution of the paste by the aggregate reduces the magnitude of shrinkage strains. Shrinkage of the concrete decreases with increasing aggregate content. Aggregates provide restraint because they do not undergo volume changes due to changing moisture conditions. The restraint provided by the aggregates reduces concrete shrinkage because the shrinkage of concrete decreases with an increase in aggregate stiffness (Alexander, 2001). The content, size, texture and stiffness of the aggregates also influence the degree of shrinkage strains of concrete. Troxell *et al*. (1958) stated that the most important aggregate characteristic influencing shrinkage cracking is the aggregate stiffness. In the study conducted by Troxell *et al*. (1958), it was found that drying shrinkage and creep of concrete increased when the high elastic modulus aggregates were substituted with the low elastic modulus aggregates.

Binders

Shrinkage cracking is also affected by the fineness of binders. The term “binders” refers to both cements and cement extenders or a blend of both. Finer cement particles generate higher amount of heat of hydration and also require a greater amount of water during the process of hydration. This may lead to high consumption of internal mix water and thus an increased risk of cracking on the overlays due to the thermal shrinkage. Cement which has been stored in unfavourable conditions for a long period of time can sometimes form larger hardened particles that could not normally undergo full hydration. These hardened particles may provide a restraint effect within overlays, similar to that provided by natural aggregates. When the overlay experiences higher degrees of shrinkage, the

restraint provided by cement particles can cause cracking. This influence was determined by Tritsch *et al*. (2005) in a research study where fine-ground cement was replaced with coarse-ground cement.

It has also been confirmed by Alexander, (1994) that addition of cement extenders influences the degree of shrinkage. With regard to the performance of the three most common cement extenders (Condensed Silica fume (CSF), Fly ash (FA) and Ground granulated blast furnace slag (GGBS)) used in construction, CSF was found to have little influence on the main shrinkage of cement based materials. Although CSF has an influence of densifying the microstructure of the mortar mixes, which help to reduce easy moisture loss, it was only found to have an impact on the rate at which shrinkage occurs. Alexander (1994) studied deformation properties of concrete made with cement blended by GGBS and CSF, and found that addition of CSF did not influence the total shrinkage but addition of GGBS seemed to reduce creep strains on concrete.

Admixtures

Addition of shrinkage reducing admixtures has been proven to improve the shrinkage cracking resistance of concrete (Weiss & Shah, 2002). Shrinkage reducing admixtures help to reduce the surface tension of the mix water and this effect has an advantage of reducing the stresses in the capillary pores. Weiss & Shah, (2002) also commented that Shrinkage reducing admixtures reduce the rate of shrinkage in concrete.

Fibre

Carlsward (2006) showed that the addition of fibre in overlays reduces the occurrence of early age shrinkage cracks. Banthia *et al*. (1996) investigated the effect of steel fibre on restrained shrinkage cracking of thin bonded overlays cast directly on the substrate beams and exposed to a drying environment. Addition of fibre was found to delay the occurrence of cracks and reduced the crack widths. Weiss & Shah (2002) also found that not only does the age of cracking prolong due to addition of steel fibre, but the rate of crack propagation also reduces. This effect is due to the fact that the fibre had the ability to arrest the cracks after their initiation.

2.4.2. Water to binder ratio

As discussed before, shrinkage and relaxation of overlays occur in cement paste because that is where water is lost and where volume change happens. The content of hydrated cement in the paste

plays an important role in the shrinkage cracking. Therefore w/b ratio is considered as one of the factors that affect drying shrinkage drastically (Mehta & Monteiro, 2006a). Carlsward (2006) observed that the extent of shrinkage is directly proportional to the amount of cement used in the paste. Decreasing w/b ratio is known to increase drying shrinkage. This result is expected because the volume of cement content is increased when the w/b ratio is decreased (Carlsward, 2006).

The w/b ratio also affects the tensile strength and elastic modulus of the cement paste, and these effects have an influence on the amount of creep experienced by the paste. The pastes with low w/b are stiffer and hence they creep less. A decreased w/b ratio implies an increased tensile strength of the overlays. Brown *et al*. (2003) suggested that higher w/b ratio should be used to reduce the risk of cracking in overlays.

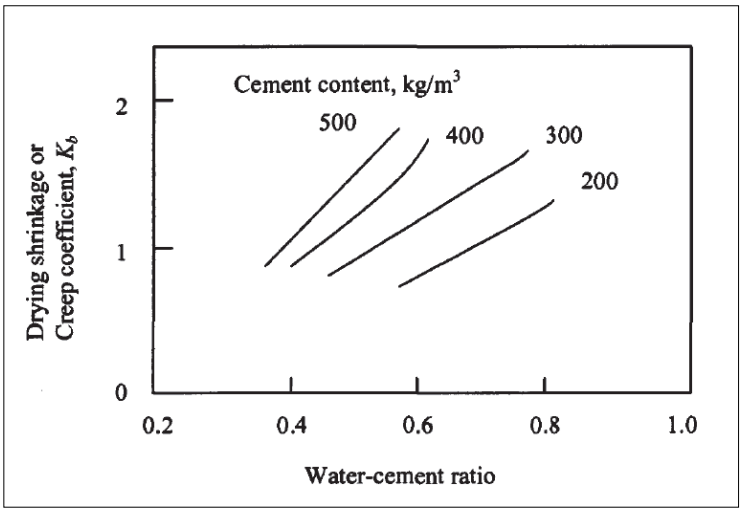

Figure 2-10: Effect of w/b ratio on restrained drying shrinkage (Mehta & Monteiro, 2006a).

2.4.3. Curing method

The degree of early age shrinkage can be reduced by applying a good curing method (Banthia & Gupta, 2006). It is also known that an increase in curing period reduces the overall shrinkage strains. Proper curing keeps sufficient moisture to prevent the surface from drying out quickly before the overlay gains sufficient tensile strength. Consequently this reduces the effects of surface shrinkage cracking. However, according to ACI Committee 364 (2006), curing only delays moisture evaporation and its associated drying shrinkage but does not reduce the overall shrinkage strain.

2.4.4. Size of a concrete member

Shrinkage cracking is also affected by the shape and size of the concrete mass. Drying shrinkage of concrete elements occurs on the exposed surfaces. Therefore it is evident that shrinkage strains depend on the geometry and dimensions of a concrete member (Alexander & Beushausen, 2009). It was observed from the study conducted by Care & Nicolle, (2005) that moisture gradient, porosity and shrinkage strain gradients were dependent on the size of the drying surface and the thickness of the concrete member.

2.4.5. Environmental conditions

In large mass concrete structures, extreme environmental conditions become some of the main parameters that influence overlay shrinkage cracking. This is because the shrinkage and creep of overlays get affected by environmental conditions such as; temperature, relative humidity (RH) and wind speed. In the case of high temperature climate, the high heat produced during the process of cement hydration results in the cement based materials having high rate of temperature rise within a few hours to days, after placement (Ballim & Graham, 2009; Beushausen *et al*., 2012). Due to the restrained thermal shrinkage that occurs at the cooling phase of concrete overlays, cracks may develop. This problem could be mitigated or reduced through the proper selection of mix constituents, constituents' content, techniques of mixing, curing methods used and proper placement (Alexander & Beushausen, 2009). It has also been proposed that the use of slag can significantly reduce the heat produced during hydration process, thereby mitigating towards the thermal shrinkage cracking problem (Mizobuchi *et al*., 2000).

The drying creep increases with decreasing ambient relative humidity (RH) and increasing temperature. Lower RH increases the creep of concrete and overlays but has much smaller effect if concrete has previously reached hygral equilibrium with the environment before application of the load. Troxell *et al*. (1958) showed that although shrinkage is still measurable even after a period of 20 years, the rate of shrinkage decreases with time (Figure 2-11). It is also shown in the figure that shrinkage becomes less when RH is high.

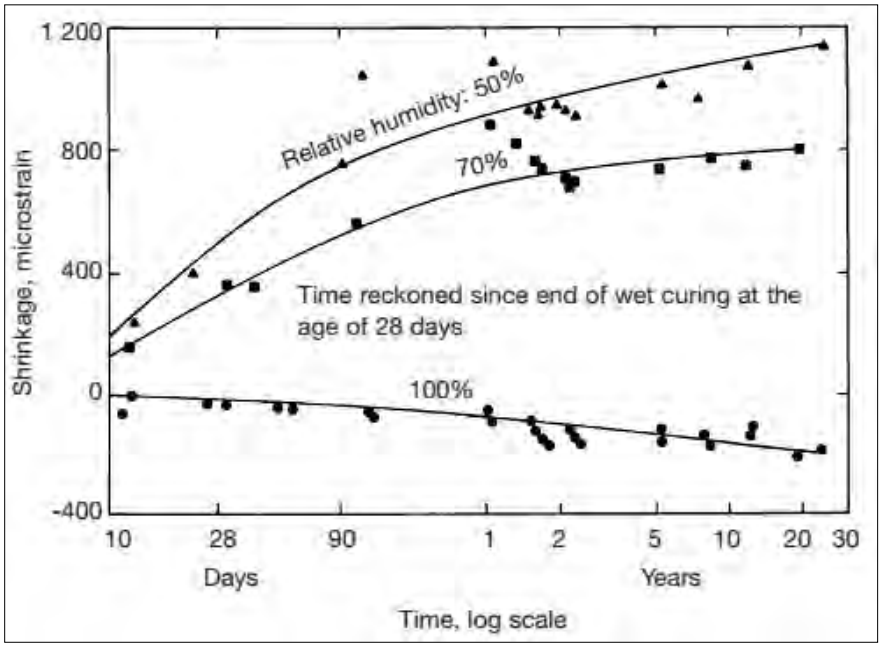

Figure 2-11: Influence of relative humidity on shrinkage of concrete (Alexander & Beushausen. 2009).

2.5. Review of recycled tyre rubber particle usage in mortars

Several authors (Turatsinze *et al*. (2005); Turatsinze *et al*. (2007); Turatsinze *et al*. (2008); Ho & Turatsinze (2009); Raghavan *et al*. (1998) and Uygunog˘lu and Topçu. (2010)) suggested an innovative technique of incorporating recycled tyre rubber particles in to concrete mortars to mitigate the effect of some of the factors that affect performance of bonded concrete overlays. This section presents the background on the use of tyre rubber particles and their potential benefits when used in overlays. First the review on production of the rubber particles and how rubber particles are incorporated in concrete mortars is presented. Mainly a summary of effects caused by rubber particles incorporation on material properties of concrete mortars is presented.

2.5.1. General review

As reported in 2012 by The South African Tyre Recycling Process Company, about 13,000,000 tyres or 225,000 tons of used tyres are generated as waste in South Africa (SA), per year. Although the tyre waste is considered as a non-hazardous waste material, it still poses a problem to the South African solid waste management. This follows from the fact that tyres are chemically none biodegradable even after long-term landfill. Shredded tyre particles can be used in a variety of rubber

and plastic products. They can also be burnt to provide energy for electricity production or get utilized in cement industries as fuel for cement kilns (Segre & Joekes, 2000).

Although the above discussed ideas of waste tyre consumption help in waste tyre management issues, they cause the problem of air pollution that in turn causes a threat to global warming and environmental sustainability. The technology of using recycled tyre rubber particles to partially replace fine natural aggregates in cement based mortars seems to be a legitimate solution. The incorporation of recycled tyre rubber particles also has the advantage of conserving some of the fine natural aggregates used in the production of concrete mortars and other cement based materials. It is thus clear that this innovative technology also fulfils some of the green engineering objectives towards a sustainable environment.

Rubber naturally has low specific gravity and the tyre rubber particles inherit the same property. The unit weight of rubberized concrete mortar therefore decreases with incorporation of rubber particles (Khatib & Bayomy, 1999). The increase in rubber particle percentage content has also been proven to reduce the elastic modulus; increase the relaxation capacity and delays age of cracking of rubberized concrete mortars (Turatsinze *et al*., 2008). These changes in material properties are necessary for cracking resistance of concrete mortars, hence are discussed in Section 3.6.3.

2.5.2. Production of tyre rubber particles

Recycled tyre rubber particles are obtained from shredded scrap tyres using either mechanical grinding at room temperature or cryogenic grinding (Goulias & Ali, 1997). ***Mechanical grinding*** is preferred because of its cost effectiveness and being the most practicable processing. In this method the scrap tyres go through ‘cracker milling’ and ‘granulation’ to get mechanically broken down into the sizes ranging from several centimetres to fractions of a centimetre (Owen, 1998). The wire mesh and steel threads from the tyres are then separated from the rubber particles magnetically in different stages of granulation. Mechanical sieve analysis is thereafter performed to sort rubber particles into various gradations (Owen, 1998). Figure 2-12 show a typical process diagram for the mechanical processing of rubber particles.

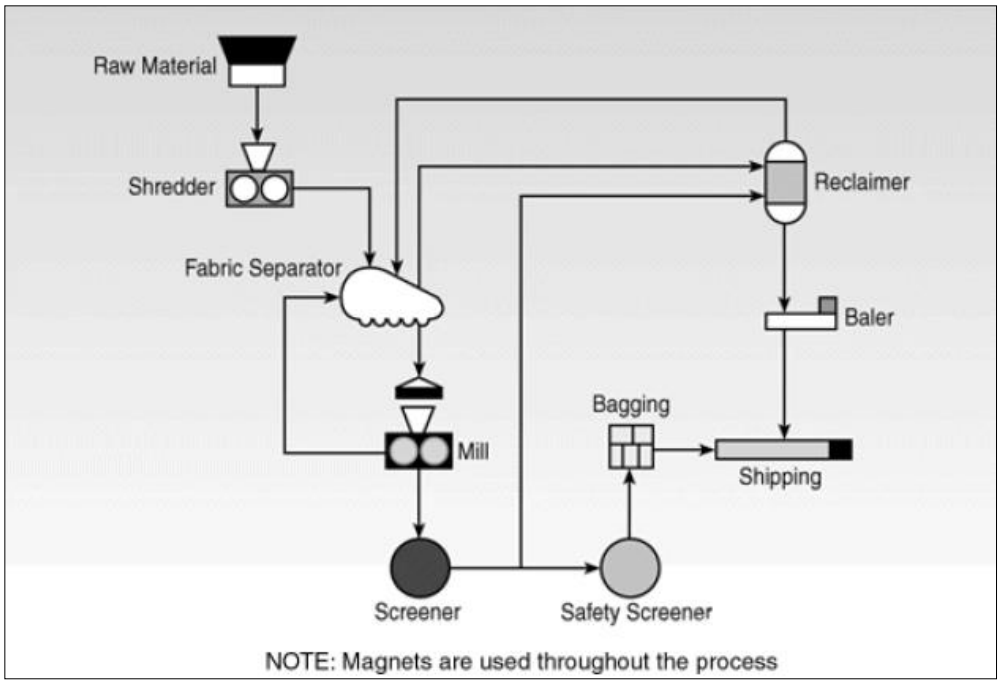

Figure 2-12: A typical process diagram for the mechanical processing of waste tyres (Gadkar, 2013).

Cryogenic processing is the other method of processing recycled tyre rubber particles into usable sizes. Cryogenic processing is performed at a temperature below glass transition temperature. At this temperature scraped tyre rubber shreds are frozen using liquid nitrogen. The cooled rubber shreds become extremely brittle. They are then crushed in to smaller desirable sizes through the closed loop of the hammer-mill. The wire mesh and steel threads are magnetically removed as in the mechanical grinding process. To avoid surface oxidation, this process is performed in a deoxygenated environment (Owen, 1998). Based on research conducted by Eldin & Senouci (1993), where the effects of rubber particles in concrete were investigated, it was argued that unlike the rubber particles that are processed mechanically, cryogenic processed rubber particles are more steel and fabric free. Cryogenic processed rubber particles are geometrically uniform in shape and finely produce desirable gradations but very expensive to produce. Figure 2-13 show a typical process diagram for the cryogenic processing of rubber particles.

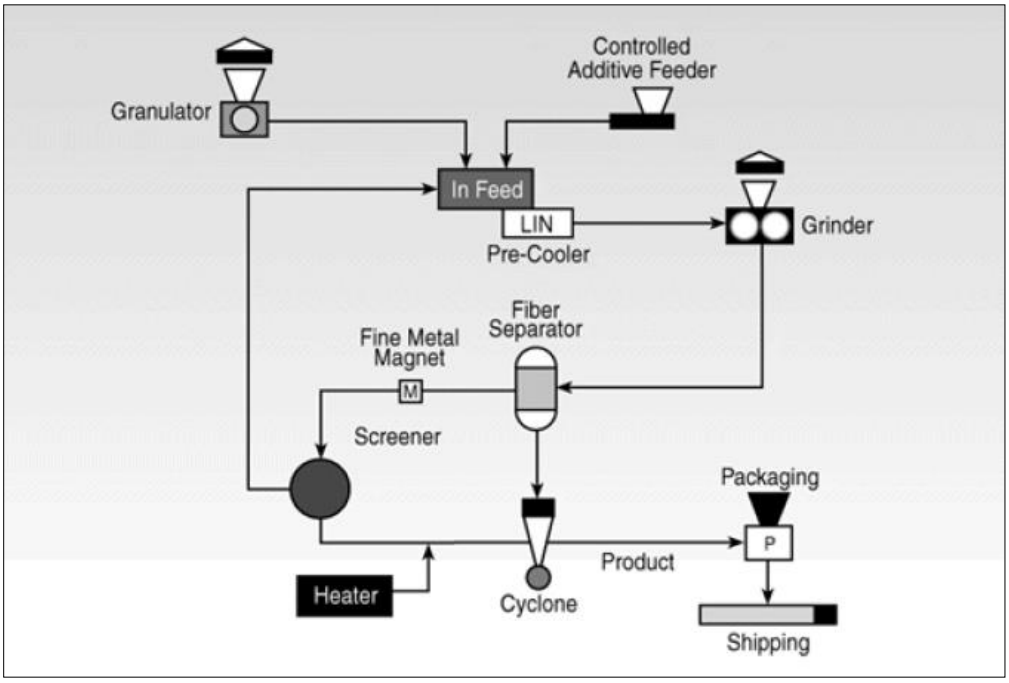

Figure 2-13: A typical process diagram for the cryogenic processing of waste tyres (Gadkar, 2013).

Ali *et al*. (1993) reported that truck tyre rubber particles and car tyre rubber particles should be considered as different materials because they have different quantities of elastomers and textile components. Figure 2-14 shows the most common compositions of tyre types from which rubber particles are usually processed.

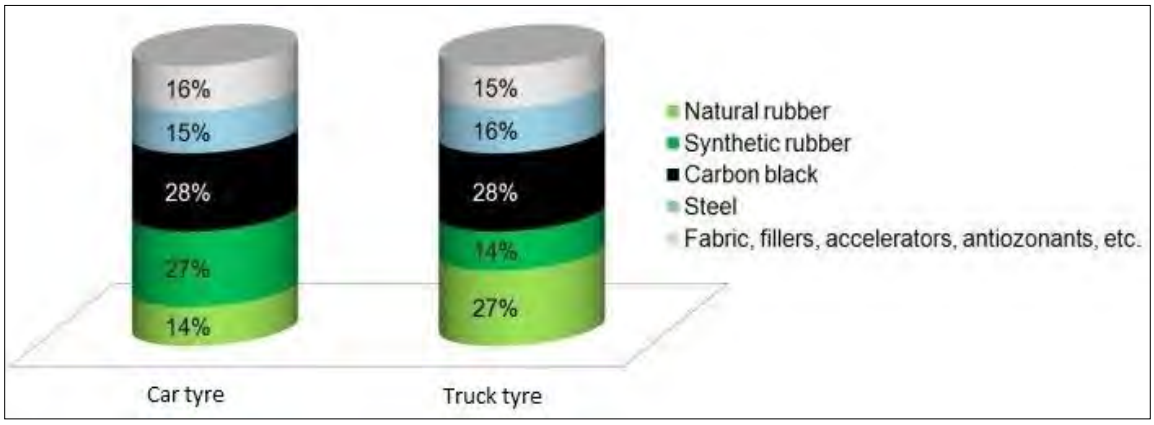

Figure 2-14: Comparison of the compositions of passenger car tyres and truck tyres (Ali *et al*., 1993).

2.5.3. The use of tyre rubber particles in concrete mortars

The main focus of concrete production is usually strength, since this is considered the major measure of quality. Nevertheless, even high strength concrete suffers from a relatively low tensile strength and poor strain capacity due to its increased brittleness. Such properties make concrete very sensitive to cracking; thus the durability and sustainability of reinforced concrete service life become compromised. This phenomenon particularly holds true for concrete overlays with large surface areas because they experience higher shrinkage and volume changes. Some researchers have proposed the usage of fibre reinforcement to mitigate against concrete overlays cracking. Unfortunately, reinforcing concrete mortars with fibres does not prevent them from cracking but only restrains the crack propagation and opening. The other solution that has been proposed include internal curing using superabsorbent polymers (SAPs) or internal sealing to prevent rapid water loss that causes excessive shrinkage.

The research project is concerned with the incorporation of recycled tyre rubber particles into concrete mortar mixes as a means of improving their cracking performance. This approach was inspired by the success of the approach used by Shkarayev, (2003) to arrest crack propagation in metals by simply drilling a hole at the crack tip or at a convenient distance ahead of the expected crack growth path. Shkarayev, (2003) found that crack stops propagating when the crack tip of the crack meets the drilled hole. Caron *et al*. (2004) discussed that the crack stops because of the decreased crack tip sharpness and also because the stress concentration dissipates in the hole, causing the material to relax.

As far as concrete mortars are concerned, the initiation points and crack growth path are unpredictable, thus making it difficult to decide the locations where holes could be drilled. In addition, the drilling of holes on concrete overlays would allow easy and abundant passage of aggressive agents to reach the reinforcing bars. The setbacks caused by drilling a multitude of holes on concrete overlays could be avoided by incorporating aggregates of a material with low stiffness. In the current research, tyre rubber particles are used. This approach seemed suitable in overlays because the resistance against shrinkage cracking is a priority. Incorporation of rubber particles in overlays promises to improve cracking resistance of overlays because, besides having the potential to arrest the cracks propagations, the relaxation capacity of the mortars increases and the elastic modulus decreases. The technique also provides the waste tyre management with an opportunity to recycle the end-of-life tyres sustainably and environmentally.

2.5.4. The influence of tyre rubber particles in concrete mortars properties

This section reports the influence that incorporation of rubber aggregates has on basic properties of concrete mortars and the impact that these influences have on the cracking performance of concrete mortars. The properties discussed are free shrinkage, tensile strength, tensile relaxation, elastic modulus and restrained shrinkage. All these material properties are important for cracking resistance of concrete overlays.

2.5.4.1. Influence on compressive strength

In general, it is reported in various published research results that incorporation of rubber particles lowers the compressive strength of concrete mortar mixes. Furthermore, it was observed that strength reduction increases with an increasing content of the rubber particles. For instance, the 28 days test results obtained by Turatsinze *et al*. (2005) showed that the control concrete mortars experienced compressive strength reduction of 80% and 50% when natural aggregates are replaced by rubber particles with the proportions of 30% and 20% by volume, respectively. This detrimental effect was described by Turatsinze *et al*. (2007) as caused by the high Poisson's ratio, which may induce premature cracking of the concrete when compressed, the low stiffness of rubber, the bond defects at the rubber–cement paste interface and the high porosity of rubberized concrete mortars.

Although the reduction in compressive strength of concrete mortar mixes may limit their application for some of the structural purposes, it was observed by Eldin and Senouci (1993) that they do not conform to a brittle failure mode when loaded in compression. Eldin and Senouci (1993) showed that when loaded in compression, specimens containing rubber particles did not exhibit a brittle failure but a gradual failure was observed. It was argued by Eldin and Senouci (1993) that since the interfacial bond of cement paste and rubber particles is much weaker in tension than in compression, the rubberized concrete specimen would start failing in tension before it reaches its compression strength limit. The resulting tensile stress concentrations around the rubber particles (see Figure 2-15a) cause multiple tensile micro cracks within the specimen (see Figure. 2-15b). These micro cracks rapidly propagate through the cement paste until they meet the rubber particles. Because of the ability of rubber particles to withstand large tensile deformations, they act as springs (see Figure 2-15c), thus causing delay in the crack widening and preventing the complete disintegration of the concrete mortar specimen.

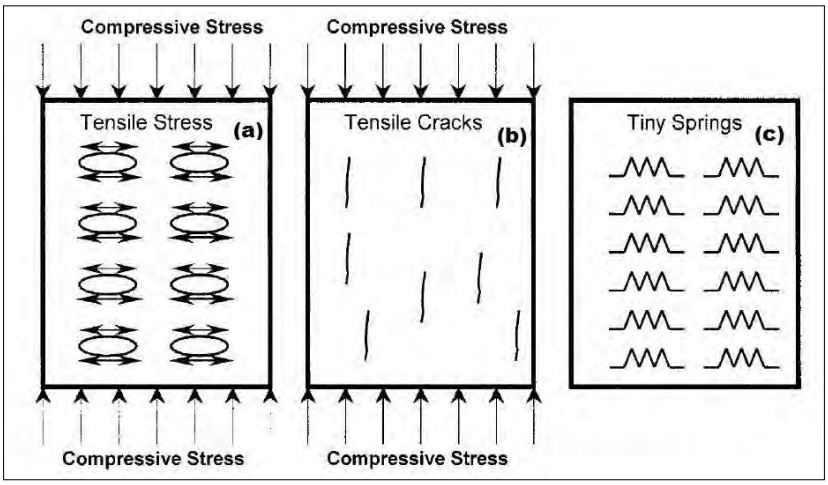

Figure 2-15: The model of the compressive failure mode of rubberized mortar specimens (Eldin & Senouci, 1993).

Due to the failure process discussed above, the continuous loading of the specimen causes development of more cracks as well as widening of the existing cracks. Rubberized concrete mortars incorporating a higher content of the rubber particles are capable of absorbing a significant amount of plastic energy, and can withstand large deformations without the complete disintegration of the test specimens.

In another experimental study conducted by Biel and Lee (1996), it was observed that the control concrete specimens failed in an explosive disintegration manner. The severity and loudness of the explosive sound of the specimens decreased with the increased content of rubber particles. It was also observed that the test specimens did not separate completely but continued to sustain compressive load after the initial ultimate failure point. When the compressive load was released, the specimens rebounded back to near their original shape. The effects of the incorporation of rubber particles on compressive strength were also observed, and reported by Tsoana (2012), from the experimental study concerning the mechanical properties of rubberized concrete.

2.5.4.2. Influence on tensile strength

Incorporation of rubber particles in concrete mortars causes reduction in tensile strength. Various researchers (Ho & Turatsinze (2009); Turatsinze *et al*. (2003); Turatsinze *et al*. (2005); Turatsinze *et al*. (2007)) observed that the tensile strength reduction increases with the increasing content of rubber particles incorporated. This was justified by the argument that; the more the interfacial transition zones (ITZ) and spaces between the rubber particles, the weaker the rubberized mortar bond

strength becomes. It was also argued that this reduction could be due to various impacts, including; the effect of rubber particles' high Poisson ratio which can cause premature micro cracking of the concrete mortar when subjected to tensile stresses; the poor bond strength between rubber particles and cement paste and the high porosity of rubberized concrete mortar (Ho & Turatsinze, 2009). Figure 2-16 shows the 28 days test results of tensile strength (f_t) and compressive strength (f_c) of rubberized concrete mortar mix as acquired by Ho & Turatsinze (2009).

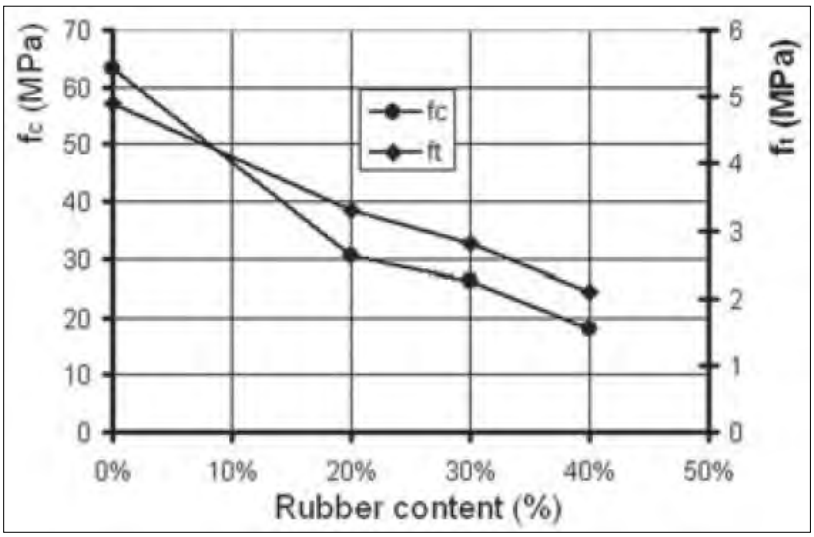

Figure 2-16: Influence of rubber particle content on tensile and compressive strength (Ho & Turatsinze, 2009).

Despite of the low ultimate tensile strength, the yield strength of rubberized concrete mortars is always higher than the yield strength of their respective control mixes. This is because of the rubber particles within the concrete having the ability to cause the mix to withstand post failure deformation (Ho & Turatsinze, 2009). Yield strength is defined as stress that can be withstood by the test specimen without permanent deformation.

2.5.4.3. Influence on tensile relaxation

In the research conducted by Turatsinze *et al*. (2003), the effect of rubber particle incorporation was analysed and was found to have the same effect as drilling small holes at the tips of a crack. This approach has been considered the simplest way of arresting the crack propagation (Shkarayev, 2003). It is because the stress concentration is relieved when the crack runs into the hole, the same way as it runs inti the interface of rubber particles with cement paste. The effect of arresting the cracks by drilling holes results in stress concentration relaxation and thus the delay of micro-crack development.

The effect of the rubber particles on tensile stress relief was further discussed by Ho & Turatsinze, (2009). They explained that the rubber particles within the concrete mortar matrix act like holes thus reducing the potential of cracks initiating at the points on high stress concentration. It is argued that the holes also reduce the sharpness of the first micro-crack tip that results from tensile stress concentration. This effect ultimately delays initiation of micro-cracks and it also slows down the kinetics of the first micro-crack to propagate (Ho & Turatsinze, 2009). This phenomenon of tensile relaxation can also be explained by the spring effect (see Figure 2-15) that occurs due to introduction of internal tensile stresses. It is the spring effect that allows for significant tensile relaxation.

2.5.4.4. Influence on elastic modulus

The reduction of the modulus of elasticity when rubber particles are incorporated in concrete mortars has been observed by many researchers (Turatsinze *et al*. (2003), Turatsinze *et al*. (2005) and Ho & Turatsinze (2009)). It was also established that the modulus of elasticity of rubberized concrete mortars decreases with increasing rubber particle content. The reduction of the elastic modulus in rubberized concrete mortars can be justified by the well-established fact that the elastic modulus of any concrete depends on the elastic modulus of the aggregates, and on their volumetric proportions in the matrix (Hobbs, 1971). Figure 2-17 shows the results of the influence of rubber particle content on the elastic modulus of a typical concrete mortar mix as presented by Ho & Turatsinze (2009).

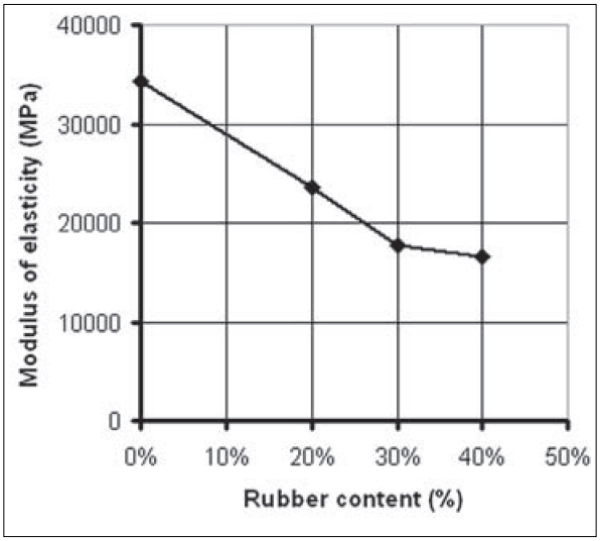

Figure 2-17: Effects of rubber particle content on the modulus of elasticity (Ho & Turatsinze, 2009).

Based on the empirical law linking elastic modulus and compressive strength, the trends observed in Figure 2-16 and Figure 2-17 were expected. According to the relationship presented in Equation 2-7, adopted from Eurocode, elastic modulus is proportional to the measured compressive strength. As it is already established that incorporation of rubber particles causes compressive strength reduction, it is implied by the equation that the elastic modulus will also be reduced. Both the empirical and experimental results demonstrate that incorporation of rubber particles in concrete mortar mixes has more effect on reducing the elastic modulus than it has on reducing the compressive strength (Ho & Turatsinze, 2009).

$$E_c = 22\left[\frac{f_c}{10}\right]^{0.3} \qquad [2\text{-}7]$$

Where; E_c = elastic modulus (GPa)

f_c = compressive strength (MPa)

Although there is a clear pattern of how the rubber particle content affect elastic modulus of cement based mortars, the influence of optimizing the content and gradation of rubber particles has not been investigated and presented. The current research study will attempt to investigate the effect of the optimized content and gradation of rubber particles on material properties that influence the cracking resistance of concrete mortars.

Uygunog˘lu and Topçu, (2010) studied the role of scrap rubber particles on the drying shrinkage and mechanical properties of self-consolidating mortars (SCMs). From the experimental results recorded, it was observed that partial replacement of natural sand with rubber particles causes a decrease in the modulus of elasticity compared with that of the control SCM. It was discussed that this effect is due to the increase of the porous structure introduced by incorporation of the rubber particles.

2.5.4.5. Influence on free shrinkage

Free shrinkage on bonded concrete overlays is caused by the excessive moisture loss from the fresh cement paste to the environment and can also be due to absorption of water by the substrate if it is relatively dry. Mechanisms of shrinkage and their influence on cracking have been discussed in Section 2.3.3.

While the incorporation of rubber particles leads to improved elastic modulus and tensile relaxation properties of concrete mortars, rubber particles are expected to induce higher free shrinkage length changes. The dependence of the free shrinkage in cement-based materials upon incorporation of rubber particles has not been sufficiently demonstrated and documented. However, there are at least few researchers who have successfully conducted experimental work to study the influence of rubber particles in free shrinkage of cement based materials.

From the shrinkage measurements recorded by Uygunog˘lu and Topçu, (2010) on self-consolidating mortars (SCM) made from both w/b ratios of 0.47 and 0.51, it was deduced that shrinkage increased with an increase in rubber particle content. As discussed before, rubber particles increase the porosity of concrete overlays. Evaporation of free water from these macro-pores causes the increase in shrinkage strains. Uygunog˘lu and Topçu, (2010) also discussed that since the stiffness of the rubber is much less than that of cement paste (and that of the sand aggregate), the rubber particles may not have the ability to restrain shrinkage. Rather an increase in shrinkage may be expected in rubberized mortar mixes. The higher shrinkage strains were observed in the SCMs with higher w/b ratio while the lower shrinkage strains were observed in the SCMs with the lower w/b ratio. However, Uygunog˘lu and Topçu, (2010) noted that an increase in drying shrinkage of all the SCMs slowed down after 100 days.

Preliminary results from the study conducted by Raghavan *et al*. (1998) revealed that the incorporation of rubber shreds in concrete mortars causes an increase in the length change due to drying shrinkage. It was also observed that shrinkage increased with increasing the content of rubber particles incorporated. The research results by Turatsinze *et al*. (2007) also showed that the free shrinkage increases with increasing the rubber particle content. It was believed that this effect is due to the fact that rubber particles offer less restraint to the shrinkage of the cement paste since they are characterized by low modus of elasticity.

2.5.4.6. Influence on restrained shrinkage

The incorporation of rubber particles in concrete mortars enhances their performance on resisting the restrained shrinkage cracking. Turatsinze *et al*. (2003) observed from restrained shrinkage test (ring test) that the delay in shrinkage cracking prolongs with increasing the content of the rubber particles. Furthermore, it was observed that the rubberized concrete mortar ring specimens were characterized by very thin crack openings compared to their respective control mortar specimens. Generally, it is

expected that the presence of less stiff aggregates within the concrete mortar will reduce the internal restraint and thus allow more shrinkage length change (Hobbs, 1971).

The rubber particles incorporated in concrete mortar mixes also changes the microstructure of the mortar. It was argued by Turatsinze *et al*. (2003) that though the surfaces of rubber particles in concrete mortar mixes could be considered as weak interfacial zones, when micro-cracks run into the interface of these rubber particles and cement matrix, stress concentrations around the crack tips are reduced. Like capillary pores, rubber particles have higher capacity of energy absorption that tends to act as crack arrestor. Turatsinze *et al*. (2003) further argued that it is this effect that leads to the delayed cracks under restrained conditions (ring test).

Most researchers use a standard method for determining the age at cracking and the induced tensile stress of concrete mortar mixes under restrained shrinkage (ASTM standard C 1581-04) to evaluate cracking performance of concrete mortars. The specimen preparation and test method are discussed in detail in Section 3.2.1.

2.5.4.7. Influence on fresh concrete mortar properties

Workability

As defined by ACI Committee 116R00, workability is the ease to mix, place, consolidate and finish a freshly mixed cement based material to a homogenous condition. Generally, the fresh rubberized concrete mortar mixes are said to show no difficulties in terms of casting, placement and finishing if an allowable amount of rubber particles is used (Toutanji, 1996). If more than allowable amount of rubber particles is used to replace the natural aggregates, the rubberized concrete mortar becomes difficult to hand-compact because of the rubber particles generating the spring action (Khatib & Bayomy, 1999).

Khatib & Bayomy (1999) further explained that even mechanical compaction performs poorly on rubberized mortar mixes because of the low density of rubber particles which force them to float during compaction. These observations often resemble poor consistency of cement based materials and are usually accompanied by bleeding and segregation (Nguyen *et al.*, 2011). Turatsinze *et al*. (2005) also observed the prominent bleeding and segregation when the rubber particles were added to concrete mortars, but claimed that addition of admixtures could stabilize the rubberized mortar mixes and improve their workability.

2.6. Durability Indexes of rubberized cement based materials

Durability of rubberized mortar and concrete was studied by Topcu and Demir, (2007). It was found by Topcu and Demir, (2007) that in despite of strength reduction, rubberized concrete and concrete mortars have higher freeze-thaw resistance compared to their respective control mixes. Savas *et al*. (1996) also conducted freeze-thaw durability tests of rubberized concrete in accordance with the ASTM C666. The results from the study conducted by Savas *et al*. (1996) showed that the freeze-thaw durability decreased with increasing content of rubber particles.

Zhang *et al*. (2006) investigated rubberized concrete exposed to wet-dry cycles under water and composite salt solution. An increase of chloride ion concentration was found to be higher in the rubberized concrete than in the control concrete. It was also found that the concentration of chloride ions increased with increasing the rubber particle content. Zhang *et al*. (2006) recommended that the rubberized concrete should not be used in applications exposed to prolonged wet-dry cycling, hot and dry weather where chloride and sulphate attack may occur.

Raghavan *et al*. (1998) studied the influence of shredded rubber particles on the durability of concrete composites in highly alkaline environments. The results from the study showed that there was a very small effect of alkaline medium on rubberized concrete. This was an indication of stability of rubberized concrete under a highly alkaline environment and hence the enhanced durability. Freeze-thaw testing results also indicated that rubberized concrete performs poorly under freeze-thaw.

In the current research study, the potential durability of rubberized concrete mortars was assessed using the Durability Index Testing Manual (2010). Oxygen permeability index (OPI), water sorptivity index (WSI) and porosity characteristics were determined. The background and detailed procedures used in this test method are discussed in section 3.3.7.

2.7. Chapter Summary

In this chapter an overview of usage of the bonded concrete overlays and the various factors that affect their performance was given. The review of usage of recycled tyre rubber particles in bonded concrete overlays was also presented. This section was concerned with a general review on rubber particles, and on details of how their incorporation in concrete overlays influences the material properties that influence shrinkage cracking.

It was found that incorporation of recycled tyre rubber particles has potential to improve the cracking resistance of concrete overlays. Although rubberized concrete overlays were characterized by reduced strength, they exhibit high toughness, low elastic modulus and higher tensile relaxation. By comparing and contrasting the results of studies reviewed in the literature, it is clear that the positive influences could outweigh the negative impacts of rubber particles in concrete mortars to improve their cracking performance. The next chapter discusses the methods used to evaluate the material properties affecting overlay performance.

CHAPTER THREE

EXPERIMENTAL METHODOLOGY

3.1. Experimental approach

This section describes an overview of the experimental approach taken to achieve the principal aim of investigating how content and grading of recycled tyre rubber particles affect material properties that influence crack resistance of concrete mortars. A systematic procedural outline of mix designs batching, main test properties and performance assessment of the mixes is given in Figure 1-2 in Section 1.5. Experimental work for this research was divided into 3 phases, trial mixing phase, initial experimental phase and main experimental phase.

3.1.1. Trial mixing phase

Incorporation of recycled tyre rubber particles in concrete mortars is a new innovation in the concrete construction industry so there are still no standard procedures that propose how to mix, cast and test rubberized cement based materials. It was therefore important to perform trial mixing of control mixes and that ensure that they were still workable when commonly used rubber particle contents were partially incorporated. This phase was aimed at establishing suitable water content suitable to produce desired slump while still maintaining target strength.

Trial mix designs were performed to establish 2 control concrete mortars of 0.45 w/b and 0.6 w/b ratios. Both trial control mixes were designed to achieve an average slump of 80 +/- 10 mm. This slump range was chosen based on literature survey of common concrete mortars used in concrete mortars. The water demand for fine aggregates (Klipheuwel sand) that was used was established to be 270 kg/m^3. The target strength for the 0.45 w/b ratio control mix was set to be 35 MPa at the age of 28 days of water curing while the target strength for 0.6 w/b ratio control mix was set to be 25 MPa at the age of 28 days of water curing. These properties were chosen because they represent common properties of cement based repair mortars in basic construction applications.

3.1.2. Initial experimental phase

This phase of experimentation was aimed at establishing the optimum recycled tyre rubber particle content and gradation. Initial material properties that were tested were restrained shrinkage (ring test), splitting tensile strength and compressive strength. The procedures used to conduct these properties are discussed in Section 3.2. Control mixes that were developed in the trial mixing phase were used in this phase as reference concrete mortars. These control concrete mortars were used to assess the effects of rubber particles incorporation on material properties that influence the cracking of concrete mortar. Table 3-1 below shows the mix proportions of the control mixes used.

Table 3-1: Mix proportions of initial control concrete mortars

Constituent	0.45 w:b control mix	0.60 w:b control mix
Cement (kg/m^3)	600	450
Water(kg/m^3)	270	270
Klipheuwel sand (kg/m^3)	1485	1600
Super-plasticizer (kg/m^3)	4.5	2.0
Desirable slump (mm)	80 ± 10	80 ± 10

A total of 18 rubberized repair mortars were then developed from both control mixes by partially replacing fine natural aggregates volumetrically with recycled tyre rubber particles of different gradations. Three different recycled tyre rubber particle gradations were used to partially replace fine natural aggregates from each control concrete mortar. Three different volumetric percentage contents of 3 different gradations were used to partially replace natural fine aggregates from each concrete mortar. The letter “R” on mix identification denotes content and “G” denotes gradation of rubber particles incorporated in the respective mix. For instance, the mix ID: 0.60:R20G3 resembles a 0.60 w/b ratio mix incorporating 20% rubber particles of gradation 3. The details on recycled tyre rubber particle content and gradation variation are discussed in Section 3.1.2.1 below.

3.1.2.1. Varying mix design parameters

Two w/b ratios were used to produce two laboratory made control mixes from which fine natural aggregates were partially replaced by rubber particles to produce rubberized concrete mortars. Recycled tyre rubber particles were the key material variable in this research experiment. Three various rubber particle contents of 3 different gradations were used to produce rubberized concrete mortar mixes. A total of 18 rubberized concrete mortar mixes and 2 control concrete mortar mixes were developed for the initial experimental phase.

Rubber particle content

An optimum percentage content of rubber particles that can be incorporated in concrete mortars has not been substantiated by researchers yet. Only the minimum and maximum contents have been commented on by previous researchers who dealt with rubberized concrete and rubberized concrete mortars. Most authors including Ho *et al*. (2012); Nehdi & Khan (2001); Nguyen *et al*. (2012); Turatsinze *et al*. (2006) and Turatsinze *et al*. (2007) speculated that concrete mortars become unworkable when the fine natural aggregate replacement by rubber particles exceeds 30%.

Turatsinze *et al*. (2005) suggested that to produce a concrete mortar with acceptable strength, the maximum content of rubber particles that could be used as partial replacement of natural aggregates should be limited to 30%. It was also observed by Ganjian (2009) that compressive and tensile strengths were detrimentally decreased by more than 40% while elastic modulus was reduced by about 17% when rubber particles incorporation was 25%. In the same research it was observed that compressive and tensile strengths were reduced by only 5% the minimum rubber particle content of 5% by volume was incorporated in the concrete mix, but unfortunately there were no noticeable improvements observed in elastic modulus and shrinkage strains.

It was therefore decided that tyre rubber particle content of 5%, 10%, and 20% by total volume of fine natural aggregates be used to partially replace fine natural aggregates. The upper volumetric content limit of 20% incorporation was chosen to avoid detrimental loss of tensile strength and poor workability of rubberized concrete mortars.

Rubber particle gradation

Three rubber particle gradations of particle sizes 0.42-0.84 mm, 1.00-2.50 mm and 0.42-2.50 mm were prepared and used as partial replacement of fine natural aggregates with the 3 contents discussed above. These gradations were readily available and were the most suitable rubber particles for use in this research. All the rubber particle samples used in this research were produced and provided by SA Tyre Recyclers (Pty) Ltd. These particle sizes were also used in this research because they represent the range of particle sizes for most of the common fine natural aggregates use in concrete mortars.

Particle gradation of all these 3 rubber particle sizes was performed using sieve analysis method in accordance to SANS 3001 – GR2: 2011 (South African National Standards, 2011). Gradations

achieved by sieving rubber particles of sizes 0.42-0.84 mm, 1.00-2.50 mm and 0.42-2.50 mm were designated gradation 1 (G1), gradation 2 (G2) and gradation 3 (G3), respectively. Their respective grading curves are shown in Figure 3-1 where they are compared to the grading curve of the fine natural aggregates (Klipheuwel sand) that they are used to replace. The rubber particle samples of gradation 1 (G1) & gradation 2 (G2) were found to be poorly graded while rubber particle sample of gradation 3 (G3) was found to be continuously graded. Gradation 3 (G3) rubber particle sample was produced by mixing G1 and G2 samples in the proportion of 40:60 to produce a grading curve similar to the one of replaced Klipheuwel sand. It was also found essential to use well graded rubber particles with continuous particle distribution in this research because well graded particles are usually known to produce better packing and compaction of fresh concrete mortars. It can be seen from Figure 3-3 that G3 was the most suitable gradation. The sieve analysis was carried out using sieves with openings that range from 4.75 mm to 0.075 mm, clamped on a mechanical shaker, illustrated in Figure 3-1.

Figure 3-1: Apparatus for mechanical sieve analysis.

Water/ binder ratio

Two water/ binder (w/b) ratios of 0.45 and 0.60 were used as the best presentation of the range of commonly used w/b ratios for concrete mortars. This variation of w/b ratios was also essential to identify the w/b ratio that can work better for rubberized concrete mortars. As it is well known that shrinkage cracking of concrete mortars is also related to the w/b ratio used, this parameter had to be studied. Various mixes of rubberized concrete mortars were prepared using these 2 w/b ratios. These mixes were tested in an initial experimental phase. The w/b ratio that produced mixes with better material properties performance was adopted and used with optimum rubber particle content and best gradation to develop concrete mortar mixes that were tested in the main experimental phase.

A total of 20 mixes were prepared in this experimentation phase by varying recycled tyre rubber particle contents and gradations. Restrained shrinkage was assessed on all 20 mixes using the ring test method. Compressive strength and splitting tensile strength loss due to incorporation of recycled tyre rubber particles were also assessed with respect to content and gradation of rubber particles incorporated. The aim of this phase was to study the influence and trends caused by incorporation of different contents and gradations of recycled tyre rubber particles in 0.45 w/b and 0.60 w/b ratio control mixes. Furthermore, this phase was aimed at establishing the best performing (optimum) rubber particle content and best performing (optimum) gradation that produced rubberized concrete mortar with enhanced properties for cracking resistance. The procedures followed for tests conducted in this phase are discussed in Section 3.2.

3.1.2.2. Fixed mix design parameters

Slump, water content, binder type, aggregate type, curing method and curing regime were considered to be fixed parameters in this research. These parameters were fixed to ensure that they do not cause any variation in mixes when studying the influence of rubber particles incorporation. Several trial mixes were performed as in trial mixing phase to determine the suitable slump and water content parameters for both 0.45 w/b and 0.60 w/b ratio mixes.

Slump

Workability for all fresh concrete mortars was assessed using the slump test in accordance to SANS 5862-1:2006. Slump test was performed to determine consistency and cohesiveness of all fresh concrete and rubberized mortar mixes as the measure of workability. A consistent slump of 80 ± 10

mm was maintained for all the mixes in initial and main experimental phase. This slump range of 80 ± 10 mm was chosen based on literature survey of common concrete mortars used as concrete overlays. It was therefore considered to be an ideal slump for concrete mortars required for horizontal placement and it was chosen because mixes inheriting this slump range are generally easy to compact even in small moulds. The target slump was achieved by addition of suitable content of Chrysopremia 310 super-plasticizer when the slump lower than target slump value was achieved. Figure 3-2 illustrates slump testing of fresh concrete mortar.

Figure 3-2: Illustration of slump test of fresh concrete mortar.

Water content

The water content of 270 l/m^3 was kept constant for all the mixes established for initial and main experimental phase testing. This water content was the suitable water demand determined from trial mixing phase conducted prior to the initial experimental phase. It was chosen on the bases of achieving the prescribed slump value and also on the basis of fine natural aggregates water demand.

It was decided that the same water content be maintained as a fixed parameter for both mixes with 0.45 w/b & 0.60 w/b ratios. This was done to ensure that shrinkage cracking trends observed in these mixes were not due to different water contents used in mixes but mainly due to incorporation of rubber particles.

Binder type

The only type of binder used in this research was CEM III/A 42.5N; commercially brand named PPC Sure-Build cement. Sure-Build cement was chosen because it is generally used for construction purposes including internal plastering, external plastering, mixing brick mortars, concrete footings, concrete walls and concrete floors. All the cement used was sourced from PPC De-Hoek production factory located in the Western Cape, South Africa. The same source was preferred to ensure that the same cement chemical properties were maintained for the sake of attaining similar hydration trends from all the mixes. This was essential because shrinkage cracking is highly and directly influenced by setting time, strength and hydration rate of cement type used. Table 3-2 below presents typical properties of Sure-Build cement as presented by PPC cement manual.

Table 3-2: Typical physical properties of CEM III/ 42.5N from PPC (PPC, 2014).

Properties	PPC requirements	SANS 50197-1 requirements
Setting times:		
Initial: minutes	165	60 minimum
Main: hours	3,5	No requirement
Compressive strength (mortar prism EN 196-1):		
At 2 days (MPa)	20	>10,0
At 28 days (MPa)	±48	>42,5 <62,5
Densities:		
Relative density	3,05	No requirement
Bulk density, aerated, kg/m^3	1100-1300	No requirement
Bulk density, as packed, kg/m^3	1500	No requirement

Aggregate type

Klipheuwel sand was the only fine natural aggregate used in all laboratory made concrete mortar mixes in this research. The other aggregates used were recycled tyre rubber particles that were incorporated to partially replace Klipheuwel sand as discussed in Section 3.1.2.1. All the sample of Klipheuwel sand used was mined from Cape Town west coast, Malmesbury siliceous pits. Prior to used, Klipheuwel sand properties were assessed. It was found to have rounded shape particles that were generally well graded. These physical properties make Klipheuwel sand exhibit a low water demand which is a suitable characteristic for concrete mortar mixes designed for applications where less shrinkage and better workability are desired. As discussed by Grieve, (2009), the percentage

fines for this type of sand is typically found to be very high (up to 20% minus-150-µm and 15% minus-75-µm) and it does not appear to cause high shrinkage.

However, it was still important to test and affirm the physical properties of Klipheuwel sand sample used because the suppliers claimed that properties of this sand change over time. The sand particle grading was performed in accordance to SANS 3001 – GR2: 2011 sieve analysis standard (South African National Standards, 2011). Figure 3-3 shows the average grading curve of Klipheuwel sand samples analysed from three different samples. The figure also includes grading curves of 3 different rubber particle gradations used to partially replace Klipheuwel sand. These curves were included to enable comparison of gradation of Klipheuwel sand and rubber particle used to partially replace it.

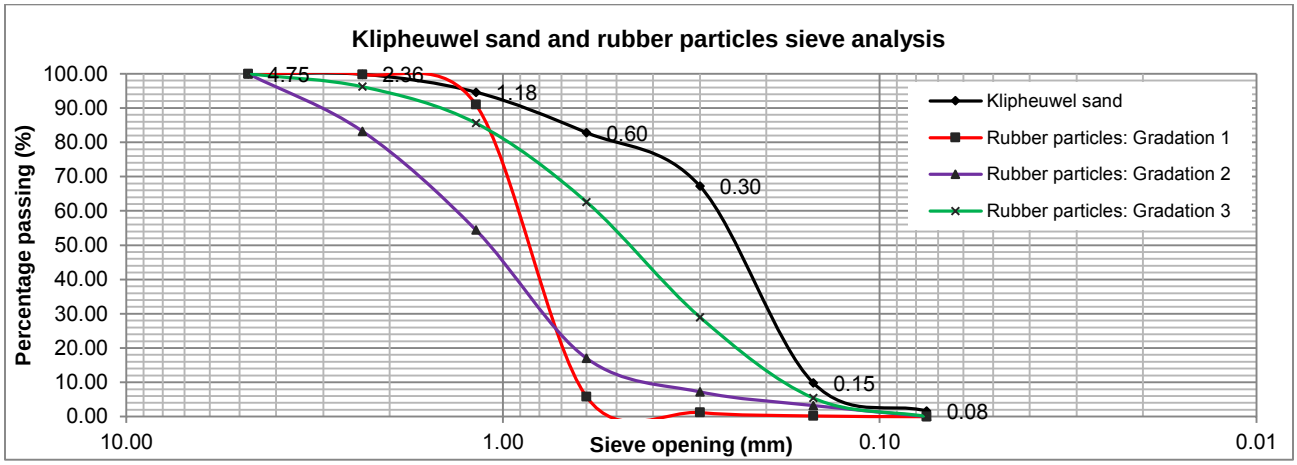

Figure 3-3 : Grading curves of 3 rubber particle gradations and Klipheuwel sand.

Klipheuwel sand was dried in the oven at the temperature of 50°C for a minimum period of 48 hours before use. That was done to ensure that the sand was completely dry and had no additional moisture that could affect w/b ratios of the concrete mortars. Moisture content of all samples of sand used was determined throughout the research experimentation to ensure consistency of sand properties. Average moisture content and relative density of Klipheuwel sand were determined to be 1.9 and 2.5, respectively.

Curing Duration

The duration of curing was considered a fixed parameter. Beside cube specimens, all the specimens that were used for testing strength and durability were cured for the period of 3 days with the curing method discussed below. Cubes were cured for the period of their testing age, 3, 7, 14 and 28 days.

Durability indexes tests were conducted on cores extracted from cubes cured for the period of their testing age, 28 days.

Curing method

The curing method considered for initial and main experimental test specimens was the wet hessian blanket curing. This curing method was considered because of its ease to implement on both inclined and horizontally applied concrete mortar overlays. The hessian blanket pieces were saturated in tap water and used to wrap specimens tightly. Thin transparent plastic sheet known as cling wrap was used to wrap and hold hessian pieces tight around specimens. This was also used as the measure to minimize the rate of moisture loss during the curing period. Cling wrap plastic sheets were preferred over the widely used black polyethylene sheet because they were easier to wrap around ring specimens, dog bone shaped specimens, cylindrical specimens and prismatic specimens. To ensure the proper sealing against moisture loss, two layers of cling rap plastic sheet were applied on each specimen and the edges were sealed with silo tape. This method was implemented immediately after the specimens were demoulding at the age of 24 hours after casting.

All the specimens; ring, prismatic, cylindrical and dog bone shaped were cured using wet hessian blanket curing method as shown in Figure 3-4. Only cube specimens prepared for compressive test and durability indexes test were cured differently using the water curing method. All the cube specimens were cured in a water tank from the time of demoulding until the desired age of testing.

Figure 3-4: Illustration of wet curing using hessian blanket and clip wrap sheets.

Ring specimens were cured for 3 days, after which plastic sheets and hessian blanket pieces were removed to expose them to open laboratory environmental conditions. The exposure of specimens' surfaces to open laboratory environmental conditions was necessary to simulate onsite environmental conditions for concrete mortar after placement. Generally, onsite applied concrete overlays have their top (outer) surface exposed to environmental conditions since their bottom (inner) and perimetral surfaces are bonded against concrete substrate. These exposure conditions were simulated on ring specimens by having their inner surfaces in contact with the inner steel ring. The top surfaces of the ring specimens were coated with paraffin wax immediately after removing plastic sheets and hessian blanket pieces to ensure that their top (perimetral) surfaces were also not exposed. This was also done as a precaution to limit moisture loss to the circumferential surface only. Generally, it is assumed that drying shrinkage along the height of the ring specimens is uniform if its height is at least four times the thickness (See *et al*., 2003).

Curing conditions

Laboratory environmental conditions (temperature and humidity) were important factors that need to be monitored as they directly influence rate of moisture loss from concrete mortars. Humidity has considerable influence on the measure of shrinkage of concrete mortars, particularly drying shrinkage. Drying shrinkage increases with decreasing relative humidity (Alexander, 2001). Higher temperatures are also known to cause higher degrees of relaxation in cement based materials. In this research it was important that these conditions were controlled to avoid their impact on the observation of effects of rubber particles incorporation on properties that affect shrinkage cracking of concrete mortars. Additional precaution was taken when testing tensile relaxation dog bone shaped specimens. Tensile relaxation was carried out for the duration of 24 hours so tensile relaxation dog bone shaped specimens were coated with paraffin wax to prevent moisture loss during the testing period, discussed in detailed in Section 3.3.4.

The temperature and relative humidity (RH) for the laboratory were not controlled. Therefore the HygroLog HL20 temperature and RH data logger was placed in the region where specimens were exposed to laboratory environmental condition to monitor temperature and RH daily. A sample of temperature data is shown in Appendix A. There was however no controlling measures available in the laboratory for RH. It was therefore accepted that laboratory temperature and relative humidity will be influenced by the outside environment conditions. An average daily RH of 60.1% and temperature of 18.8 ^{0}C were recorded during the duration of experimentation. It was observed that the daily

conditions stayed almost the same throughout the duration of experimentation (see raw data in Appendix A. Figure 3-5 shows the data logger used to record the temperature and RH readings daily in the laboratory.

Figure 3-5: A data logger used to record temperature and RH readings in the laboratory

3.1.3. Main experimental phase

This experimental phase was aimed at investigating the influence of incorporation of rubber particles on material properties that influence cracking resistance of concrete mortars. The optimum rubber particle content and gradation established in the initial experimental phase were used in this phase.

3.1.3.1. Identification of main experimental phase mixes

An optimum gradation of rubber particles was determined based on observations and analysis of the test results from the initial experimental phase. The age of cracking, crack area and crack growth from the ring test were the main properties used to assess the cracking resistance performance of rubberized concrete mortars tested in the initial experimental phase. Compressive strength and splitting tensile strength were also analysed with respect to content and gradations of rubber particles incorporated to determine optimum rubber particle content and gradation.

Based on results achieved from the initial testing phase, the rubber particle gradation that performed best in cracking resistance in all rubberized concrete mortars was determined as gradation 3. It was observed that cracking resistance of concrete mortar mixes increased with increasing rubber particle content. The best performing content of rubber particles was found to be 20% by volume

replacement. The optimum rubber particles incorporation was therefore determined to be 20% content of gradation 3 in this research. This optimum rubber particle sample was adopted and used in main experimental phase. An optimum rubberized concrete mortar from initial experimental phase was therefore considered to be the 0.60 w/b ratio incorporating an established optimum rubber particle sample (0.60:R20G3).

For the purpose of assessing the influence of this established rubber particle sample clearly, it was decided that two more different mortars be developed to also enable assessment of incorporating optimum rubber samples in various mortars. The other laboratory made concrete mortar of a higher w/b ratio (0.80) was chosen as another ideal mortar mix to be used in this exercise. It was also considered necessary to assess performance of this optimum rubber particle sample in cracking resistance of at least one commercial repair mortars (CRMs). One commercially available polymer modified mortar (CRM) was identified to be another suitable mortar mix for this exercise too. Both the CRM and the 0.80 w/b ratio mortar mixes were chosen based on their good cracking resistance performance as tested by Bester, (2014) in his study of influence of different curing methods on cracking resistance of concrete mortars.

3.1.3.2. Preparation of main experimental phase mixes

The two laboratory-made mixes, 0.6 and 0.8 w/b ratio mixes were prepared and set as control mixes for the main experimental phase. The optimum recycled tyre rubber particle gradation and content that was adopted from the section above was incorporated in both control mixes to produce two rubberized laboratory-made concrete mortars. A total of four laboratory-made mixes were prepared in this phase. Table 3-3 below presents the mix proportions of two main laboratory-made mixes.

Table 3-3: Mix proportions of main experimental phase control mortar mixes.

Constituent	0.60 w:b control mix	0.80 w:b control mix
Cement (kg/m^3)	450	356
Water (kg/m^3)	270	285
Klipheuwel sand (kg/m^3)	1600	1555
Super-plasticizer (kg/m^3)	2.0	none
Desirable slump (mm)	80 ± 10	80 ± 10

As discussed in the section above, the commercially available repair mortar that was selected as the suitable mortar to use in this phase was the CRM. This mortar was also selected because it is commonly used for overhead, horizontal and vertical concrete patch repairs and overlays applications. It is a high performance cementitious polymer modified repair mortar that could be used in concrete repairs of thicknesses ranging from 5 mm to 70 mm. This repair mortar inherits good resistance to freeze/thaw, water and chloride penetration. It is also described to have excellent workability characteristics, excellent thixotropic behavior, it is wet sprayable and has compressive strength ranging from 35-40 MPa (CRM product data sheet, 2012).

The CRM was prepared according to the manufacturer's instructions specified in the CRM product data sheet (2012). This mix was also set to be a control mix. The optimum recycled tyre rubber particle gradation and content that was adopted from the initial phase was then incorporated in this control mix to produce the rubberised commercial mortar. Rubber particles were used as partial volumetric replacement of the CRM powder. Table 3-4 presents characteristics of the CRM mix.

Table 3-4: Mix proportions of control CRM mix.

Constituent	CRM
CRM powder (kg/m^3)	1670
Water (kg/m^3)	250
Super-plasticizer (kg/m^3)	None

A total of 3 control mortar mixes and 3 rubberised mortar mixes were prepared in this experimentation phase. Material properties that influence shrinkage cracking resistance of concrete mortars were tested on all these 6 mixes. The aim was to study the influence and trends on cracking resistance performance due to incorporation of optimum recycled tyre rubber particle gradation and content in all the 3 control mixes. The test procedures followed for testing these material properties are discussed in the section below.

3.2. Initial experimental testing

The properties tested at this experimental phase were restrained shrinkage test (ring test), tensile splitting strength and compressive strength. This section discusses the preparation, sampling and testing of these test properties. The other material properties associating to restrained shrinkage cracking were tested in the main experimental phase.

3.2.1. Testing for restrained shrinkage

The ring test is the common experimental test method used to evaluate cracking resistance of concrete mortars in restrained shrinkage conditions. A ring apparatus similar to one used in American Society for Testing and Materials (ASTM C1581-09a, 2009) standard test method (but with a slight difference in dimensions) was used in this research. The mould was assembled with the outer stainless steel sheet ring of thickness 3 mm and the inner steel ring of thickness 12.7 mm. Both rings were placed concentrically on a ply wood base. Detailed dimensions of the ring mould are shown in Figure 3-6 (i).

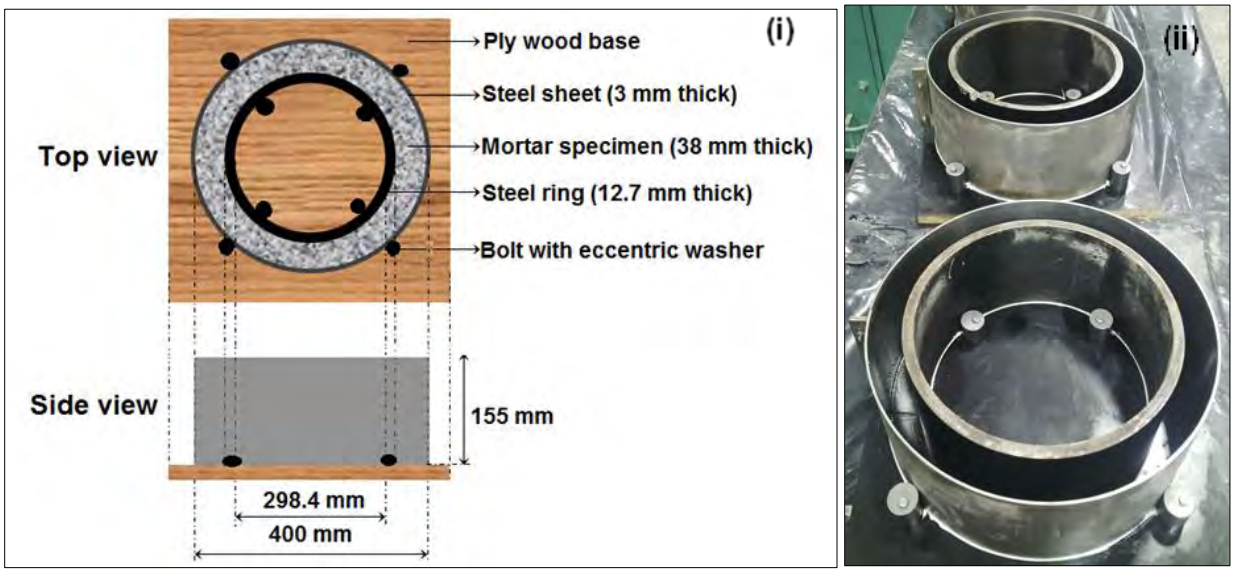

Figure 3-6: Dimensions and preparation of ring specimen mould.

The ring specimens for all 6 mixes were prepared in accordance to ASTM C1581-09a (2009) but a different curing method was used. Prior to casting mortars specimens, the outer surface of the steel sheet and inner surface of the steel ring were coated with oil to make demoulding easy. The bottom edges of both steel rings were sealed with silicon sealant 24 hours before casting, see Figure 3-6 (ii) above. This was done to minimize water loss from the mortar mixes during compaction. A total of 3 rings were cast per mortar mix, the outer steel ring sheets were then demoulded after 24 hours of casting. It is known that when internal stresses that develop within the ring specimens due to the shrinkage restraint provided by the inner steel rings exceed the tensile strength of repair mortar, cracks start to initiate on rings specimens (See *et al*, 2003). The inner steel rings were therefore left to provide the shrinkage restraint on the mortar ring specimens. The top surfaces of the ring

specimens were sealed with paraffin wax to allow drying to occur only from the outer circumferential surface during crack inspection period.

Cracking resistance of concrete mortar ring specimens was evaluated on the bases of time of the 1st crack occurrence and crack area growth. In this research 3 ring specimens prepared from each mix were inspected twice a day, morning and evening, for occurrence of the 1st crack. An average number of days that the 3 specimens took for a crack to initiate was recorded as the age of cracking for a respective mortar mix. Since crack occurrence inspection was conducted twice a day, morning and evening, age of crack was recorded to the nearest half a day. The ring specimens were further inspected for total crack area which was calculated as the sum of product of all average crack widths and crack lengths measured from 3 ring specimens for each mortar mix. An average crack width was determined from 3 width readings measured from different points along each crack path using a 0.02 mm accurate hand microscope. Figure 3-7 (i) shows approximated width measuring points along a crack path on one of the ring specimens. The red marks shown on the figure indicate directions in which the microscope scale was orientated along the crack path to ensure proper crack width estimation. The hand microscope used to measure crack widths in this research is shown on Figure 3-7 (ii).

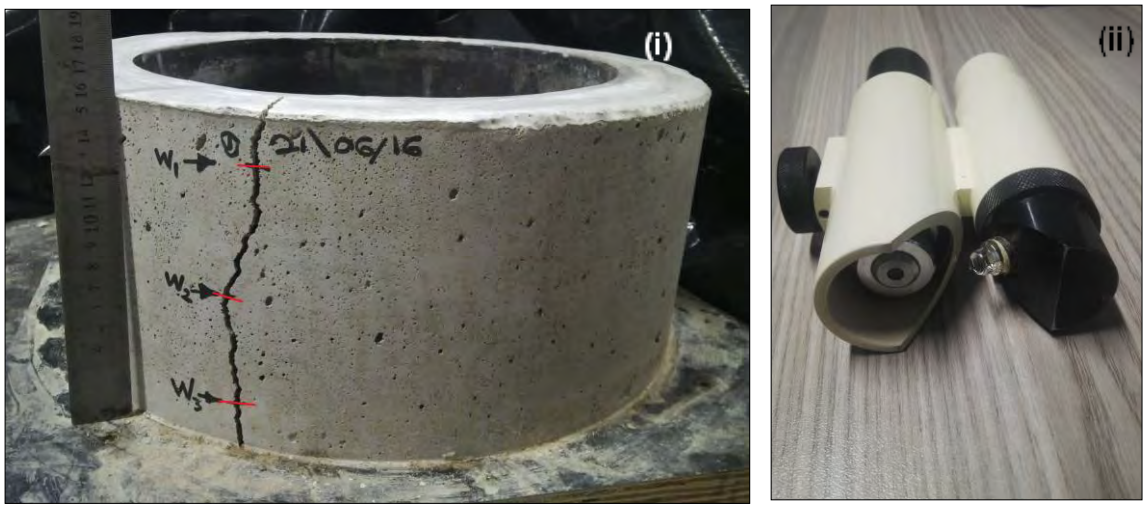

Figure 3-7: A ring specimen showing crack width measuring points and a hand microscope.

The crack lengths were approximated by measuring the length of a wetted woolen thread stuck along each crack path; see Figure 3-8. The total crack area of a mortar mix at each test age was recorded as the sum of crack areas measured from all 3 ring specimens. Furthermore, crack area growth was

inspected and determined by measuring the total area of each mix at ages of 3, 7 and 14 days after initiation of the 1st crack.

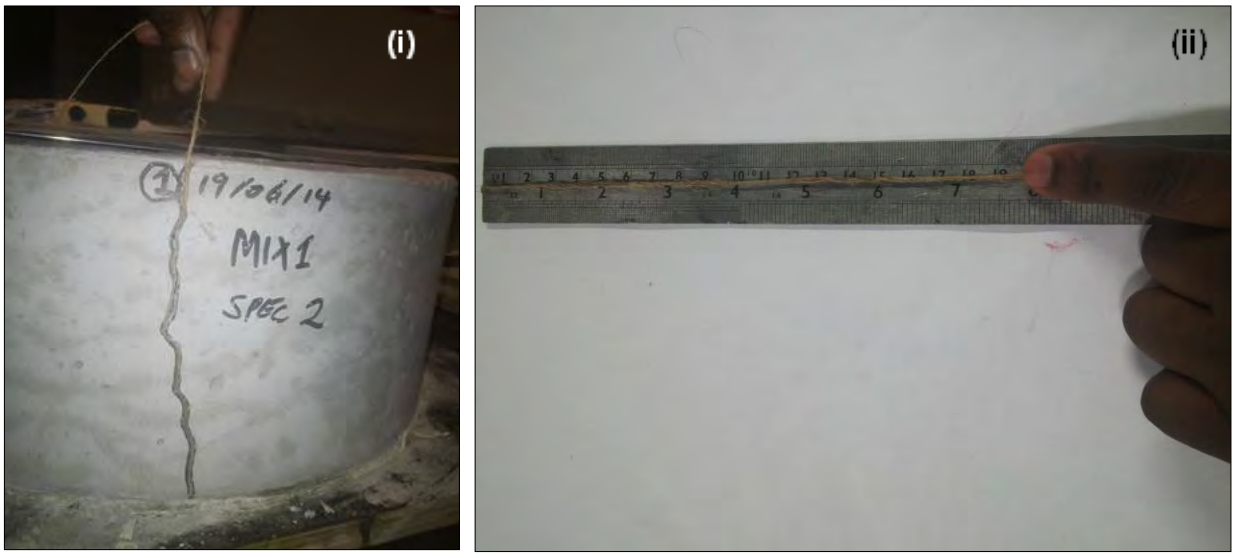

Figure 3-8: Illustration of the crack length measurement using a woolen thread.

3.2.2. Testing for splitting tensile strength

Splitting tensile strength tests were performed on all mortar mixes using cube specimens with standard dimensions of 100 x 100 x 100 mm^3, shown in Figure 3-9. The results were used to assess strength development of rubberized concrete mortar mixes compared to their respective control mixes. This was necessary to study the strength loss trends caused by incorporating recycled tyre rubber particles of various gradations and contents.

Three cube specimens per mortar mix were tested at each test age in accordance to South African National Standards (SANS 6253:2006) specifications using the Amsler compression machine. The test was performed with a cube specimen centrally placed on Amsler compression machine test plate with two halved steel rod pieces carefully positioned along the faces of the as-cast specimen to cause the fracture plane crossing at right angle to the trowelled surface. The cube specimens were tested at the ages of 3, 7 and 14 days after being cured in water tanks set at the temperature of 23 ^{0}C. Figure 3-9 (i) and (ii) show a cube specimen set up for splitting tensile strength test.

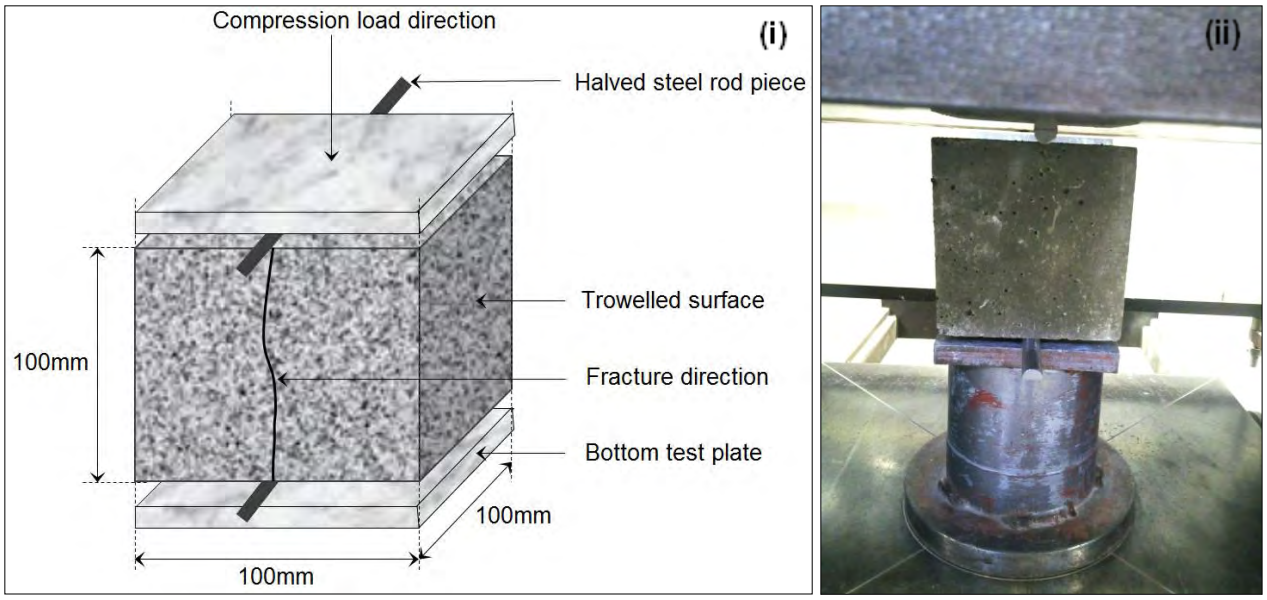

Figure 3-9: A cube specimen under splitting tensile strength test.

3.2.3. Testing for compressive strength

Compressive strength testing was performed on mortar mixes using cube with the standard dimensions of 100 x 100 x 100 mm^3. The results were used to assess compressive strength development of rubberized concrete mortar mixes compared to their respective control mixes.

Three specimens per concrete mortar mix were tested in accordance to South African National Standards (SANS 5863:2006) specifications using the Amsler compression machine. The cube specimens were tested at the ages of 3, 7 and 14 days after being cured in water tanks set at the temperature of 23 ^0C.

3.3. Main experimental testing

Material properties that influence cracking resistance of concrete mortars were tested in this experimental phase. These properties were free shrinkage, tensile strength, tensile relaxation and elastic modulus. The restrained shrinkage test (ring test) was also performed to assess cracking age, crack area and crack growth of all prepared main mortar mixes. The testing was performed on rubberized mortar specimens and also on their respective control mortar specimens to assess the influence caused by incorporation of the optimum rubber particle content and grading.

It was acknowledged that the cracking of any cement based material is mainly caused by differential shrinkage. Some of the important factors that influence differential shrinkage of laboratory made mortar specimens are their exposed surface area and mass volume. The surface area/ volume ratio was therefore kept similar for all the specimens used to test free shrinkage, tensile strength, tensile relaxation and elastic modulus. It was essential that the dimensions of specimens used to test these material properties conformed to a relatively similar surface area/ volume ratio since drying shrinkage depends also on this ratio. This was important in this research to ensure that the influence of incorporating optimum rubber particle sample was observed without confounding it to the influence of differential shrinkage due to different exposed surface area/ volume ratios.

3.3.1. Testing for restrained shrinkage

Restrained shrinkage testing (ring testing) was conducted again in this experimental testing phase using specimen and test procedures same as the ones discussed in Section 3.2.1.

3.3.2. Testing for free shrinkage

Free shrinkage strains were measured using prismatic specimens with dimensions of 300 x 50 x 50 mm^3 (Figure 3-10 (ii)). The free shrinkage results from three rubberized mortar mixes were compared to free shrinkage results of their respective control mixes in order to analyze how rubber particles incorporation influences mortar mixes' cracking.

Two pairs of demec targets were attached on 2 long sides of specimens after demoulding. Each pair of demec targets were attached with a spacing gauge length of 100 mm. Figure 3-10 (i) shows the hand strain gauge that was used to measure shrinkage strains daily.

Specimens were cured using hessian blankets and cling wrap plastic sheet and left covered under a black plastic sheet for 3 days. After the curing period, specimens were uncovered and exposed to laboratory conditions. This was done to simulate the common onsite preparation and curing conditions of mortar overlays.

Free shrinkage was determined as the sum of the average displacements from the 2 pairs of attached demec targets determined from 3 specimens. Initial readings were taken immediately after the specimens were uncovered and exposed to laboratory conditions. Free shrinkage was then

measured daily for the period of 28 days. The curing method and laboratory conditions under which the free shrinkage specimens were exposed were the same as the ones discussed in Section 3.1.2.1.

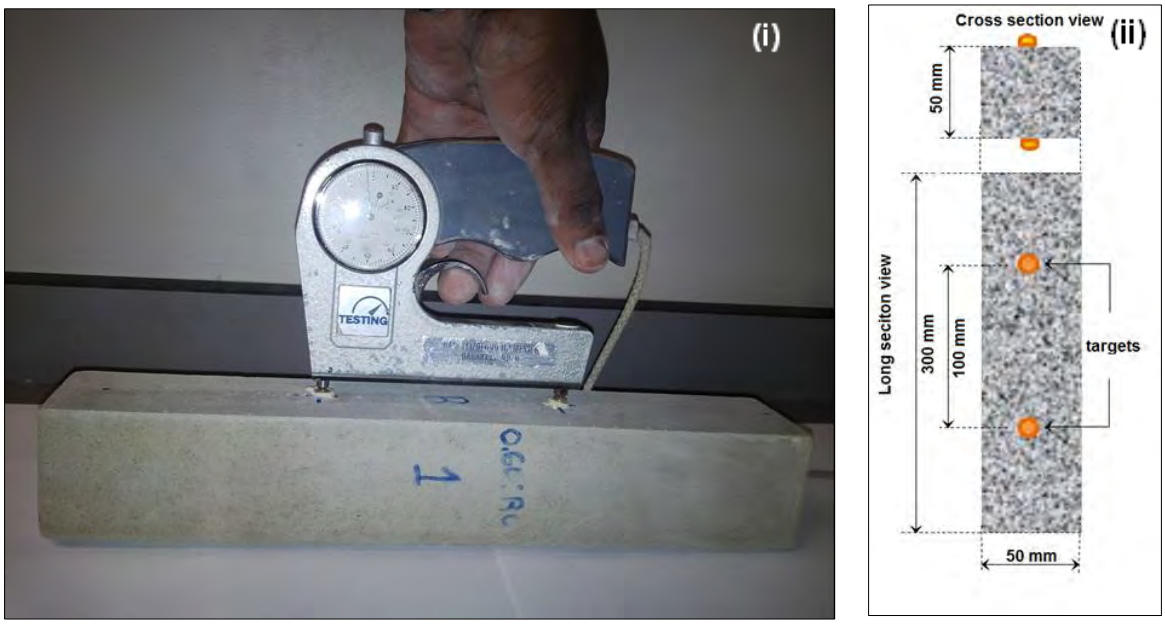

Figure 3-10: Dimensions of a prismatic specimen and an illustration of shrinkage strain measurement.

3.3.3. Testing for tensile strength

Tensile strength strains were measured using notched dog bone shaped specimens of dimension shown in Figure 3-11 (ii). Notched specimens were used for tensile strength to ensure that failure occurs along the prismatic section of the specimens and to avoid fracturing at the dove-tail section. A notch helps to initiate a fracture plane at the middle of the specimen's prismatic section, across the 40 mm x 30 mm cross sectional area.

Three specimens per mortar mix were tested. The tests were conducted by placing a specimen in ZwickRoell Z020 grips and applying a uniaxial tensile force at the rate of 0.2 mm/min until specimen failure. The test set up is shown in Figure 3-11 (i). The tensile load of a respective mortar mix was recorded as the average value of failure load from 3 specimens tested. The specimens were tested at ages of 3, 7, 14 and 28 days. Only about 10% of all notched specimens that were tested failed undesirably. Some developed continuous cracks on the dove-tail sections while others failed both on dove-tail sections and along the notch. Figure 3-12 (i) shows some undesirable tensile failure modes on notched dog bone shaped specimens while Figure 3-12 (ii) shows an expected typical tensile strength failure mode. The test results from specimens that did not fail along the notch were

disregarded. The ultimate tensile load was then recorded as the average value from the remaining 2 specimens. In the case where more than 2 specimens failed in an undesirable mode, new specimens were cast and retested.

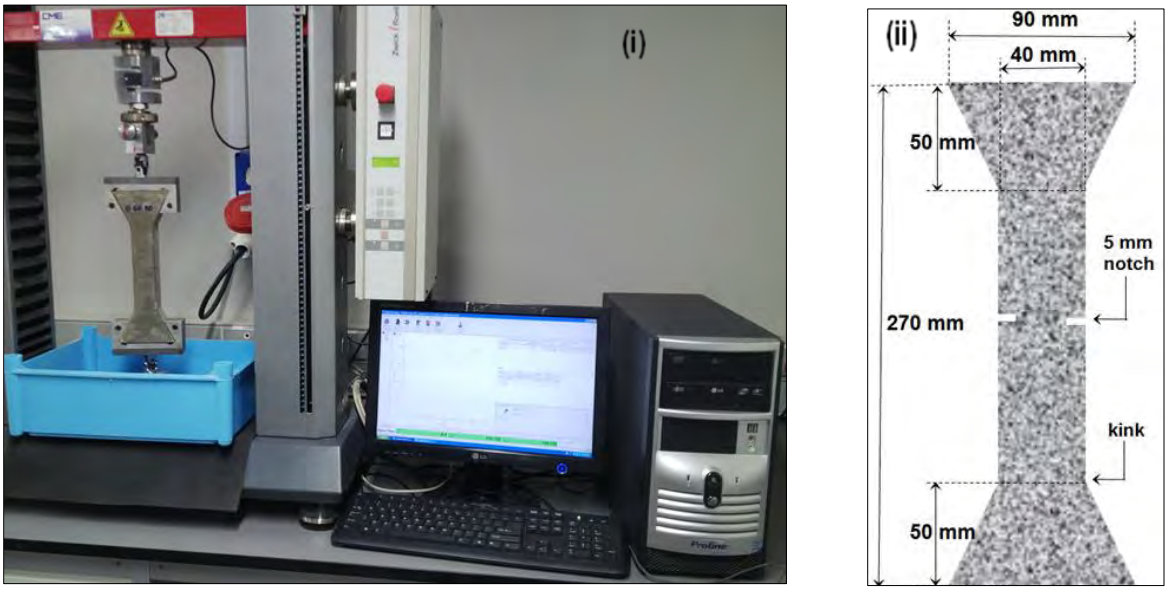

Figure 3-11: Dimensions of a notched dog bone shaped specimen and a ZwickRoell Z020 machine used testing tensile strength.

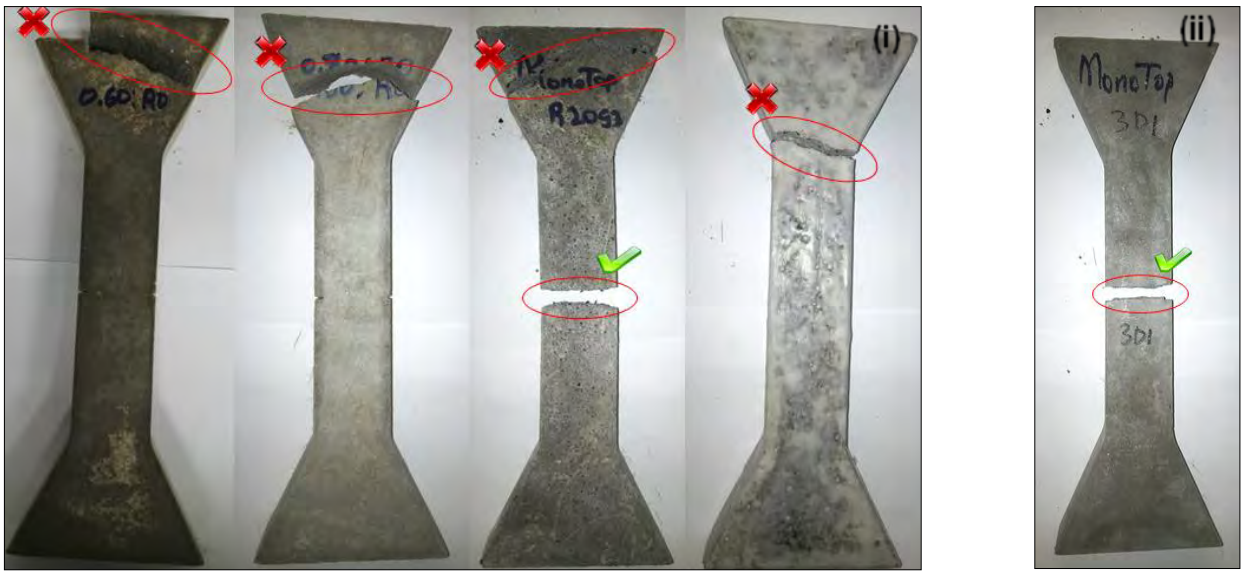

Figure 3-12: Failure modes on notched dog bone shaped specimens under tensile strength testing.

3.3.4. Testing for tensile relaxation

Tensile relaxation was tested using dog bone shaped specimens (without notches) with dimensions same as the dimensions of notched dog bone shaped specimens used for testing tensile strength. Two specimens per mortar mix were simultaneously tested in tension using ZwickRoell Z020 and ZwickRoell Z100 testing machines for the period of 24 hours.

All surfaces of tensile relaxation specimens were coated with paraffin wax to avoid the effects of drying shrinkage due to moisture loss during the testing period of 24 hours. The stress load equivalent to 80% of the respective mortar ultimate tensile strength was applied as the standard stress level for determining tensile relaxation. The loading of specimens was maintained at the rate used in tensile strength tests (0.2 mm/min). The resulting strain due to applied standard stress was then kept constant for the period of 24 hours. The tensile relaxation of the respective mortar mix was determined from the main stress value recorded on the computer after the stress decay had occurred during the testing period. The testing was conducted at ages of 3, 7 and 14 days for all mortar mixes.

The relaxation values at the 24^{th} hour (ultimate relaxation value) were used as input data in the analytical modeling of age of cracking. This was done to study the influence of rubber particles incorporation on cracking resistance of mortar mixes. The equations used and details about analytical modeling are discussed in section 4.4.

3.3.5. Testing for compressive strength

Compressive strength testing was conducted again in this experimental testing phase using specimen and test procedures same as the ones discussed in Section 3.2.3.

3.3.6. Testing for elastic modulus

Elastic modulus was tested using the cylindrical specimens with dimensions shown in Figure 3-13 (ii). Three specimens per mortar mix were tested in compression using a ZwickRoell Z100 testing machine as illustrated in Figure 3-13 (i). It was acknowledged that concrete overlays perform under tensile stresses in their application thus testing elastic modulus in tension was the most ideal test method, however it has been proven very difficult to test elastic modulus of cylindrical specimens in tension. It was therefore assumed that there is little variation between elastic modulus tested in compression and the one tested in tensile load.

The test surfaces of cylindrical specimens were ground flat to avoid possible eccentricity of loading forces when tested. Their longitudinal surfaces were cleaned and dried up to allow firm attachment of demec strain targets. Two pairs of demec strain targets were attached on two adjacent sides of each specimen at the 100 mm gauge length using X 60 fast adhesive. This was done to enable recording of 2 alternative readings in case the specimen compressed unevenly during the process of testing. The initial zero strain measurements were taken using demec strain gauge and the specimens were placed laterally on the test plate such that the axial force applied acts through their central axis.

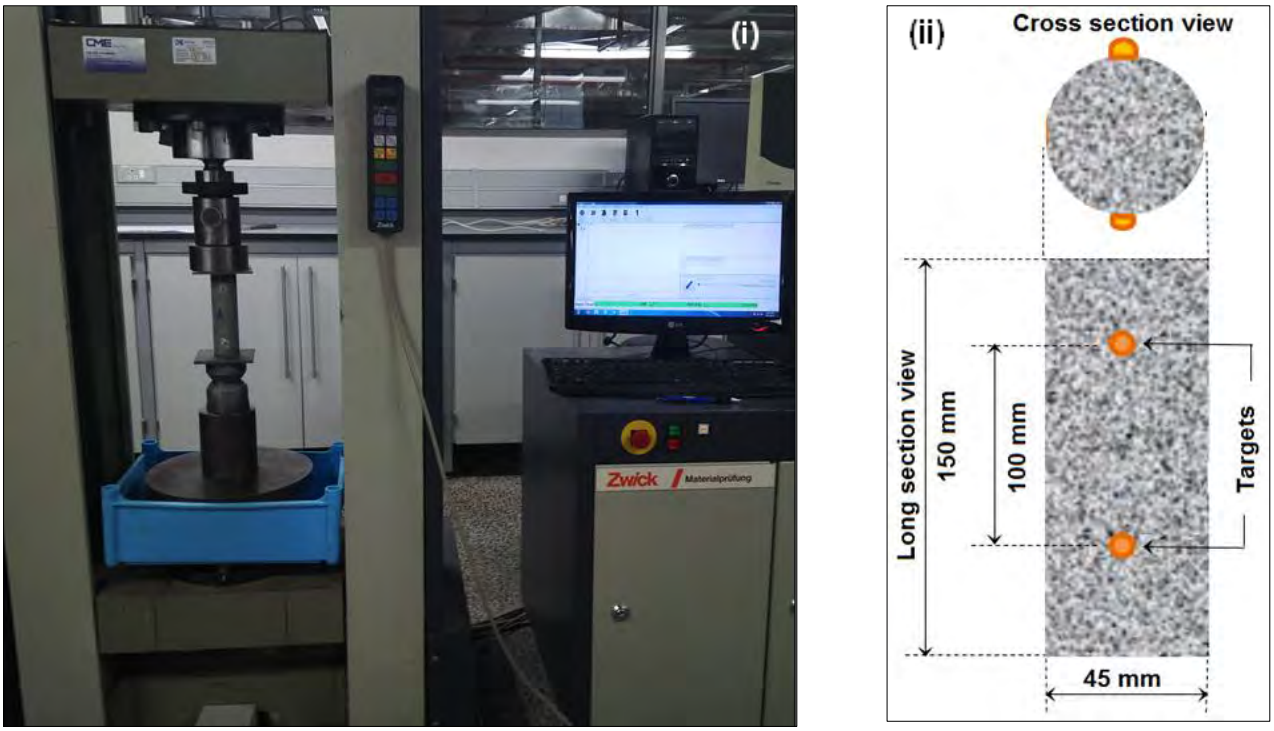

Figure 3-13: Dimensions for cylindrical specimen and a ZwickRoell Z100 machine used to test elastic modulus.

After grinding the test surfaces of the rubberized mortar specimens, it was observed that their test surfaces became rough due to the spiky rubber aggregates projecting out from the surface, see Figure 3-14 (ii). To ensure accurate data acquisition, the test surfaces of these specimens were cushioned with hard boards during the process of testing. The test setup is shown in Figure 3-14 (i).

Elastic modulus was tested at the ages of 3, 7 and 28 days. At the age of 7 days specimens were first loaded to 10% and then 20% of their cube ultimate compressive strength. This was done to ensure that the same specimens could still be tested at ages of 14 and 28 days without any cracks within their matrix and that they were still performing within their elastic limits. The secant elastic modulus for 0-10% loading and 0-20% loading were determined. The tangent elastic modulus for 10-20%

loading was also determined. The ultimate elastic modulus of the respective mortar mix was recorded as the average of all these elastic moduli determined 3 specimens.

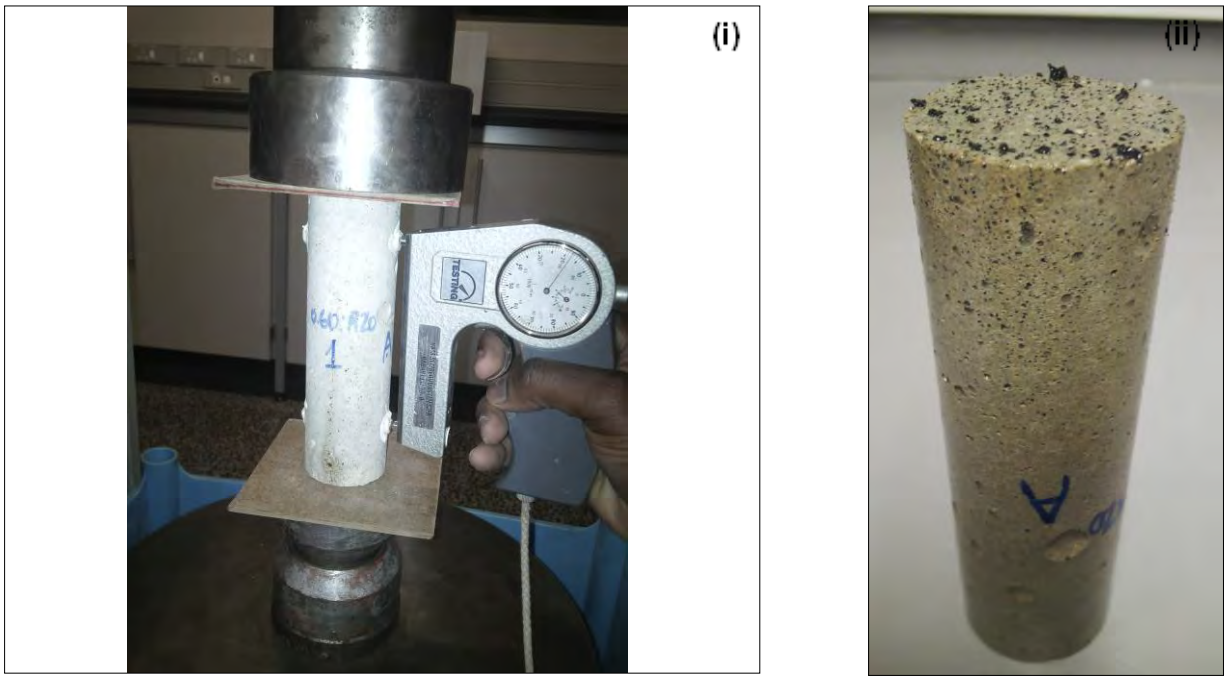

Figure 3-14: (i). Illustration for elastic modulus test set up and a cylindrical specimen showing spikey rubber particles on its ground test surface.

3.3.7. Testing for durability indexes

Durability as defined in ISO 13823:2008 (E) is; 'the capability of a structure or component of the structure to satisfy the design performance requirements over a specified period of time, with planned maintenance, under an influence of environmental actions in a given area'. The durability characteristics of the main mortar mixes were assessed based on their Oxygen Permeability Index (OPI), water sorptivity index (WSI). Both tests were performed in accordance to the UCT durability index test method presented in the Durability Index Manual, Version 1.0 (2009). The test results were evaluated using the durability index performance specifications proposed by Alexander and Mackechnie (2001)

3.3.8. Durability Index based Performance design and specifications

The values from the durability index tests provide a quantifiable measure of the concrete mortars penetrability. For the durability index based performance design method, the durability index values are used as compliance limiting values for design performance specifications. An earlier version used

in classification of concrete for durability based on a range of values, is given in Table 3-5. This method was proposed by Alexander and Mackechnie (2001). There were some limitations that were identified Grieve et al. (2003) in this approach. Grieve et al. (2003) identified that it fails to give estimates of expected service life of a structure and does not take into consideration environmental conditions. It is hence, currently, considered an outdated approach but it is used in the current research to simply quantify the measure of penetrability for the rubberized concrete mortar mixes.

Table 3-5: Suggested range for durability classification using DI values (Alexander and Mackechnie, 2001)

Durability class	OPI (log scale)	Sorptivity ($mm/hr^{0.5}$)	Conductivity (mS/cm)
Excellent	>10	<6	<0.75
Good	9.5-10	6-10	0.75-1.50
Poor	9.0-9.5	10-15	1.50-2.50
Very poor	<9.0	>15	>2.50

3.3.9. Testing procedures

The cube specimens with standard dimensions of 100 mm x 100 mm x 100 mm were used to prepare mortar discs specimens for durability index tests. Cubes were cured using water curing for the period of 28 days and then cored using a coring machine with a core bit of 70 mmϕ. Three 30 mm thick discs specimens were sliced from each mortar core and placed in drying oven set at 50 ± 2° C for a minimum period of 7 days to ensure complete drying of specimens. Specimens were then allowed to cool for 2 hours in a desiccator before testing. It was ensured that the same specimens used in OPI test did not come in contact with moisture after OPI test so as to re-use them for the WSI test.

Oxygen permeability index (OPI)

The test was developed by Ballim (1991) and involves testing the permeability of a concrete sample when subjected to a falling head of pressure. After preconditioning of a concrete mortar sample, the disc specimens were placed in the testing cells and pure oxygen was pressured to 100 ± 5 kPa. A data logger connected to pressure cells was used to record the pressure decay for a period of 6 hours or until the pressure had dropped below 50 ± 2.5 kPa. The collected data was used to calculate a D'Arcy coefficient of permeability for each specimen. Figure 3-15 (ii) shows the pressure cells used for testing OPI.

Using computer software the pressure drop readings are automatically logged and transferred to Microsoft Excel spreadsheets where the computation of the permeability coefficient (k) is done using the equation of D'Arcy coefficient of permeability, as given by:

$$k = \frac{\omega V g dz}{RA\phi} \qquad [3\text{-}1]$$

Where k = coefficient of permeability of test specimen (m/s)

ω = molecular mass of oxygen (32 g/mol)

V = volume of oxygen in the test cell (m^3)

g = acceleration due to gravity (9.81 m/s^2)

d = average specimen thickness (m)

z = slope of line determined in regression analysis1.

R = universal gas constant (8.313 Nm/K mol)

A = cross-sectional area of the test specimen (m^2)

ϕ = temperature (K)

The OPI value for a respective mortar mix was then calculated from determining an average k value from four test specimens and converted it into a negative log scale as shown in equation 3-2.

$$OPI = -\log_{10}[\tfrac{1}{3}(k_1 + k_2 + k_3)] \qquad [3\text{-}2]$$

Where: K_n= coefficient of permeability of each test specimen ($k_1 - k_3$).

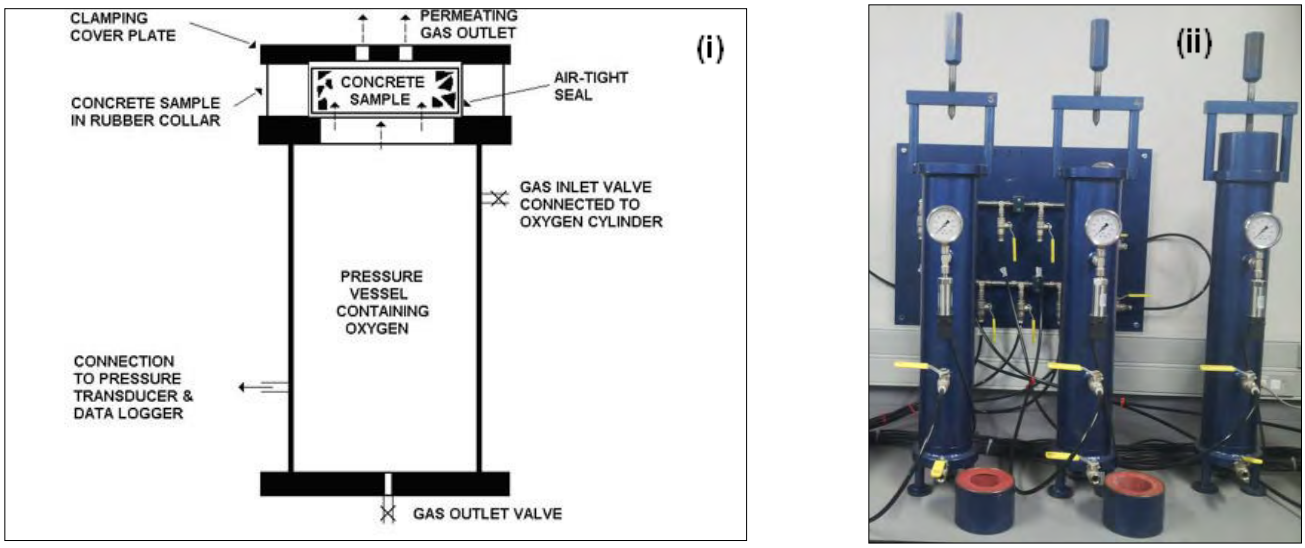

Figure 3-15: (i). A schematic diagram of OPI apparatus (Alexander and Mackechnie, 2001) and pressure cells used for the testing.

Water sorptivity index (WSI)

The test determines a potential measure of the sorptivity and porosity of concrete. The water sorptivity index test was performed on the same specimens used in the OPI test. The circumferences of the disc specimens were sealed tight with silo tape to ensure that no water was absorbed from the circumferential surfaces. The specimens were then placed in a tray, on top of paper towels saturated with calcium hydroxide solution (Figure 3-16 (ii)). The mass of each specimen was recorded at regular intervals for the period of 25 minutes. The specimens were enclosed and fully submerged in a vacuumed tank (-75 kPa) of 5 mol calcium hydroxide solution for 3 hours. The vacuum was then released and specimens were left to soak in calcium hydroxide solution for further 18 hours.

The saturated mass of the specimen was measured and the mass gain due to water absorption at each measurement interval was plotted against the square root of time. A best-fit line was obtained from the plot and water sorptivity was determined using the gradient of the best-fit line;

$$S = \frac{Fd}{M_{SV} - M_{SO}} \qquad [3\text{-}1]$$

Where, S = sorptivity of the specimen (mm/√hour)

F =slope of the best-fit line from plotting M_{WT} against √t (g/√hour)

D = average specimen thickness (mm)

M_{SV} = vacuum saturated mass of the specimen (g)

M_{S0} = dry mass of the specimen at the beginning of the test (g)

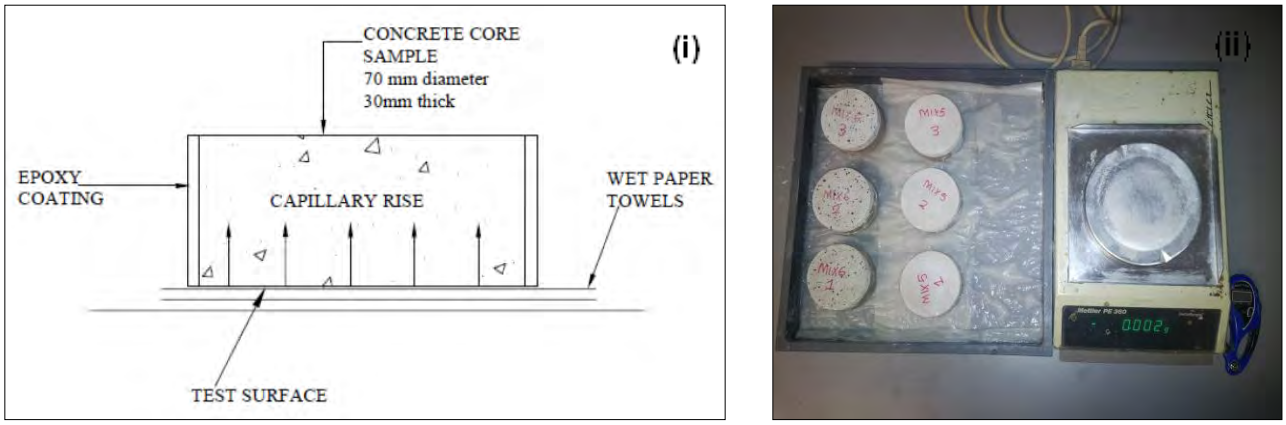

Figure 3-16: (i). A schematic diagram of sorptivity apparatus (Alexander and Mackechnie, 2001). (ii). Sorptivity test apparatus

3.4. Analytical modeling of results

An existing material properties analytical model used by Chilwesa (2012) was used to predict ages of cracking of concrete mortars mixes that were tested in the main experimental phase. The results of age of observed cracking of mortar mixes tested in main experimental phase were the compared and contrasted with the ages of cracking results predicted by the model. This exercise was performed to aid in evaluating efficiency of material properties analytical model on predicting cracking age of rubberized concrete mortars mixes. The details of application of analytical modeling are fully discussed in Section 4-4.

3.5. Chapter summary

The sections in this chapter have given information on the materials used, mix design parameters of concern, test methods employed, as well as the details of curing method and the curing conditions. The test results and discussions for initial and main testing are then given in chapter 4, Section 4.4 of

this chapter discussed details of an analytical modeling technique and the analysis of the results achieved.

CHAPTER FOUR

EXPERIMENTAL RESULTS AND DISCUSSIONS

4.1. Introduction

Results analysed in this chapter are from both initial experimental testing and main experimental testing. The initial experimental phase comprised testing of ring specimens, compressive strength and splitting tensile strength. The main experimental phase comprised testing of ring specimens, free shrinkage, tensile strength, tensile relaxation and elastic modulus. This chapter also presents results from analytical modeling and results obtained from Durability Index tests.

4.2. Initial experimental test results

The results from the initial experimental testing phase were used to determine the optimum rubber particle gradation and optimum rubber particle content that worked best to delay cracking. The established optimum rubber particle gradation and content were then used in main experimental phase to test its influence on cracking resistance performance of main phase concrete mortar mixes.

4.2.1. Ring test

Ring test (restrained shrinkage tests) were performed on concrete mortar ring specimens. The main parameters of concern were cracking age, crack area (width x length) and crack area growth as the function of age after cracking. It was established that incorporation of rubber particles delays the occurrence of shrinkage cracking. With respect to this test, results show a positive synergetic effect from optimizing rubber particle content and gradation. The following sub-sections summarize ring test results for the 20 initial experimentation phase concrete mortar mixes.

4.2.1.1. Age of cracking

The cracking age was determined as the number of days it took each repair mortar specimen to develop a crack after completion of curing. Figure 4-1 and Figure 4-2 present the results for age of cracking for 0.45 w/b and 0.60 mixes, respectively. The figures show trends of cracking age observed

after 14 days from rubberized concrete mortars while compared to their respective control mixes. The 0.45:R0 control concrete mortar mix cracked earlier than its respective rubberized mixes, at the age of 4.5 days after curing. According to both figures, incorporation of different rubber particle gradation produces different trends of crack delays in all the mixes.

According to Figure 4-1 and Figure 4-2, different gradations of rubber particles produce different crack age delays when incorporated in different mixes. Incorporation of gradation 3 rubber particles seemed to have more influence on increasing the crack age more than the other gradations. For instance, crack ages of 5 days, 4 days and 2 days were observed for 0.45:R5G3, 0.45:R10G3 and 0.45:R20G3, respectively. Compared to their respective control mixes, cracking age delays of 0.5, 2.5 and 3.5 days were recorded. For gradation 2, cracking age delays of 0.5 days, 1.5 and 2.5 days were recorded with respect to 5%, 10% and 20% incorporation of rubber particles. For gradation 1, cracking age delays of 0.5 days, 0.5 and 2 days were recorded with respect to the 5%, 10% and 20% incorporation of rubber particles. It is seen from the Figure 4-2 that 0.60:R20G3 mix is the one that recorded longer cracking age amongst all the mixes. Therefore the 20% content of gradation 3 is considered the optimum rubber particle sample.

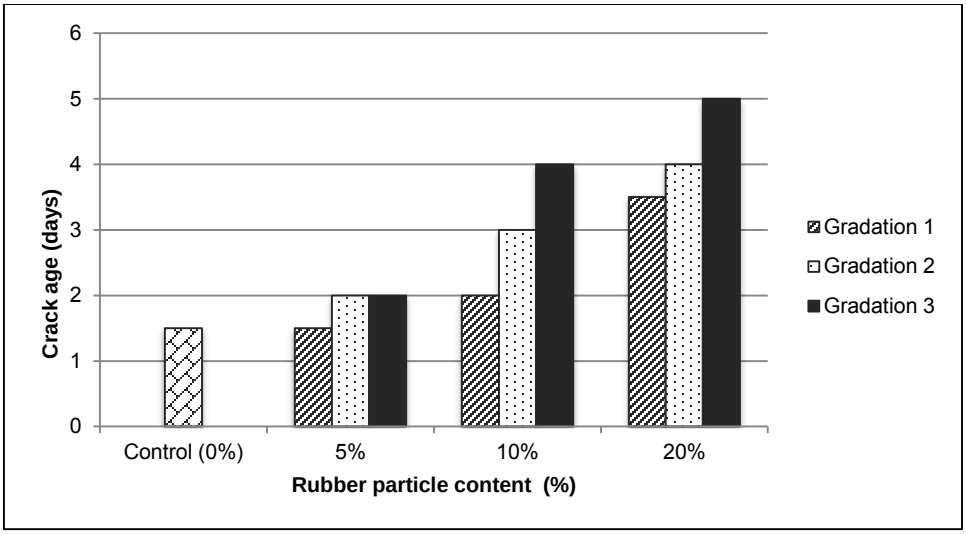

Figure 4-1: Crack ages for rubberized concrete mortars of 0.45 w/b ratio.

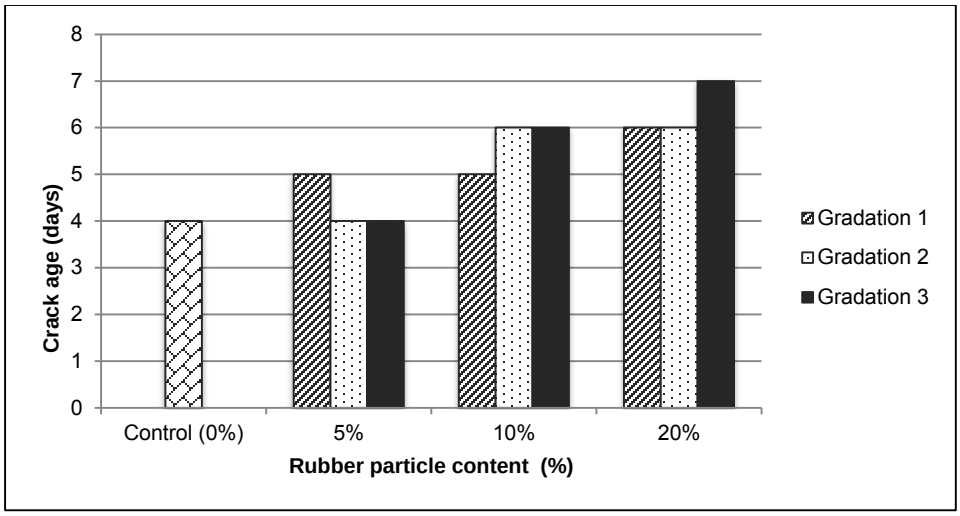

Figure 4-2: Crack ages for rubberized concrete mortars of 0.60 w/b ratio.

As seen from Figure 4-3 and Figure 4-4, all concrete mortar mixes incorporating gradation 3 rubber particles experienced lower total crack areas compared to mixes incorporating rubber particles of gradation 1 and gradation 2. It was also observed that crack area reduced with increasing rubber particle content for all the 3 gradations. In crack area development, the content of 20% rubber particles was identified the best performing content for crack resistance for all tested concrete mortar mixes. It is concluded that mix 0.60:R20G3 recorded the longer cracking age amongst all the mixes; therefore it is identified as an optimum concrete mortar mix with regard to the inspection of age of cracking. Further discussion on crack area is provided in Section 4.2.1.2.

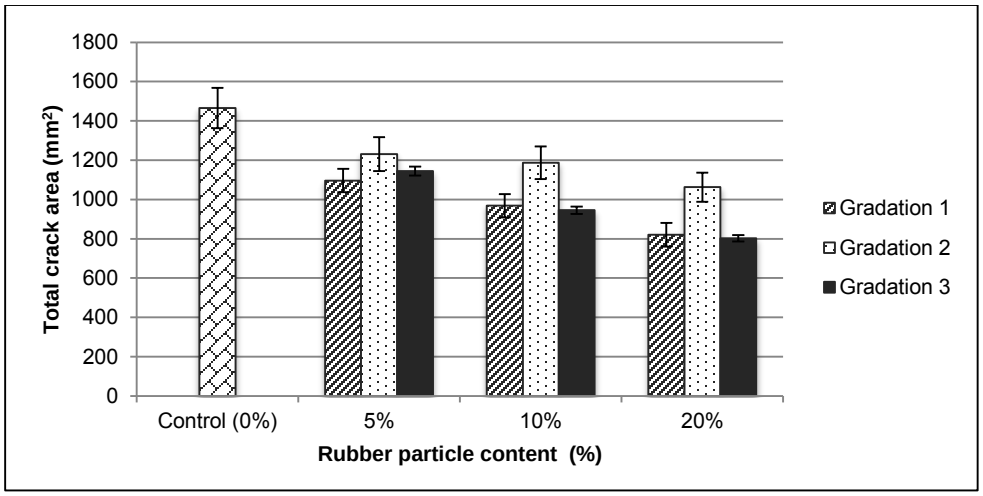

Figure 4-3: Total crack areas for rubberized concrete mortars of 0.45 w/b ratio.

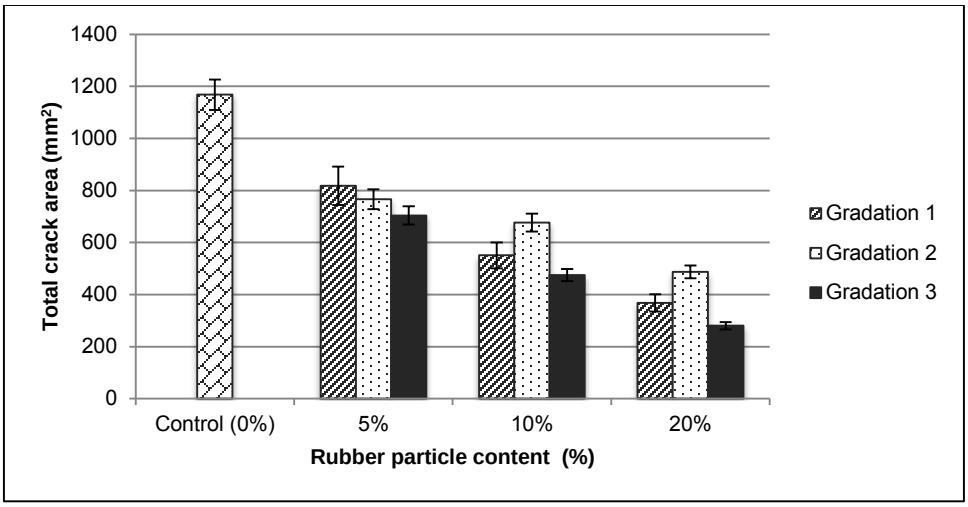

Figure 4-4: Total crack areas for rubberized concrete mortars of 0.60 w/b ratio.

4.2.1.2. Crack area growth

Crack area growth for all concrete mortar mixes was monitored for a period of 28 days after cracking. Crack areas were recorded at ages of 3, 7, 14 and 28 days after an occurrence of the 1st crack. The definition of crack area and the procedure of how it is determined are presented in section 3.2.1. Crack area growth trends for all the mixes incorporating rubber particles of gradation 1, 2 and 3 are illustrated in Figure 4-5 (a-c), respectively.

Each chart illustrates the effect of rubber particle content incorporation for the 3 gradations used. As observed from the 3 figures, rubber particle content seems to affect crack opening considerably, more especially at the later age (14 days). However this influence appeared moderate in all other ages. In overall, it is evidenced that an increase in content of rubber particles reduces the crack width opening, hence crack area. It was also observed that gradation does not influence the crack area growth in both mixes with 0.45 w/b ratio and 0.60.

Mix 0.60:R20G3 recorded the longer cracking age amongst the mixes. It was therefore concluded that the rubber particle content of 20% of gradation 3 is an optimum incorporation with regard to the age of cracking age performance.

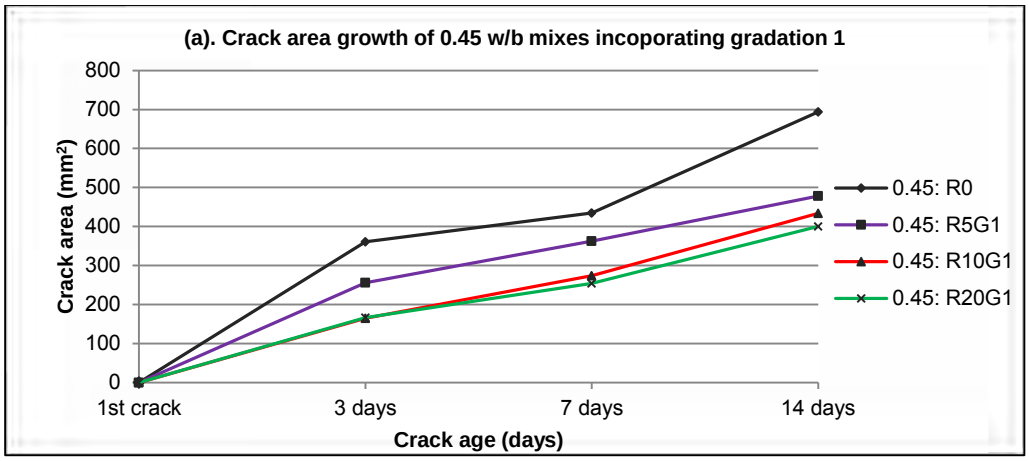

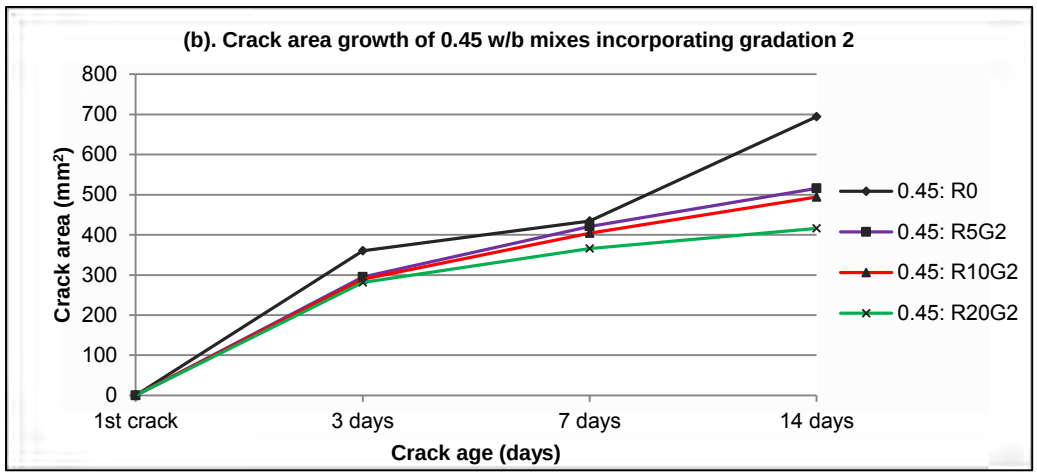

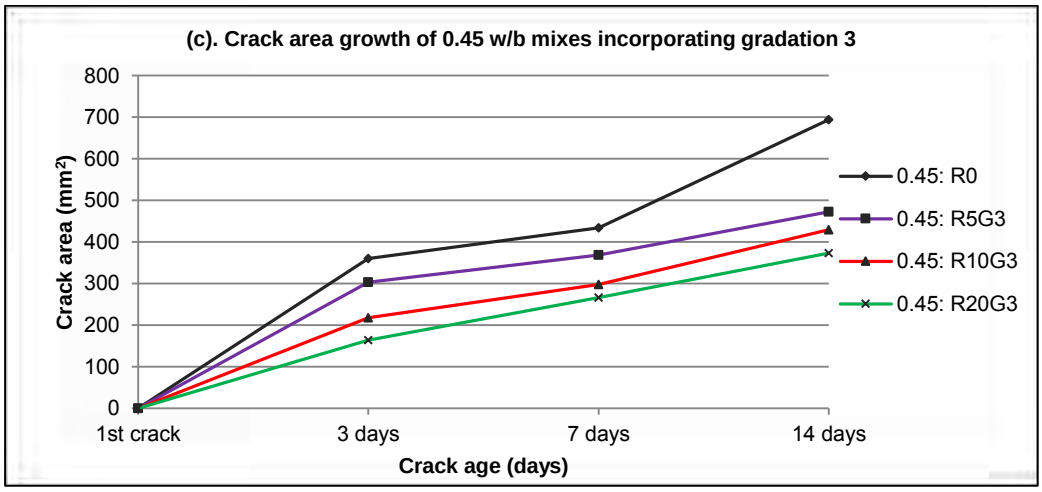

Figure 4-5 (a-c): Cracking area growth for the 0.45 w/b rubberized mortar mixes.

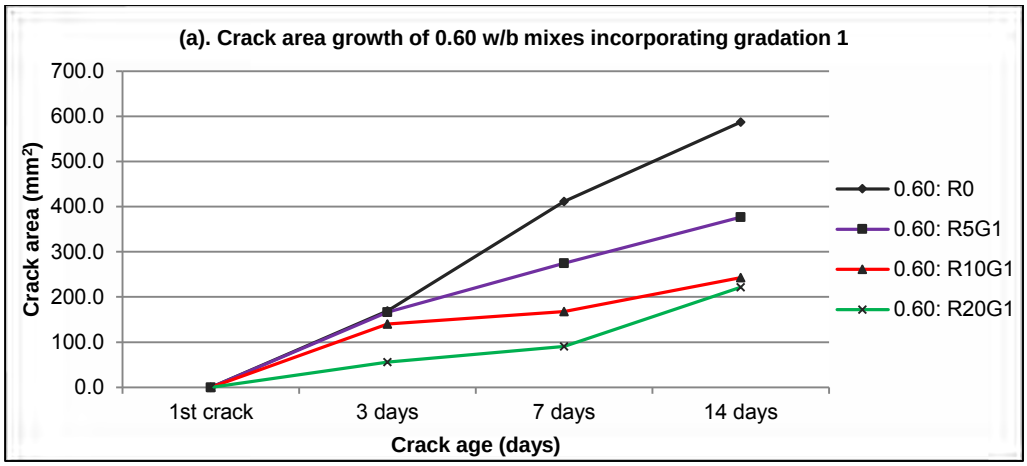

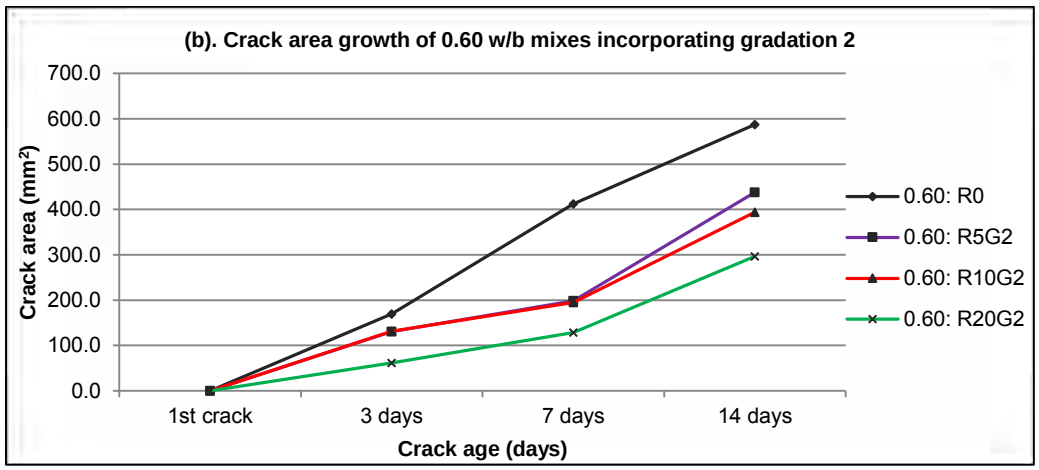

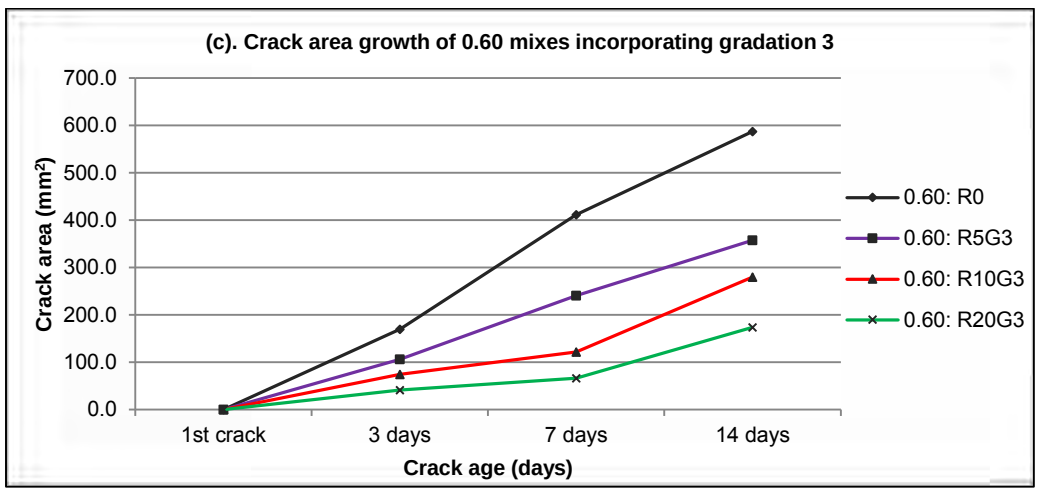

Figure 4-6 (a-c): Cracking area growth for the 0.60 w/b rubberized mortar mixes.

Generally, one crack was observed from all concrete mortar specimens except for mix 0.60:R10G2 and 0.60:R20G2 which developed the average of 2 cracks. For these mixes, both cracks ran through the entire height of the ring specimens. The main crack was determined to be the one that initiated first. It was observed that the width of the main crack opened wider than a secondary crack and it is the main crack that showed a progressive growth while approximately no crack width growth was observed from the secondary cracks. For mortar mixes that developed two cracks, the crack area was calculated as the sum of the areas determined from both cracks.

These results are a reflection that incorporation of optimum content and gradation of rubber particles can improve the cracking resistance of concrete mortars. It is therefore proposed that the natural aggregates should only be replaced by the rubber particles that have similar/close gradation when producing rubberized concrete mortar. In the current research study, it was observed that the concrete mortars incorporating the rubber particles that had the gradation close to that of Klipheuwel sand (Gradation 3) performed well in resisting cracking.

4.2.1.3. Summary of ring test results

The purpose of the initial experimental testing was to determine which gradation and content of rubber particles can perform best in cracking resistance using the ring test.

Generally, comparing the mixes with the 2 different w/b ratios, it is observed that the control mixes with w/b of 0.6 cracked at a later age (7 days) than the mixes with w/b of 0.45 (4.5 days). This could be due to a higher tensile relaxation margin and lower free shrinkage strains expected in the mixes with w/b of 0.6 compared to mixes with a w/b of 0.45. It is also expected that mixes with a higher w/b of 0.60 exhibit lower elastic modulus thus causing a combined effect of relaxation and elasticity that has more influence than the higher tensile strength recorded in mixes with 0.45 w/b to prolong the cracking time. The 0.60 w/b was hence identified to be an optimum w/b ratio. It is also important to note that there was a consistent correlation that was observed between the cracking age and the crack area. It appears that the mixes exhibiting the shorter cracking age experienced the highest crack area at all ages.

Based on the above assessment of results, the 20% content of gradation 3 is the rubber particle sample that performed best in resisting cracking (optimum sample) for concrete mortars tested in this phase. It was therefore proposed that mix 0.60:R20G3 be subjected to further testing relating to other important bonded concrete overlay properties.

4.2.2. Strength development

4.2.2.1. Compressive strength

Compressive strength for all mixes was tested on cubes at the ages of 3, 7 and 14 days. Figure 4-7 present the compressive strengths for rubberized concrete mortar mixes with w/b ratio of 0.45. Figure 4-8 present the compressive strengths for rubberized concrete mortar mixes with w/b ratio of 0.60.

Effect of rubber particle content

It is observed from the results that compressive strength reduction on concrete mortars depended on both rubber particle gradation and the percentage content added. It can be seen from Figure 4-7 and Figure 4-8 that generally, compressive strength reduced with an increasing percentage of rubber particle replacement. The highest strength reduction was related to 20% rubber particles incorporation for all 3 rubber particle gradations used. Nevertheless, this content proved to be the most optimum content that can be incorporated in concrete mortars to delay cracking. From this observation it was concluded that the optimum tested rubber particle content that could be incorporated in concrete mortars to delay cracking while still achieving workable mix is 20%. This conclusion is also in agreement with an observation made by Turatsinze *et al*. (2005) that incorporation of rubber particles greater than 20% produced undesirable workability and detrimental strength loss of about 50% when tested at the age of 28 days.

Effect of rubber particle gradation

For 3 day compressive strength test results in Figures 4-7 it is observed that concrete mortar mix incorporating 20% of gradation 2 rubber particles (0.45:R20G2) recorded the lowest compressive strength compared to other mixes. Similar trend was observed from the test results of test ages of 7 and 14 days. The lowest compressive strength reduction due to incorporation of optimum rubber particle content was 23% on 0.45:R20G3 at the age of 7 days. On the other hand, the highest compressive strength reduction due to incorporation of optimum rubber particle content was 71% on 0.60:R20G2 at the age of 3 days. From these observations it is still concluded that the optimum rubber particle gradation that could be incorporated to achieve minimum strength reduction is gradation 3 (0.42-2.50mm).

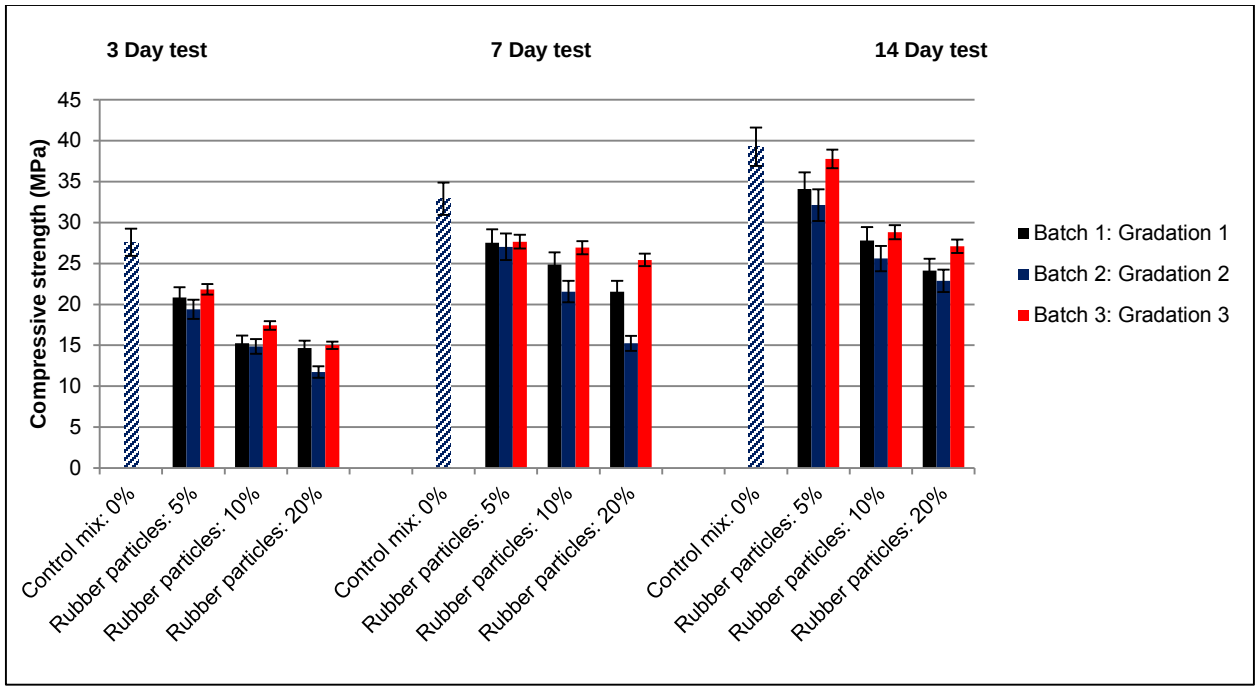

Figure 4-7: Compressive strength of 0.45 w/b rubberized mortar mixes.

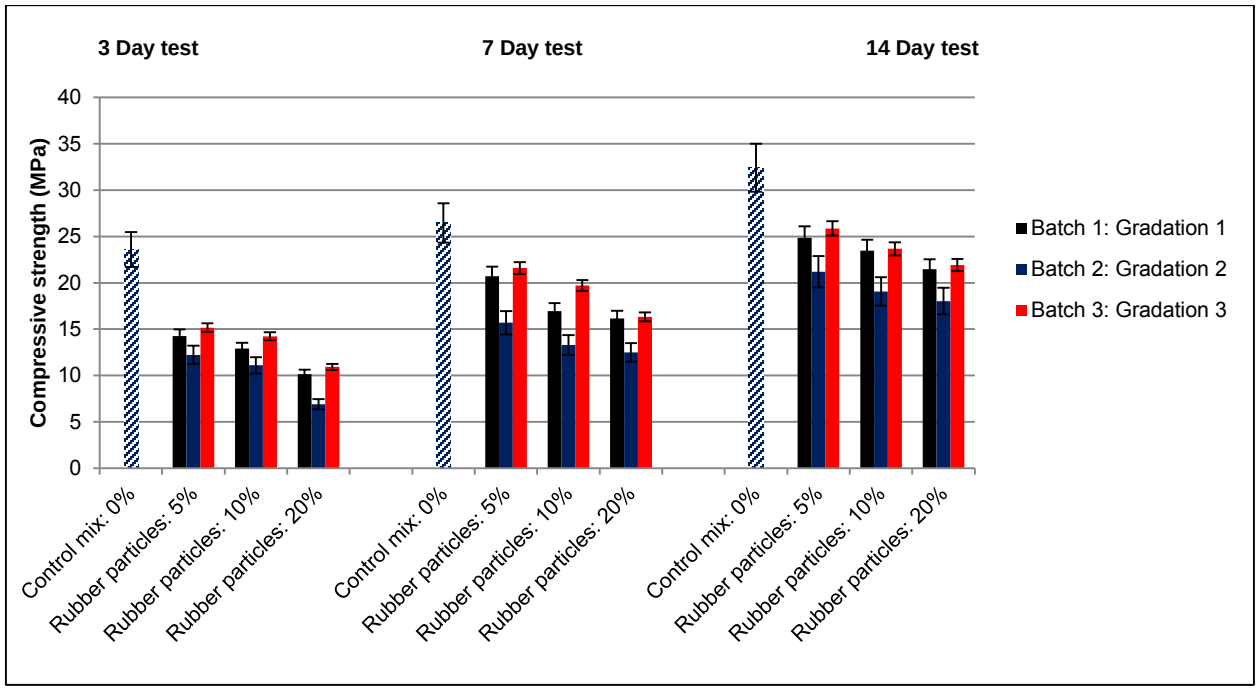

Figure 4-8: Compressive strength of 0.60 w/b rubberized mortar mixes.

4.2.2.2. Splitting tensile strength

Splitting tensile strength for all mixes was tested on cubes at the ages of 3, 7 and 14 days. Figure 4-9 present the splitting tensile strength for rubberized concrete mortar mixes with w/b ratio of 0.45. Figure 4-10 present the splitting tensile strengths for rubberized concrete mortar mixes with w/b ratio of 0.60.

Effect of rubber particle content

It is observed from the results that splitting tensile strength reduction on concrete mortars also depended on both rubber particle content and gradation. It can be seen from Figure 4-9 and Figure 4-10 that generally, splitting tensile strength reduced with an increasing percentage of rubber particles replacement. The highest strength reduction was also related to 20% rubber particles incorporation across all test ages, mostly when rubber particles of gradation 2 were used. This trend is also in agreement with the observation made by Turatsinze *et al*. (2005) that the incorporation of 30% rubber particles caused more that 30% tensile strength loss at the age of 28 days. Tensile strength is the very important property for overlays cracking performance. Therefore the percentage content of rubber particles incorporation was limited to 20% to avoid detrimental tensile strength reductions.

Effect of rubber particle gradation

For 3 day splitting tensile strength test results in Figures 4-9 it is observed that concrete mortar mix incorporating 20% of gradation 3 rubber particles (0.45:R20G3) had the lowest splitting tensile strength loss compared to other mixes. Similar trend was observed from test results of test age of 7 and 14 days. The lowest splitting tensile strength loss that was calculated from mixes incorporating optimum content (20%) was 31% on 0.60:R20G3 at the age of 14 days. On the other hand, the highest splitting tensile strength loss that was calculated from mixes incorporating optimum content (20%) was 70% on 0.60:R20G2 at the age of 3 days. From these observations it was still concluded that the optimum rubber particle gradation that could be incorporated to achieve minimum strength loss is gradation 3 (G3).

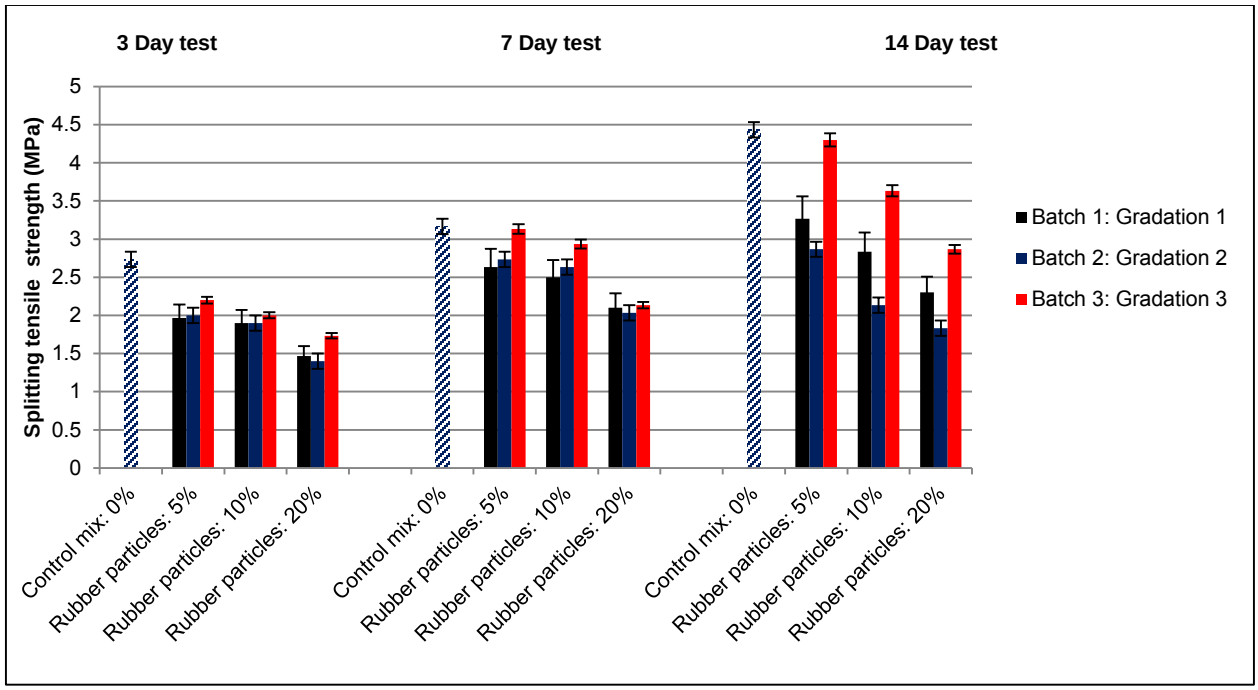

Figure 4-9: Splitting tensile strength of 0.45 w/b rubberized mixes.

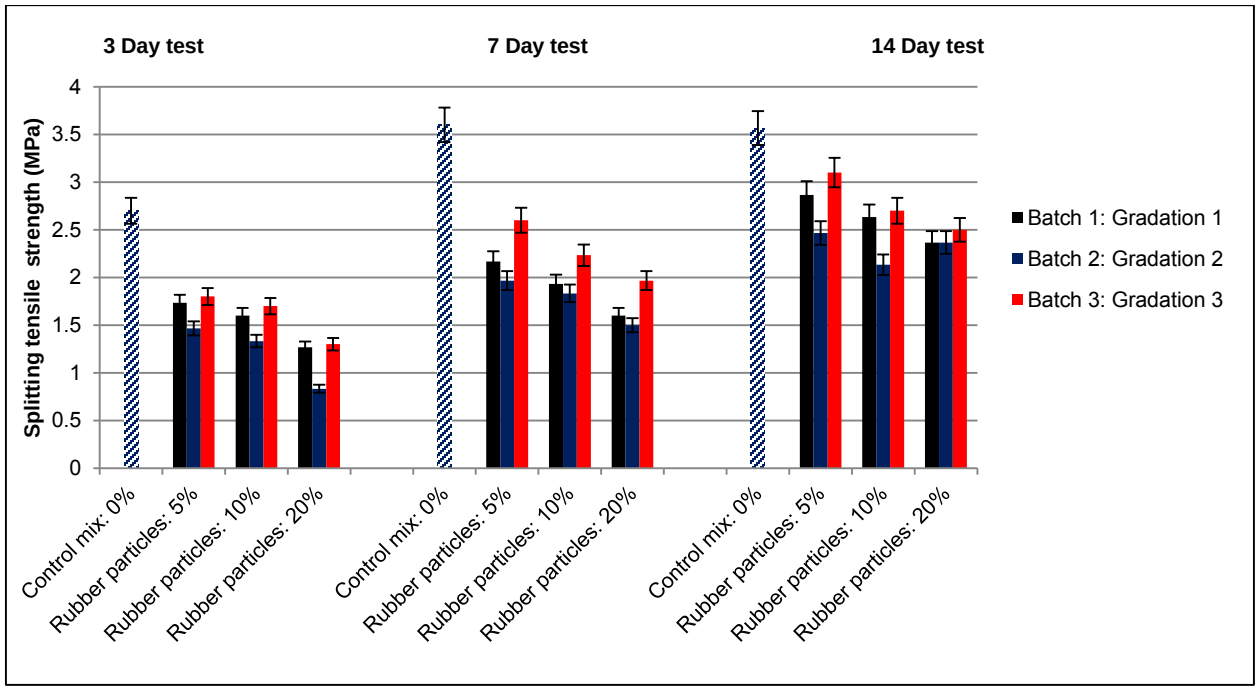

Figure 4-10: Splitting tensile strength of 0.60 w/b rubberized mixes.

Summary of strength development results

Incorporation of rubber particles resulted in strength reduction at all test ages for all mixes. Strength reduction increased with an increasing incorporation of rubber particle content for all 3 rubber particle gradations incorporated. Goulias *et al*. (1998) attributed that the observed detrimental loss of both compressive and tensile strength is due to effectively high void content introduced by incorporation of rubber particles.

The results of the splitting tensile and compressive strength testing showed that an increase in rubber particle content results in a decrease in strength across all types of gradations. However, the strength of specimens incorporating rubber particles of gradation 3 was the least negatively affected followed by specimens incorporating rubber particles of gradation 1.

4.3. Main experimental test results

In order to assess the influence of rubber particle grading and the optimization of rubber content on cracking resistance of rubberized repair mortars, the material properties discussed in Chapter 3 were tested on the optimum mix (0.60:R20G3) that was identified from the initial testing. One more laboratory made concrete mortar of w/b ratio of 0.80 and one commercially available repair mortar (CRM) were also used to incorporate the optimum rubber particles and investigations were made on the cracking performance. The rationale for the choice of these mixes was discussed in Section 3.1.2.1. Material properties that were tested in this main experimental phase were free shrinkage, compressive strength, tensile strength, tensile relaxation and elastic modulus. Restrained shrinkage (ring test) was also done to assess cracking age, crack area and crack growth of all prepared main mixes.

4.3.1. Compressive strength

Compressive strength tests were performed for the purpose of mixes material characterization. Compressive strength was tested on typical 100 mm x 100 mm x 100 mm concrete mortar cubes at the ages of 3, 7, 14 and 28 days. These ages were simply chosen to obtain data that can be used to monitor the mortars strength development. Compressive strength of all 3 selected control mortar mixes and their 3 respective rubberized mortars were tested. Figure 4-11 presents compressive strength development test results for all the main mixes.

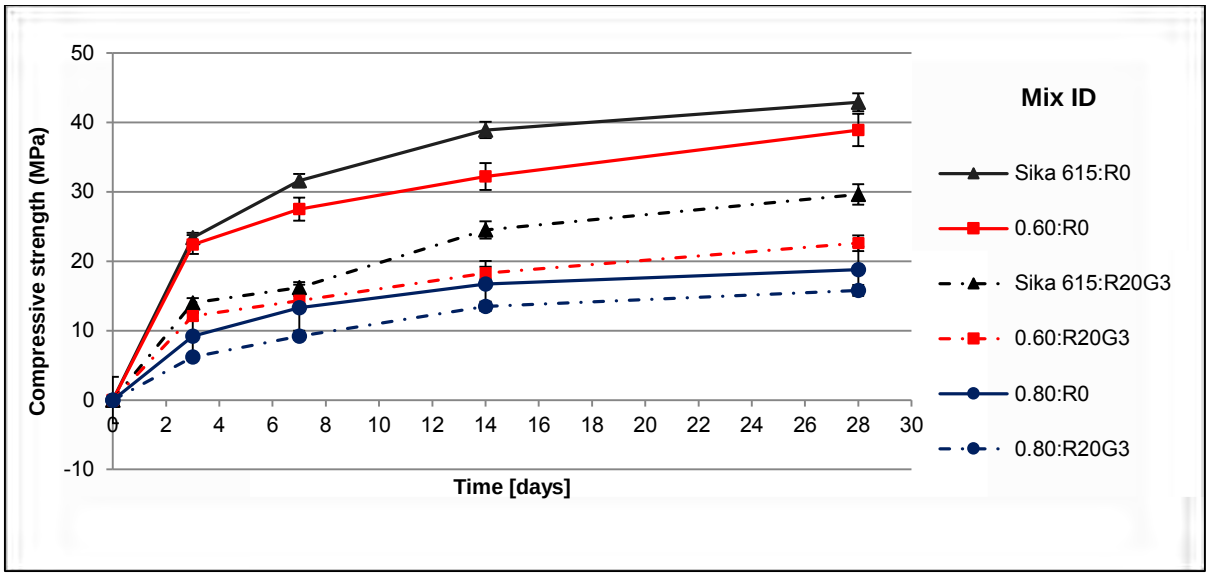

Figure 4-11: Compressive strength development of main rubberized mixes.

As in the initial experimental testing phase it was observed that replacement of natural aggregates by rubber particles causes reduction in compressive strength. From Figure 4-11, it is observed that the CRM control mix (CRM:R0) had the highest compressive strength across all test ages, followed by control mix of the 0.60 w/b (0.60:R0) and then their respective rubberized mixes, CRM:R20G3 and 0.60:R20G3. Although the 0.80:R0 mix recorded the lowest compressive strength at the age of 28 days, it underwent the lowest strength reduction of 16% when rubber particles were incorporated.

It was observed that the compressive strength failure mode for control concrete mortar specimens was different from that of the rubberized concrete mortars. Control mix specimens failure mode exhibited the typically failure mode (see Figure 4-12 (i)). The snapping sound due to internal stress release was heard at points of failure for some of the control mix specimens, more especially at the age of 28 days. Rubberized concrete mortar specimens did not exhibit neither the typical compressive failure mode nor the snap sound at failure. Most of the rubberized specimens only developed straight cracks along the edges longitudinal to loading axis (see Figure 4-12 (ii)). As discussed in the literature, this could be because rubber particles within the concrete mortars act as holes to release internal stress concentrations during the test. Figure 4-12 (i) and (ii) below show failure modes experienced by control mix specimen and rubberized mortar mix specimen, respectively.

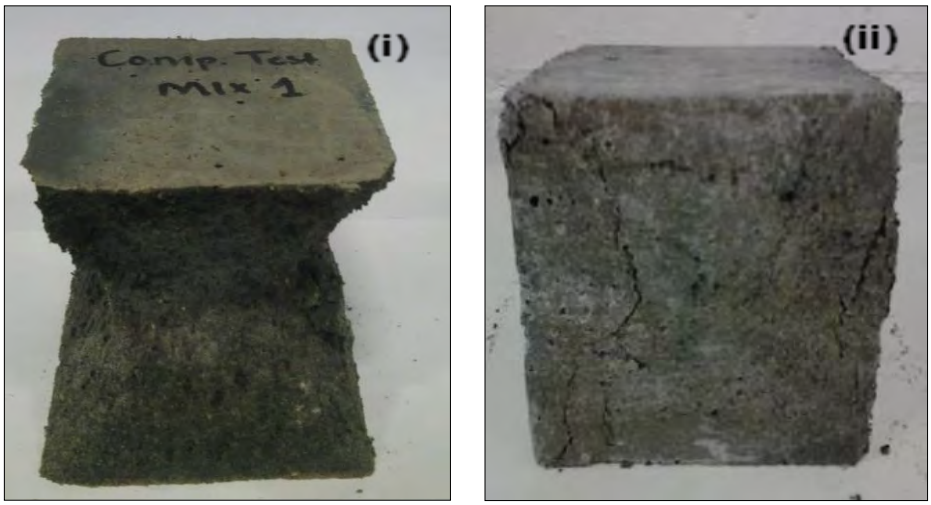

Figure 4-12: Failure modes for cube specimens tested under compressive test.

4.3.2. Tensile strength

Tensile strength is one of the important material properties needed by overlays to resist cracking. Tensile strength for all mixes was tested on notched dog bone shaped specimens at the ages of 3, 7, 14 and 28 days. Tensile strength of each mortar mix was determined as an average of test results of 2 dog bone shaped specimens. This was because of the large number of samples that needed to be tested and the shortage of moulds, as well as time constraints. Figure 4-13 presents tensile strength results for main experimental testing.

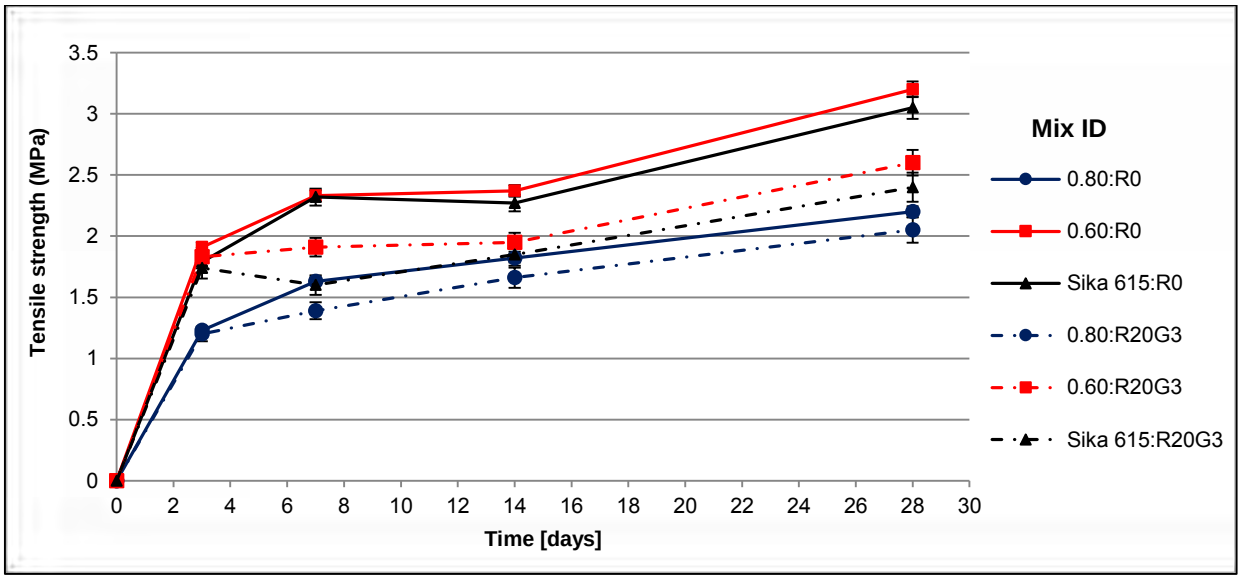

Figure 4-13: Tensile strength development of main rubberized mixes

As seen from Figure 4-13, the control mix with w/b ratio of 0.60 (0.60:R0), together with CRM:R20G3 recorded the highest tensile strength than all other mixes across all test ages. The highest tensile strength of 3.2 MPa was recorded for 0.60:R0 at the age of 28 days. This was followed by CRM:R20G3 with a tensile strength of 3.1 MPa. The mix that recorded the lowest tensile strength at the age of 28 days was 0.80:R0 with strength of 2.1 MPa.

At an age of 3 days, the strength reduction was less than 5% for all the 3 mixes with incorporation of 20%. This is significant because good early age tensile strength plays a big role in cracking resistance of cement based materials. This result suggests that the incorporation of optimum rubber particles does not cause detrimental effects on tensile strength at the early ages. It can therefore be concluded that rubberized mixes could still develop good tensile strength at early ages and will thus be able to resist any tensile stresses that could develop within the rubberized overlay at the early ages.

At an age of 7 days, the tensile strength recorded for CRM:R20G3 was lower than the strength recorded at the age of 3 days. This was possible because of minor cracks that developed on the dovetail section of both test specimens during the test. It was observed that these minor cracks that occur before the specimens could break at notched prismatic section causes an uneven gripping on the holding mechanism of the test machine. Due to this unevenness the specimens that started cracking at the dovetail sections recorded lower strengths. The results were accepted only in the cases where specimens just cracked at dovetail but eventually failed at the notched section. For specimens that failed with the modes demonstrated on Figure 3-12 (i), the results were discarded. At this age, it was observed that 0.60:R20G3 mix still outperformed the other 2 rubberized concrete mortars.

The tensile strength reduction in concrete mortars due to incorporation of rubber particles was observed in all mixes across different test ages. The ultimate reason for this reduction was discussed to be caused by high void content or holes that are assumed to be effectively introduced by the incorporation of rubber particles. The other reason for this behavior may be due to the weak interface zone between rubber particles and cement matrix. These weak interface zones may act as a micro-crack due to the weak bonding between rubber particles and cement matrix during tensile loading (Ganjian *et al.,* 2009).

4.3.3. Ring test

Ring tests were performed on concrete mortar ring specimens as in the initial testing phase. It was evident from the initial testing phase that incorporation of rubber particles delays the occurrence of the shrinkage cracks. Therefore, it was necessary to perform the ring test on the main mortar mixes for the purpose of comparing experimental cracking age to the predicted cracking age using the analytical model for material properties. The following sub-sections summarize ring test results for 6 mortar mixes.

Cracking age

Table 4-1 presents ring tests results of all 6 mixes tested in the main experimental phase. The table shows trends of crack areas, age of cracking and maximum recorded crack width observed from 3 control mixes and their respective rubberized mortar mixes.

Table 4-1: Ring test results for main experimental phase mixes.

0.60 w/b ratio mixes						
Mix ID	***0.60:R0***			***0.60:R20G3***		
Cracking age (days)	**7**			**11**		
Test age (days)	3 days	7 days	14 day	3 days	7 days	14 day
Crack area (mm^2)	145.5	506.5	798.3	135.0	186.0	267.0
Max crack width (mm)	3.8 ± 0.6			1.6 ± 0.2		
0.80 w/b ratio mixes						
Mix ID	***0.80:R0***			***0.80:R20G3***		
Cracking a (days)	**10**			**15**		
Test age (days)	3 days	7 days	14 day	3 days	7 days	14 day
Crack area (mm^2)	169.2	411.8	587.0	41.2	65.9	173.4
Max crack width (mm)	3.2 ± 0.5			1.2 ± 0.1		
CRM mixes						
Mix ID	***CRM:R0***			***CRM:R20G3***		
Cracking age (days)	**10**			**18.5**		
Test age (days)	3 days	7 days	14 day	3 days	7 days	14 day
Crack area (mm^2)	203.0	494.2	704.4	49.0	98.0	190.0
Max crack width (mm)	2.6 ± 0.2			0.9 ± 0.5		

It can be seen that the 0.60 w/b control concrete mortar (0.60:R0) cracked earlier than all the other mixes. Indeed, all control mortar mixes developed cracks earlier than their respective rubberized repair mortar mixes. CRM:R20G3 recorded the longer crack age of 18.5 days, followed by 0.80:R20G3 which recorded cracking age of 15 days. Amongst the rubberized mortars 0.60:R20G3

recorded the shorter cracking age of 11 days. The cracking delays on rubberized mortars were also determined. It was found that 0.60:R20G3 only had the delay of 4 days while 0.80:R20G3 and CRM:R20G3 had delays of 5 and 8.5 days, respectively.

Total crack area growth

The total crack area growth for all mixes was monitored for the period of 14 days. The definition of total crack area and the procedure of how it is determined are presented in section 3.2.1. Crack areas were recorded at ages of 3, 7 and 14 days after an occurrence of 1st crack. Crack areas for control mortar mixes and their respective rubberized mortar mixes are illustrated in Table 4-1.

The table also shows the summary of the maximum width of the main crack opening measured on ring specimens at the age of 14 days after the development of the 1st crack. Beside CRM:R0 and 0.60:R0 which developed 2 cracks, only one crack was observed on the other mortar specimens. Contrary to this observation, Nguyen *et al*. (2012) observed that 2 cracks predominantly occurred on rubberized mortar mixes and only one crack on control mortar mixes from the research they conducted.

For specimens that developed 2 cracks, both cracks ran through the entire height of the ring specimens. The crack growth trends observed on Table 4-1 are mainly due to the evolution of the opening of the main crack. It was observed that the width of secondary crack stayed relatively the same since it developed thus having no effect in crack area growth. These 2 interesting observations made it conclusive that the crack area growth is the function of the crack width widening of the main crack only. The biggest average crack width that was measured at the 14th day was 3.8 mm recorded on 0.60:R0. While the smallest average crack width was recorded on CRM:R20G3 as 0.9 mm. It can be observed also that its crack width reduced by approximately 65% compared to the value recorded on CRM:R0. It is evident that incorporation of rubber particles reduces the crack width widening caused by restrained shrinkage. As seen from the main experimental phase, results show a positive synergetic effect of incorporating rubber particles of optimum gradation and content.

4.3.4. Free shrinkage

All specimens were cured for 3 days under the same curing regime discussed in Section 3.1.1.2. Specimens were then exposed to drying in an open laboratory. The Figures 4-14 (a-c) present the

influence of rubber particles incorporation on free shrinkage strains of main experimental phase mixes.

It was assumed that plastic shrinkage was no more occurring at the time when free shrinkage strains were recorded. As suggested in the literature, plastic shrinkage only occurs at the very early age (<3 days) when the concrete mortar is still in the plastic state. It should therefore be acknowledged that the shrinkage strain readings are as a result of autogenous and drying shrinkage. However, Alexander (2001) state, that shrinkage during curing is noteworthy particularly for concrete mortars with a low w/b ratio of less than 0.40. Therefore it was assumed that autogenous shrinkage is negligible in this research because all the mixes had w/b ratios greater than 0.40.

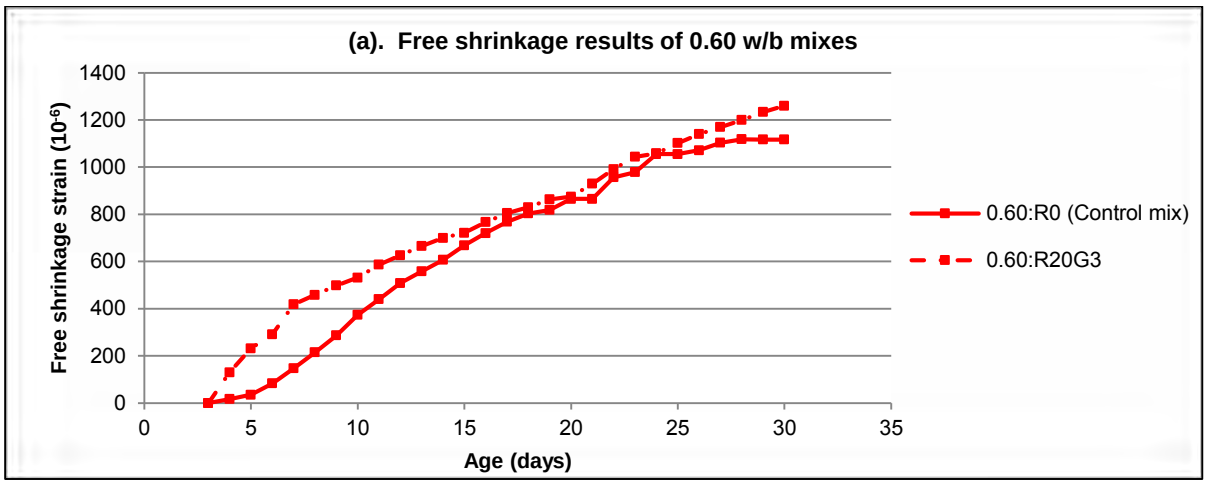

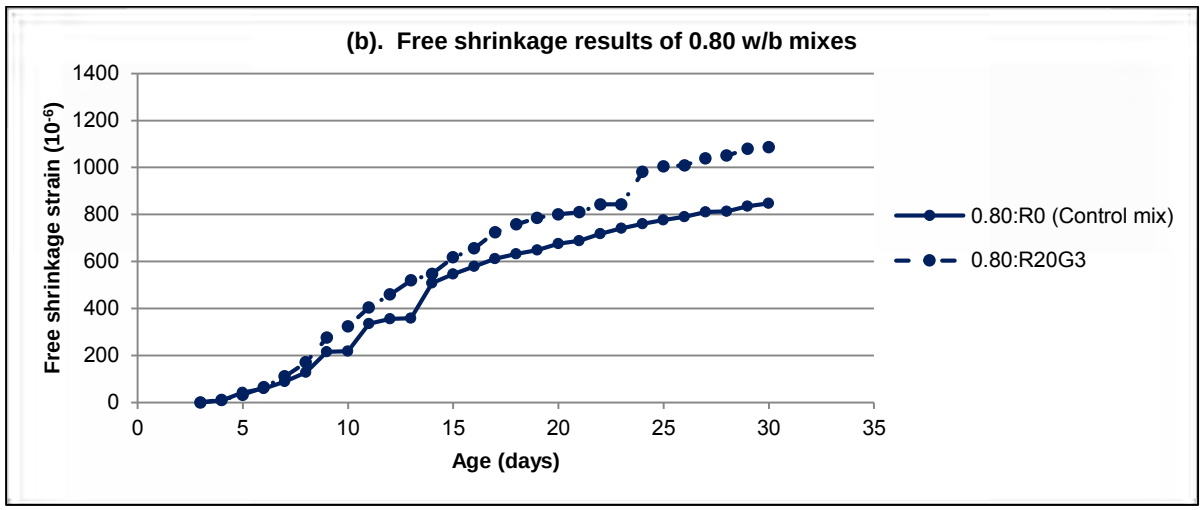

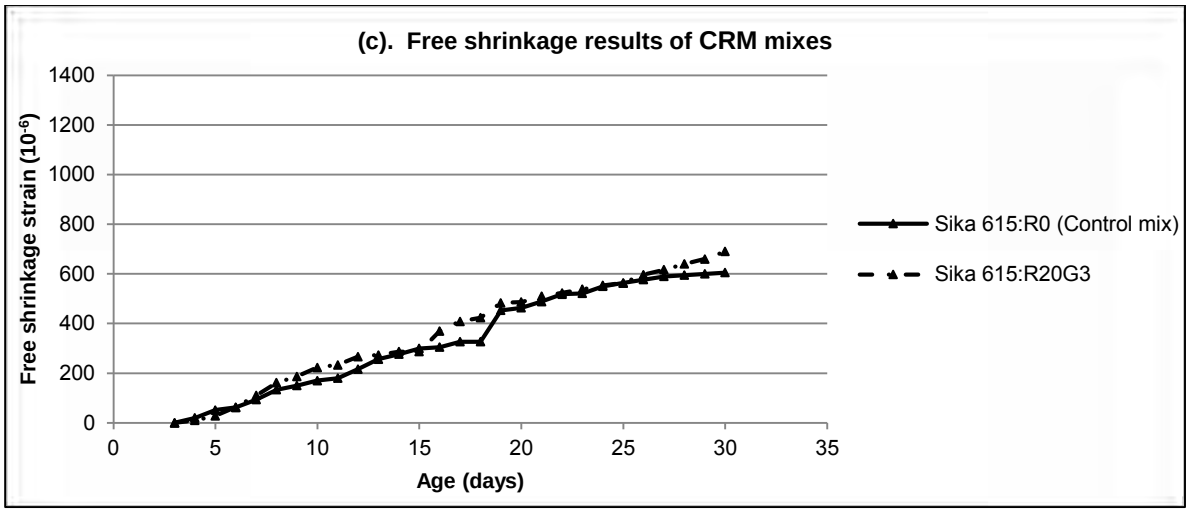

Figure 4-14 (a-c): Free shrinkage results of main experimental phase mixes

It is observed from the Figure 4-14 (a-c) that higher free shrinkage was experienced by the 0.60 w/b ratio concrete mortar mix (0.60:R0) than the 0.80 w/b ratio concrete mortar mix (0.80:R0). This observation agrees with the statement drawn from the literature that drying shrinkage is directly influenced by w/b ratio. Mortar mixes with lower the w/b ratio experiences higher shrinkage strains. Higher shrinkage in 0.60:R0 mix may have been due to higher cement and paste content compared to 0.80:R0 (shrinkage take place in cement paste). These results agree with the experimental findings by Masuku (2009) and Chilwesa (2012) who found that free shrinkage strain was higher in mixes with w/b of 0.45 than in mixes with w/b of 0.60. Amongst the 3 control mixes CRM:R0 recorded the lowest free shrinkage strains.

The trends from the results show that incorporation of rubber particles has less or no influence on free shrinkage capacity of 0.60:R0 and CRM:R0 mixes. When comparing free shrinkage degree of rubberized mortars and control mixes, it can be seen that the incorporation of rubber particles only had little influence on shrinkage of 0.80 w/b ratio mix. The increased shrinkage in this mix may be because of the higher void content introduced by incorporation of rubber particles. It is argued that high moisture loss happens through these introduced capillary pores and excessive voids.

4.3.5. Tensile relaxation

The ultimate tensile relaxation of each mortar mix was recorded as the difference between 100% and the percentage stress ratio achieved from 2 dog bone shaped specimens per mortar mix. Tensile relaxation was determined for all mortars at ages of 3, 7 and 14 days. Due to time constraints and

overbooking of the Zwick machines, tensile relaxation testing was conducted for the duration of 24 hours instead of the suggested 72 hours per specimen. Figure 4-15 shows a typical relaxation curves as the function of stress ratio for 0.80R:20G3.

The tensile relaxation results presented as the difference between 100% and the percentage stress ratio are shown in Figure 4-16. It is observed from the figure that the margin of tensile relaxation decreases with an increase in age of testing. Specimens tested at the younger age seem to undergo higher margin of relaxation than the specimens tested at the older age. This observation was made on both control mortar specimens and rubberized mortar specimens. This observation is consistent with the findings by Masuku (2009) and Chilwesa (2012). Masuku (2009) commented that due to higher degree of hydration in later age, specimens seem to undergo lower relaxation because of higher strength they have gained.

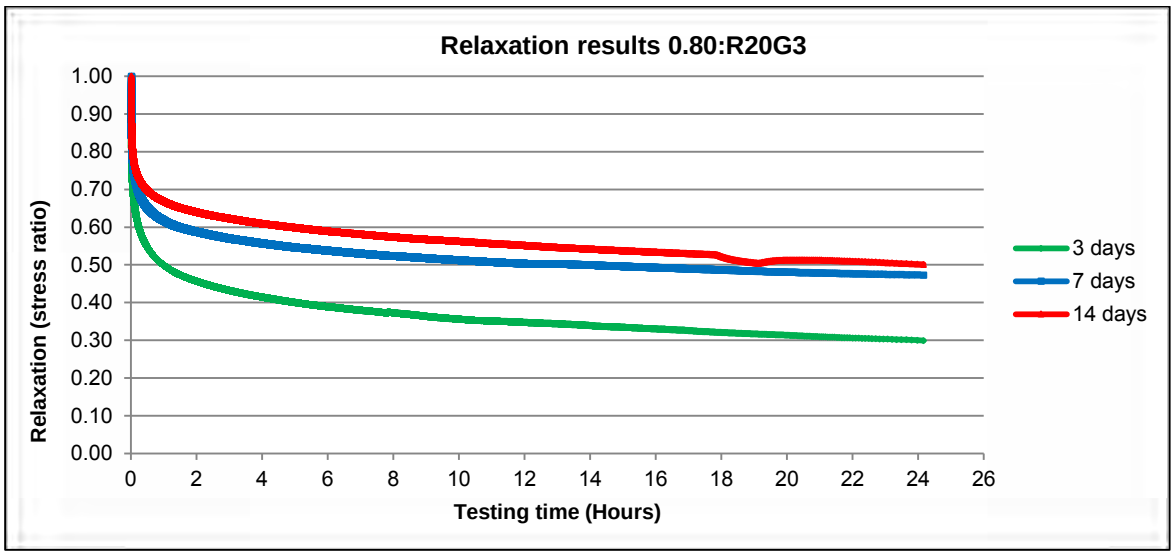

Figure 4-15: Typical relaxation curves for 0.80R:20G3 across all test ages.

From Figure 4-16 it is observed that rubberized mortar specimens undergo higher tensile relaxation than their respective control mortar specimens. The results indicate that an incorporation of rubber particles results in an increased margin of tensile relaxation. Comparison of tensile relaxation results between the rubberized specimens and their respective control specimen is presented in Table 4-2.

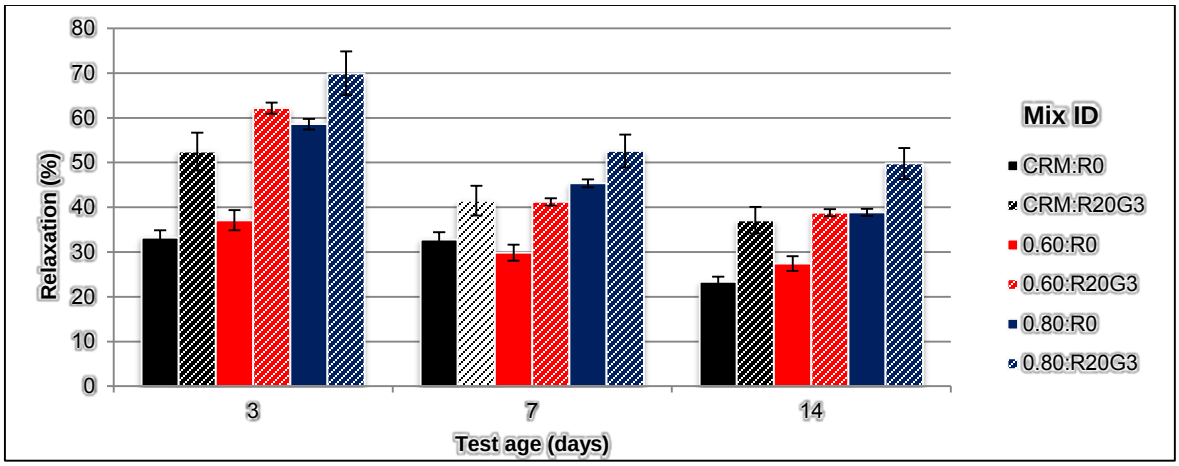

Figure 4-16: Tensile relaxation results for main experimental phase test specimens

Table 4-2 is provided aid with the details of the margins of relaxations that rubberized mortars undergo compared to their respective control mixes. It shows relaxation increase from each test age.

Table 4-2: Tensile relaxation results for main experimental phase test specimens.

0.60 w/b ratio mixes							
Mix ID		***0.60:R0***			***0.60:R20G3***		
Test age	(days)	***3 days***	***7 days***	***14 day***	***3 days***	***7 days***	***14 day***
Relaxation	(%)	37	30	27	62	41	39
Relaxation increase at age of 3 days	(%)	25					
Relaxation increase at age of 7 days	(%)	11					
Relaxation increase at age of 14 days	(%)	11					
0.80 w/b ratio mixes							
Mix ID		***0.80:R0***			***0.80:R20G3***		
Test age	(days)	***3 days***	***7 days***	***14 day***	***3 days***	***7 days***	***14 day***
Relaxation	(%)	59	45	39	70	53	50
Relaxation increase at age of 3 days	(%)	11					
Relaxation increase at age of 7 days	(%)	7					
Relaxation increase at age of 14 days	(%)	11					
CRM mixes							
Mix ID		***CRM:R0***			***CRM:R20G3***		
Test age	(days)	***3 days***	***7 days***	***14 day***	***3 days***	***7 days***	***14 day***
Relaxation	(%)	33	33	23	52	41	37
Relaxation increase at age of 3 days	(%)	19					
Relaxation increase at age of 7 days	(%)	9					
Relaxation increase at age of 14 days	(%)	14					

Comparing the rubberized mortar mixes, 0.80:R20G3 specimens showed the highest margin of tensile relaxation at all testing ages, followed by 0.60:R20G3 specimens and then CRM:R20G3

specimens. The highest tensile relaxation of 70% was recorded for 0.80:R20G3 at the age of 3 days, then relaxations of 62% and 50% were recorded for 0.60:R20G3 and CRM:R20G3, respectively. The lowest tensile relaxation of 37% was recorded in CRM:R20G3 at the age of 14 days, then relaxations of 39% and 50% were recorded for 0.60:R20G3 and 0.80:R20G3, respectively.

The results reflect that at the age of 3 days, the tensile relaxation increase between 0.60:R0 and 0.60:R20G3 was approximately 25%. This is by far the highest relaxation increase caused by an incorporation of rubber particles. CRM:R0 recorded the lowest relaxation increase of 9% when rubber particles were incorporated.

As seen below in Section 4.3.6, the elastic modulus of all the tested mortar mixes also decreased when rubber particles were incorporated. This observation is significant for overlays performance and it is agrees with the findings from relaxation test. The overlay exhibiting a lower elastic modulus undergoes a higher margin of tensile relaxation hence relieve some internal tensile stress that develops within the overlay.

4.3.6. Elastic modulus

Elastic moduli of all 3 control mortar mixes and their 3 respective rubberized mixes were determined from stress-strain curves acquired from test results. Tests were performed at the ages of 7, 14 and 28 days using 3 specimens per test.

Figure 4-17 shows elastic modulus results of main phase testing across 3 different test ages. It can be seen that the values obtained fall within the common range of elastic moduli for repair mortars (5 GPa to 30 GPa). The 0.80:R20G3 recorded the lowest elastic moduli at all testing ages. At the age of 28 days it recorded 17 GPa as compared to 19 GPa for 0.80:R20G3 and 26 GPa for CRM:R20G3. The highest elastic modulus reduction of 18.5 % at the age of 7 days was recorded for 0.80 w/b ratio when rubber particles were incorporated. Reduction of elastic modulus due to rubber particles incorporation was also observed on 0.60:R0 and CRM:R0 mortar mixes. At the age of 7 days, 0.60:R0 and CRM:R0 experienced elastic moduli reduction of 15% and 8.2%, respectively.

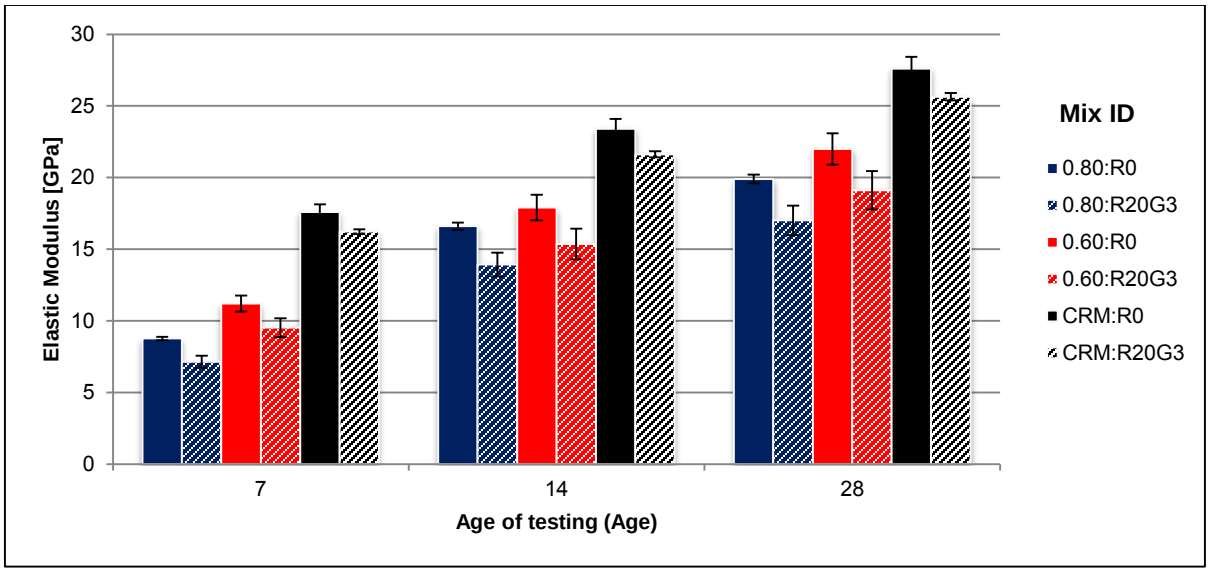

Figure 4-17: Elastic modulus results for main experimental phase test specimens.

As seen from Figure 4-17, CRM:R0 had the higher elastic moduli across all 3 testing ages, followed by 0.60:R0 and 0.80:R0 mixes, respectively. It can be seen that CRM:R20G3 achieved higher elastic modulus earlier than other mortars mixes. At age of 7 days CRM:R20G3 was found to have achieved about 64 % of its 28 days elastic modulus while 0.80:R20G3 only achieved 44 % of its 28 days elastic modulus. As discussed in the literature, the higher early age elastic modulus development like the one recorded from CRM mix is usually undesired for overlays where higher cracking resistance is a priority.

The reduction of elastic modulus in mortar mixes incorporating rubber particles was expected. This effect can be rationalized by the coherent fact that the elastic modulus of any concrete mix is governed by the elasticity of its constituents, characteristics of constituents interface and their volumetric content (Goulias & Ali, 1997). It was therefore concluded that incorporation of optimum rubber particles reduces stiffness of mortar mixes.

4.4. Analytical modeling of results

4.4.1. Overview

This chapter discusses the application of an existing analytical model used by Masuku (2009) to predict the age at cracking. This section comprises of the theoretical background behind the analytical model used, and the results analysis of the age of cracking predicted for main experimental phase mixes. The predicted ages of cracking are also compared and contrasted with the cracking age results observed experimentally. The comparison of these results is done on effort to answer the key question concerned with the effectiveness of an analytical model to predict the age of cracking of rubberized mortar mixes.

There are various numerical methods which could be used to predict the shrinkage cracking age of concrete materials. These methods use the stress and strain relationship of tested materials and predict their shrinkage cracking ages. In the current research study, the most relevant analytical model is the material properties analytical model that was used by Masuku (2009) and Chilwesa (2012). Masuku (2009) and Chilwesa (2012) both observed that the results predicted by this model fitted well with the experimental results, thus why it was considered relevant in the current research study. The model predicts the time of the first crack for mortar mixes based on the measured material properties. Figure 4-18 shows a schematic of the approach used in this analytical model.

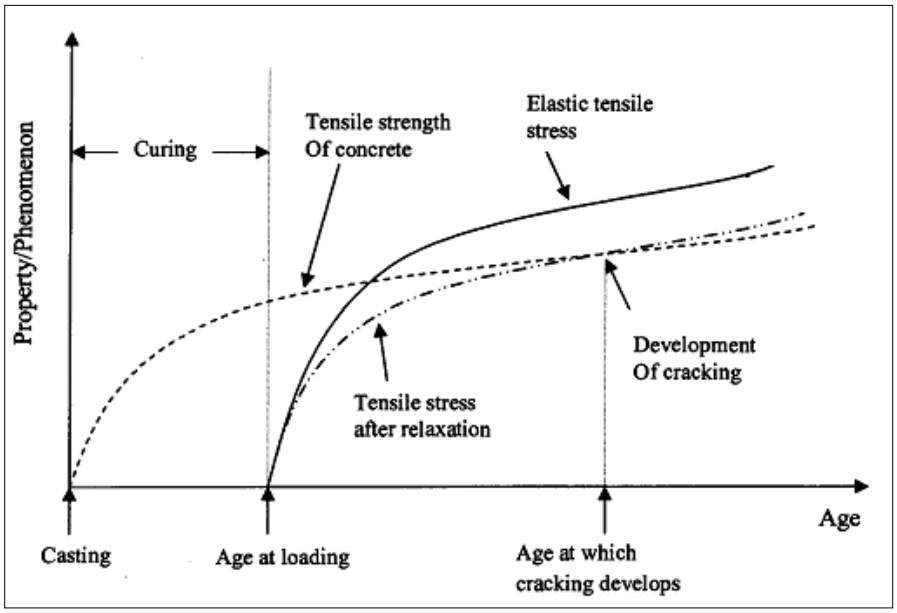

Figure 4-18: Schematic of cracking delay of mortars due to the effect of relaxation (Masuku, 2009).

In order to use this analytical model to predict cracking age of mortar mixes, the results of the measurable material properties from the main experimental phase were needed. These parameters included tensile strength, elastic modulus, tensile relaxation and restrained shrinkage strains. In the current research study, the material properties were tested only at specific ages i.e. tensile strength was tested at the ages of 3, 7, 14 and 28, elastic modulus was tested at the ages of 7, 14 and 28 days, tensile relaxation was tested at the ages of 3, 7 and 14 days. Therefore regression functions were needed to interpolate the intermediate values for the ages that were tested.

Different researchers (Gilbert (1988); Weiss *et al*. (1998); Masuku (2009) and Yoshitake *et al*. (2011)) have used functions such as power functions, exponential functions, hyperbolic functions or logarithmic functions to model the trends in concrete materials. For instance, Weiss *et al*., (1998) used an exponential function to obtain regression fits for elastic modulus of normal concrete. It was however found that the shape of the curve did not correlate with the experimental results so it had to be modified. Yoshitake *et al*. (2011) used a hyperbolic function to predict the tensile modulus at early age for normal mortars. Their equation included two coefficients that accounted for the effect of w/b ratio and age of the mortar specimens. The function could therefore not be used for commercially available mortars because w/b ratio is usually not defined.

On the other hand, Masuku (2009) who studied the "Tensile relaxation of bonded concrete overlays" and Chilwesa (2012) who assessed "The age of cracking of concrete overlays subjected to restrained drying shrinkage" employed an algebraic function expressed in equation 4-1 to predict the margin of tensile relaxation ($\Psi_{(t)}$) of mortar specimens. Masuku (2009) found out that the results from equation 4-1 showed a good match to experimental results. It was therefore decided that the algebraic function used by Masuku (2009) and Chilwesa (2012) should be employed in this research.

$$\Psi(t) = 100 - A * t^{(B)} = 100 - \sigma_t / \sigma_0 \ (\%) \qquad [4\text{-}1]$$

Where; $\Psi(t)$ = mean relaxation function

σ_t = stress at time t_i

σ_0 = Initial stress

A, B= empirical constants

t = time in hours

The other material properties intermediate values that were not measured experimentally were interpolated using the logarithmic based regression functions shown in Equations 4-2 to 4-5. These functions were chosen because they show good fit with experimental data, as shown by Chilwesa (2012). Figure 4-19 shows typical curves used to estimate; tensile strength, elastic modulus and tensile relaxation for mortars. The values interpolated from these curves were used in the analytical model to predict the time of cracking.

$$E_i(t_i) = A\ln(t_i) + B \quad [4\text{-}2]$$

$$F_{Yi}(t_i) = C\ln(t_i) + D \quad [4\text{-}3]$$

$$\beta_i(t_i) = N\ln(t_i) + M \quad [4\text{-}4]$$

$$\Psi_i(t_i) = 100 - \beta_i(t_i) * {}^{1}\!/_{100} \quad [4\text{-}5]$$

Where; $E_i(t_i)$ = mean elastic modulus in the interval t_{i-1}

$F_{Yi}(t_i)$ = tensile strength at time t_i

$\beta_i(t_i)$ = mean relaxation in the interval t_{i-1}

$\Psi_i(t_i)$ = tensile relaxation function in the interval t_{i-1} - t_i

A, B, C, N and M = regression analysis constants

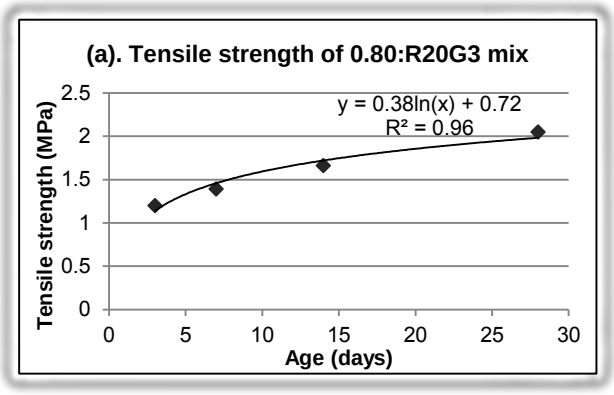

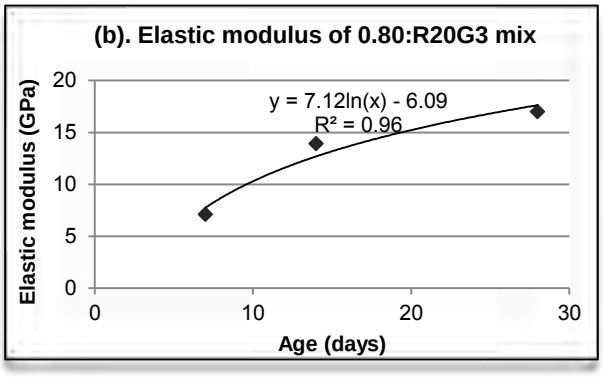

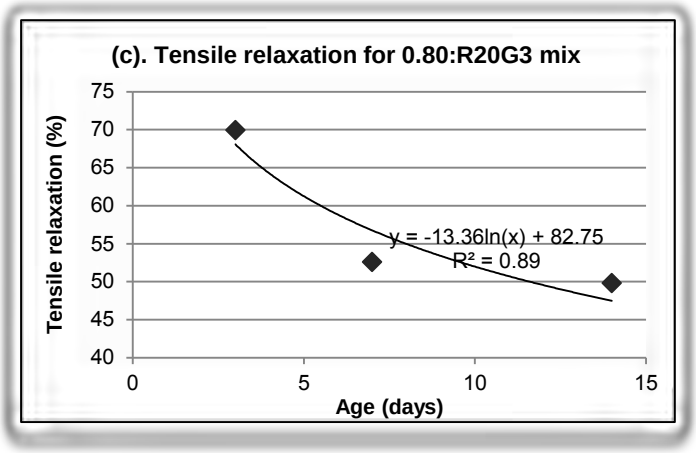

Figure 4-19: Regression curves of; (a) Tensile strength, (b) Elastic modulus and (c) Tensile relaxation for 0.80:R20G3 mix

Unfortunately, there was no direct method that could be used to measure the elastic stress of the mortars. The elastic stress of each mix was therefore estimated from the product of the restrained shrinkage strain and the elastic modulus of the respective mix (see Equation 4-8). The principle of superposition, as discussed by Gilbert (1988) provided the basis on which the time development of the elastic stress was calculated. The elastic stress was required for comparison with the time development of the tensile strength of the mortar in order to predict the age of cracking.

The principle of superposition suggests that the elastic stress (σ_i) can be determined using equation 4-6. It assumes that the concrete mortar is subjected to a time varying strain. Figure 4-20 shows a typical time varying strain history that a concrete mortar can undergo.

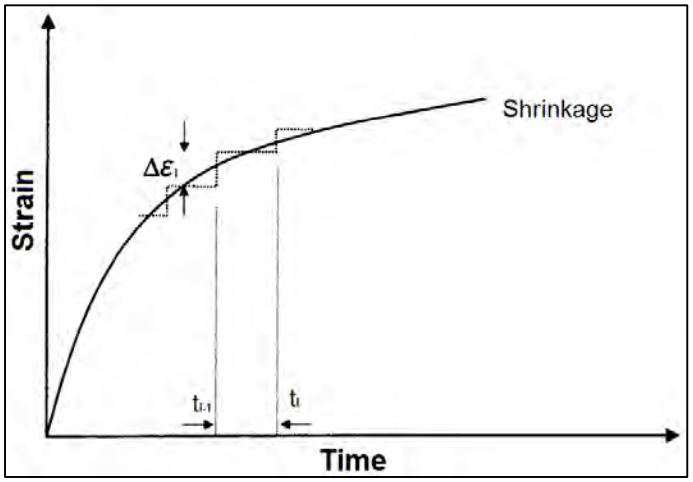

Figure 4-20: Time varying strain history due to shrinkage.

If the strain history is assumed to be varying continuously with time, the strain increment that occurs at the i^{th} time interval and the mean elastic modulus are taken to be applied at the middle of the interval.

$$\sigma_i = \sigma_{i-1} + \Delta\varepsilon_i E_t \qquad [4\text{-}6]$$

Where ; σ_i = stress at time t_i

σ_{i-1} = stress at time t_{i-1}

$\Delta\varepsilon_i$ = change in shrinkage strain in the interval t_{i-1} - t_i

E_i = mean elastic modulus in the interval t_{i-1}

The stress remaining ($\ddot{\sigma}_i$) after accounting for the effects of tensile relaxation (Ψ_i) is also estimated using the approach presented above. Equation 4-7 represents the remaining stress.

$$\ddot{\sigma}_i = \ddot{\sigma}_{i-1} + \Delta\varepsilon_i E_t \Psi_i \qquad [4\text{-}7]$$

Where ; $\ddot{\sigma}_i$ = remaining stress at time t_i

$\ddot{\sigma}_{i-1}$ = remaining stress at time t_{i-1}

$\Delta\varepsilon_i$ = change in shrinkage strain in the interval t_{i-1}- t_i

E_i = mean elastic modulus in the interval t_{i-1}

Ψ_i = mean relaxation factor in the interval t_{i-1}

When predicting the age of cracking, the tensile strength, the elastic stress resulting from restrained shrinkage and the stress remaining after tensile relaxation are all plotted against the age of concrete mortar. The age of cracking is considered to be at the point when the elastic stress curve intersects with the tensile strength curve. This point depicts the age at which the stresses within the mortar exceed the tensile strength of the mortar. The age of cracking could be prolonged by the effect of stress relaxation. If the effect of tensile relaxation is considered, the elastic stress curve intersects with the tensile strength curve at a later age. The point on the graph at which the remaining stress exceeds the tensile strength of the mortar indicates the age of cracking predicted by the model.

4.4.2. Main assumptions about material properties inputs

There are a lot of factors that influence the cracking resistance of the overlays, thus making it very complex to predict their age of cracking. However, there are three main assumptions that were made regarding the calculations of stress development required to perform modeling of cracking age. These assumptions are employed to simplify the process of predicting the age of cracking on mortar mixes;

- ***Shrinkage does not occur during curing period***: This assumption is meant to facilitate the stress calculation resulting from the restraint condition after curing. It is reasonable to employ this assumption because it is assumed that shrinkage occurs only after the period of curing. Figure 4-19 presents the commencement of assumed shrinkage on placed overlays.

- ***Tensile relaxation of overlays is instantaneous***: It has been established by many researchers (Beushausen & Alexander (2006), Masuku (2009) and Chilwesa (2012)) that the tensile stress relaxation develops rapidly just after loading. The results from this research also agree to this finding. The rate at which stress relaxation occurs is way faster than the rate at which shrinkage stress develops in overlays. This assumption is aimed at facilitating easy analytical modeling of results. In this research the relaxation function was taken as a constant value (24 hours) because tensile relaxation was measured for the duration of 24 hours.

- ***Restrained shrinkage is proportionally equivalent to free shrinkage***: It was established from the research conducted by Beushausen (2005) that restrained shrinkage in bonded overlays is approximately 60% of the measured free shrinkage strains. The change in restrained shrinkage strains is therefore estimated by simply applying a factor of 60% to the change in free shrinkage strains.

$$\Delta\varepsilon_i = 0.6\Delta\varepsilon_{FSSi} \quad [4\text{-}8]$$

Where ; $\Delta\varepsilon_i$ = estimated restrained shrinkage strain change for time interval $t_{i-1} - t_i$

$\Delta\varepsilon_{FSSi}$ = measured free shrinkage strain change for time interval $t_{i-1} - t_i$

4.4.3. Modeling the age of cracking for mortar mixes

Figures 4-21 to 4-26 present the predicted ages of cracking for the mixes tested at the main experimental phase. The results were achieved using an analytical model discussed above. The model shows time development of elastic stress and remaining stress starting from the age of 3 days because all the specimens were cured for the period of 3 days. The time development of tensile stress and remaining stress was 28 days because the tensile strength was recorded up to 28 days. This time development of 28 days was also selected because it was observed from the ring test results that all the ring specimens cracked within the duration 28 days.

The elastic stress and remaining stress were plotted against age of mortar once the regression constants were determined. The tensile strength was also plotted on the same curve for each mix. The age of cracking of a respective mortar mix is predicted to occur when the tensile strength curve and remaining stress curve intersect (indicated with the blue arrows from the figures).

The model predicted that 0.80:R20G3 takes 11 days to develop the first crack. This is 4 days earlier than the age recorded experimentally. Compared to its control mix (0.80:R0), the model predicts that the incorporation of rubber particles delayed the occurrence of the crack by 2 days as opposed to 5 days recorded experimentally. From this observation it can be concluded that the model underestimates the age of cracking for 0.80 w/b mix. However, the delay that was observed from both the model and experimental results may still be attributed to the combined effect of increased margin of tensile relaxation and reduced elastic modulus that were observed in 0.80:R20G3 at the early age, due to incorporation of optimum content of rubber particles. The results of modelling the age of cracking for the 0.80 w/b ratio mixes are show in Figure 4-21 and Figure 4-22.

For the mixes with w/b of 0.60, the model predictions of age of cracking were closer to the experimental observations. The model predicted that 0.60:R20G3 takes about 10 days to develop the first crack. This result almost corresponds to the 11 days cracking age that was observed experimentally. Compared to its control mix (0.60:R0), the model predicts that the incorporation of rubber particles delayed the occurrence of the crack by only 0.5 days as opposed to 4 days recorded experimentally. These delays are also attributed to the increased margin of tensile relaxation and reduced elastic modulus in 0.60:R20G3 at the early age, due to incorporation of optimum content of rubber particles. The results of modelling the age of cracking for the 0.60 w/b ratio mixes are show in Figure 4-23 and Figure 4-24.

The model predicted that CRM:R20G3 takes about 11 days to develop the first crack. This age is far way less than the age recorded experimentally (18.5 day). Compared to its control mix (CRM:R0), the model predicts that the incorporation of rubber particles did not have any influence on the age of cracking while it was observed experimentally that incorporation of rubber particles delayed the occurrence of the crack by a total of 8.5 days. The results of modelling the age of cracking for the CRM mixes are show in Figure 4-25 and Figure 4-26.

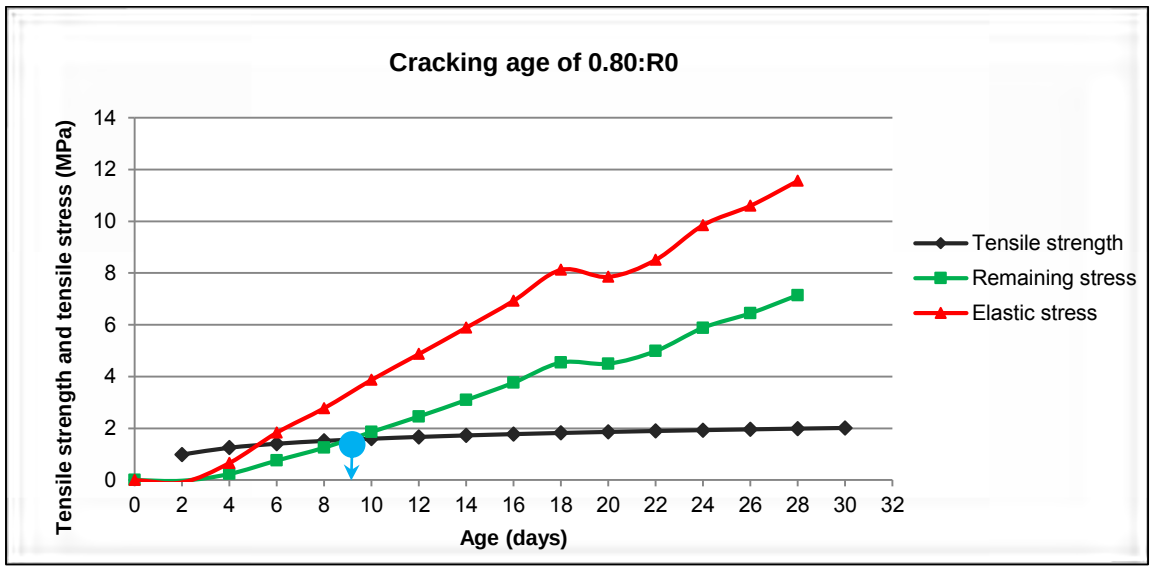

Figure 4-21: Tensile strength and tensile stress development for 0.80:R0 mix.

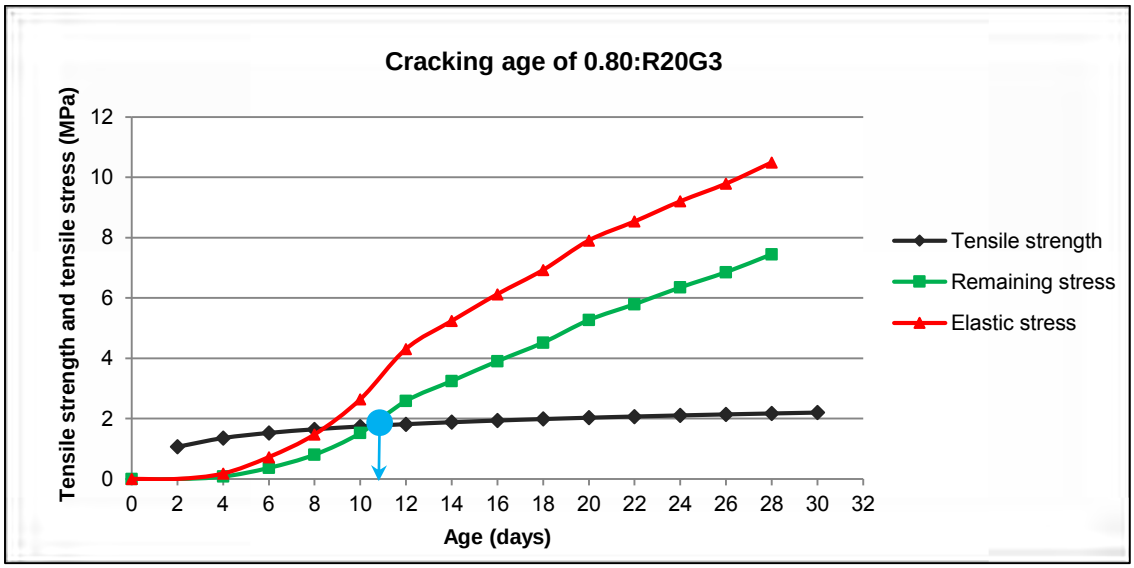

Figure 4-22: Tensile strength and tensile stress development for 0.80:R20G3 mix.

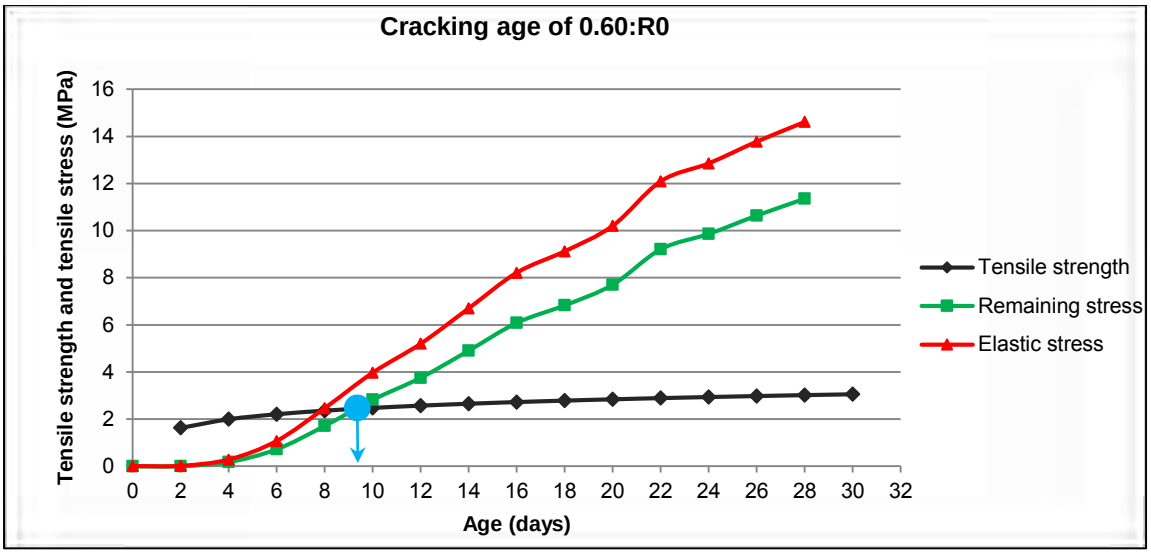

Figure 4-23: Tensile strength and tensile stress development for 0.60:R0 mix.

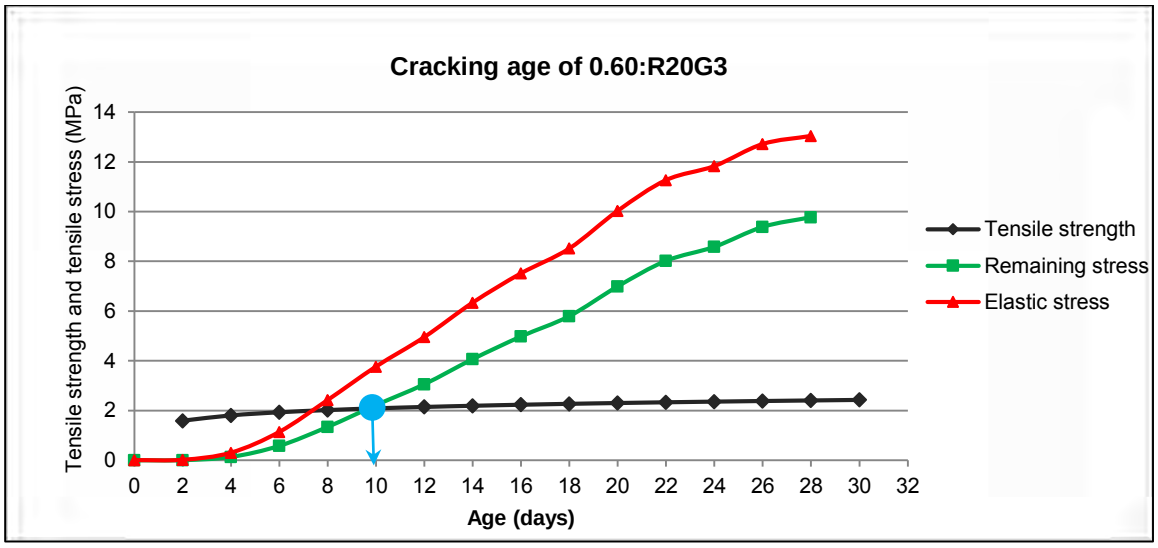

Figure 4-24: Tensile strength and tensile stress development for 0.60:R20G3 mix.

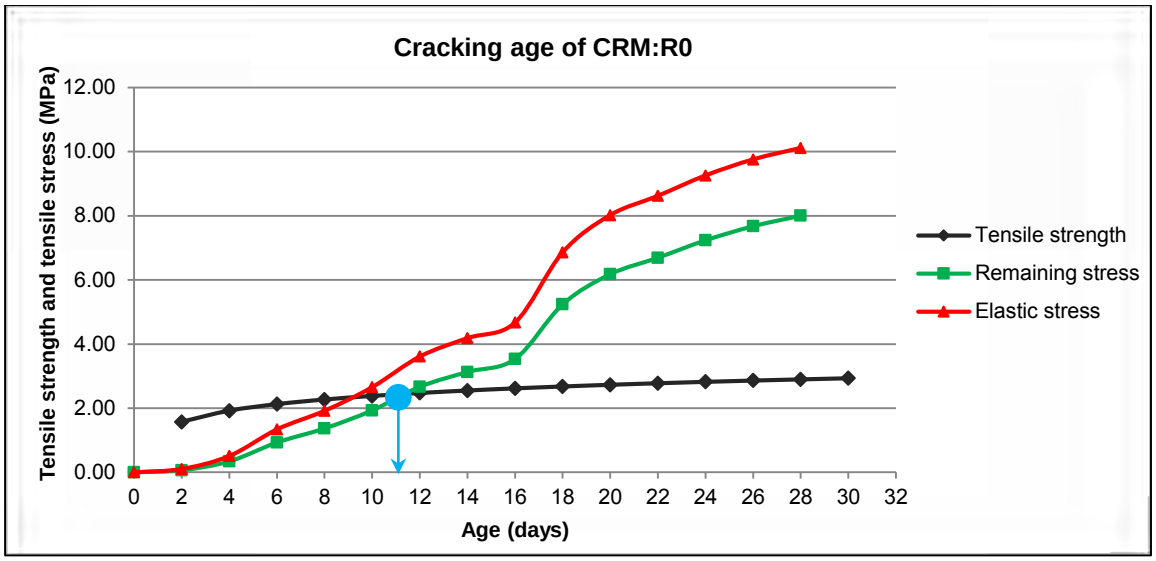

Figure 4-25: Tensile strength and tensile stress development for CRM:R0 mix.

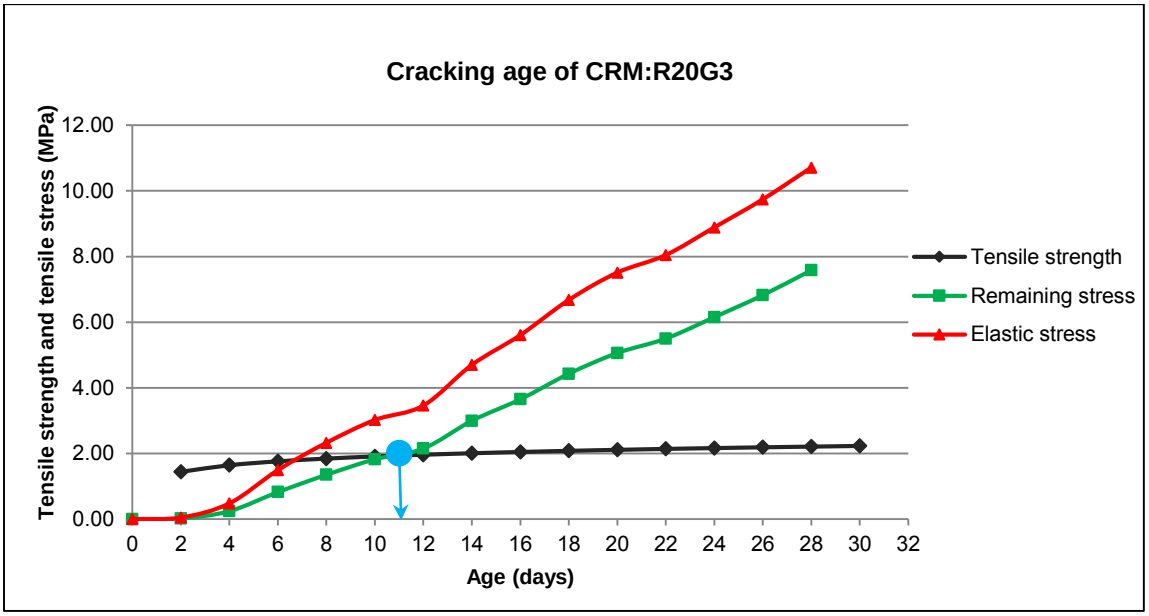

Figure 4-26: Tensile strength and tensile stress development for CRM:R20G3 mix.

4.4.4. Summary of predicted age of cracking compared to experimental age of cracking

It was observed in all the figures that the rate at which the elastic stress develops is much faster than the rate that tensile strength develops. Table 4-3 below presents a comparison of age of cracking results predicted by an analytical model and as observed experimentally. Even though the model

underestimated the influence of rubber particles on the age of cracking, it was still obvious that incorporating rubber particles in mortar mixes delays the age of cracking.

It is anticipated that the delays are due to the rate of increase in relaxation that is higher than the rate of tensile strength gain at the earlier ages. The ultimate effect may be due to a combined effect of the increased relaxation and reduced elastic modulus that outperforms the reduced tensile strength.

Table 4-3: Comparison of experimental age of cracking and modeling age of cracking

0.60 w/b ratio mixes		
Mix ID	***0.60:R0***	***0.60:R20G3***
Experimental age of cracking (days)	7.0	11.0
Predicted age of cracking (days)	9.5	10.0
0.80 w/b ratio mixes		
Mix ID	***0.80:R0***	***0.80:R20G3***
Experimental age of cracking (days)	10.5	15.0
Predicted age of cracking (days)	9.0	11.0
CRM mixes		
Mix ID	***CRM:R0***	***CRM:R20G3***
Experimental age of cracking (days)	10.0	18.5
Predicted age of cracking (days)	11.0	11.0

Beside the age predicted for 0.80 w/b ratio mixes, the table shows that model predictions were very close to the experimental observations. From the Table 4-3 it can be noted that the prediction model has proven to be reasonably accurate in predicting the age of cracking for control mixes, considering the assumptions made in 4.4.2. It was also noted that the model underestimated the cracking ages of (rubberized mixes) 0.60:R20G3, 0.80:R20G3 and CRM:R20G3 by 1 day, 4 day and 7.5 days, respectively.

4.5. Durability Index results

Durability of concrete mortars has been an issue for the concrete structures exposed to various environmental conditions such as; chemical or highly alkaline environment, cyclic wetting and drying in marine environment, temperature changes, salts and chemical environments. Excessive exposure to these conditions often causes expansive stresses in concrete causing cracking. It is therefore necessary to investigate the effect of incorporating rubber particles on durability properties of

rubberized concrete mortars. The durability analysis in this study is with regard to OPI (and k-values) and sorptivity (and porosity) values of the main phase mixes. The results are shown in Figures 4.27 and 4.28.

4.5.1. Oxygen Permeability Index (OPI)

The OPI tests were conducted as per the Durability Index Testing Manual (2010). Specimens were obtained from the 100 mm x 100 mm x 100 mm cubes that were water cured for 28 days. Cubes were cored to obtain the required 70 mm diameter core. The cores were then cut into three 30 mm thick discs for testing. The OPI value is determined by obtaining the negative logarithm of the average of coefficient of permeability (k) values from 3 specimens per test.

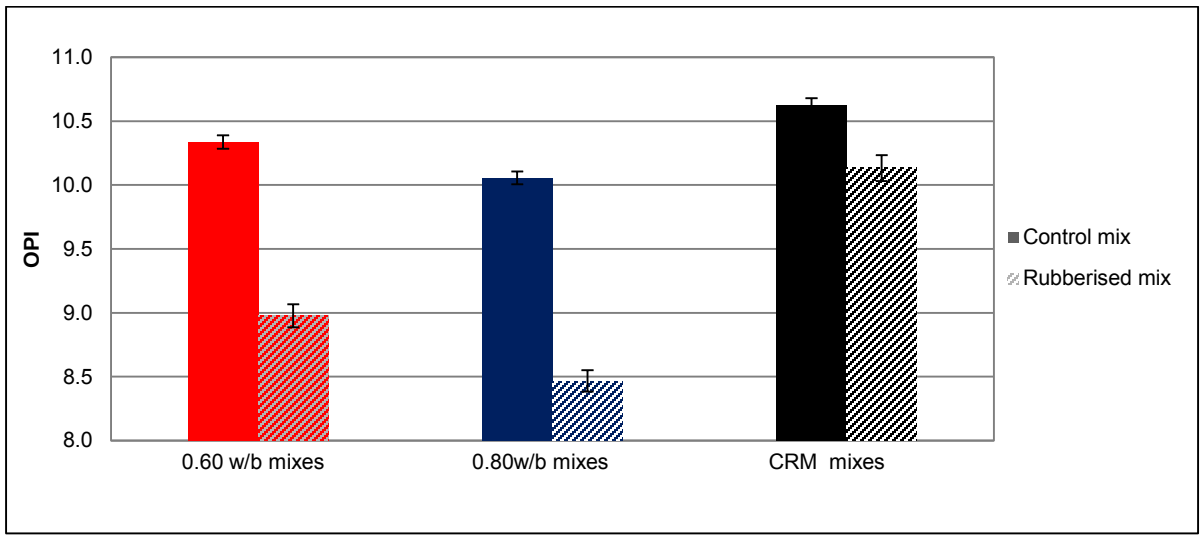

Figure 4-27: OPI results of the main mortar mixes.

The results of the OPI testing on the 0.60 w/b ratio mixes and 0.80 w/b ratio mixes show that an incorporation of rubber particles results in a decrease in OPI. The incorporation of rubber particles has no influence on the OPI results of the CRM mixes. The results of all the testing on the main phase mixes are all similar for control mixes and are all above 10. However, the results of rubberized laboratory made mixes (0.60:R20G3 & 0.80:R20G3) show that OPI decreases to 9.0 and 8.5, respectively. From these results it could be concluded that incorporation of optimum rubber particles in concrete mortar does reduce their OPI but not detrimentally.

4.5.2. Water Sorptivity Index (WSI)

The same specimens that were used for the OPI test were used in the water sorptivity tests. Tests were carried out in accordance with the Durability Index Testing Manual (2010). The results are shown in Figures 4.28.

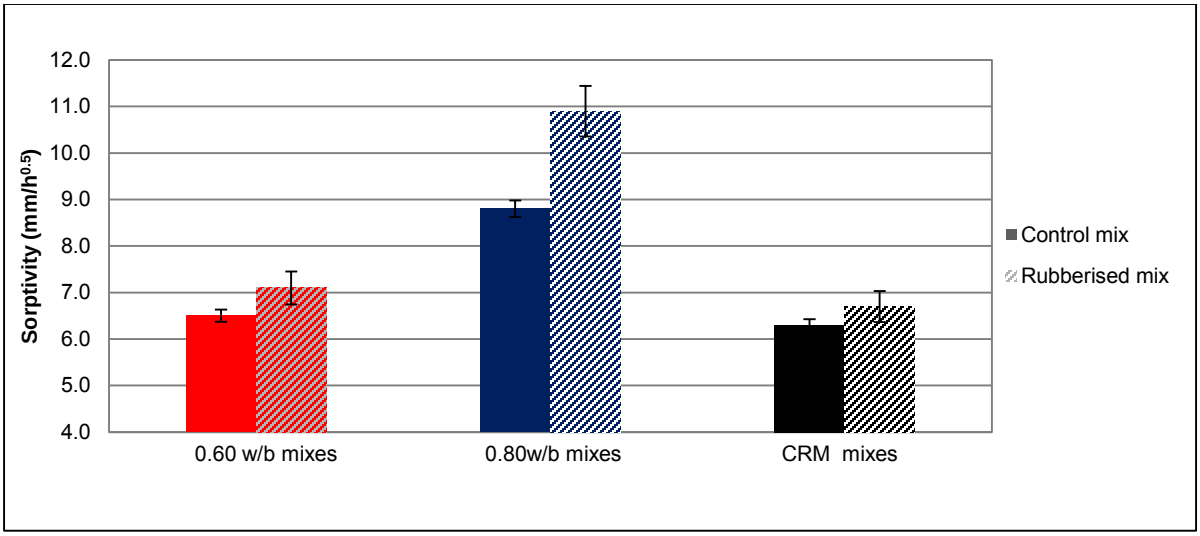

Figure 4-28: Sorptivity results of the main mortar mixes.

The results of the sorptivity testing on the 0.60 mixes and CRM mixes show that an incorporation of rubber particles does not have any influence or sorptivity. But it is however acknowledged that there was a very small increase in sorptivity of these mixes when rubber particles were incorporated. The results of the 0.80 w/b ratio mixes show that an incorporation of rubber particles results in an increases in sorptivity. From these results it could be concluded that an incorporation of rubber particles only has an influence in sorptivity for concrete mortar with higher w/b ratio.

4.5.3. Porosity

The porosity measure for each concrete mortar mix was obtained from the sorptivity testing as per the UCT Durability Index test methods. The results of the porosity testing are shown in Figure 4-29.

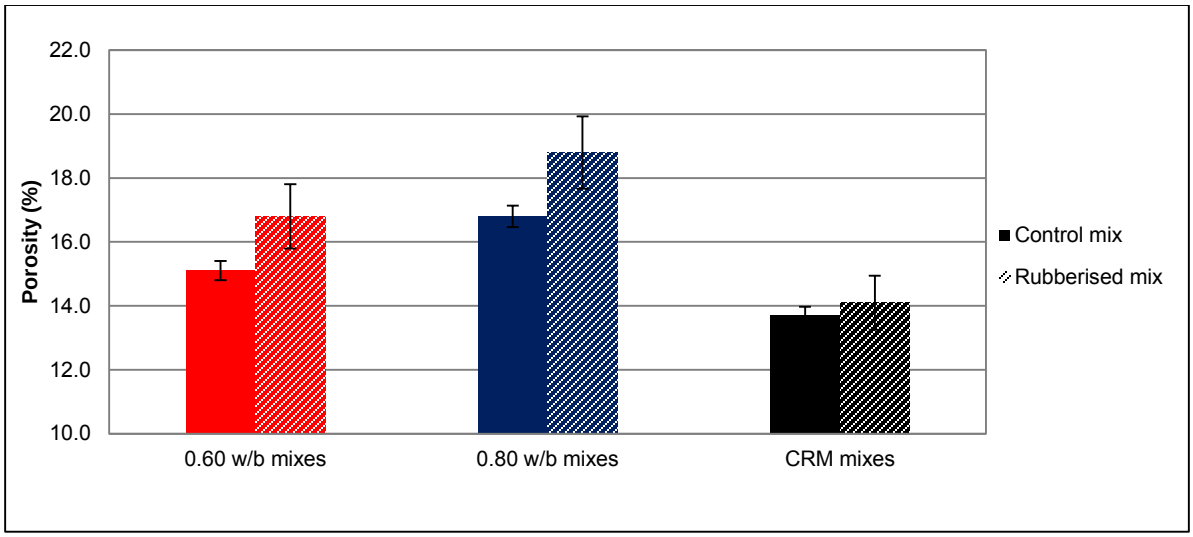

Figure 4-29: Porosity results of the main mortar mixes.

The results of the porosity testing indicate that the incorporation of rubber particles in concrete repair mortars results in an increase in porosity. This is true for both 0.6 w/b and 0.80 w/b ratio mixes, as well as the CRM mix. A possible reason for this effect could be the increase in pore size and distribution introduced by the presence of rubber particles in mortar mixes. Research conducted by Ho & Turatsinze (2009), showed that mortar mixes incorporating rubber particles had behave like mortar mixes with regularly spaced holes which act like macro pores within the mortar. Literature suggests that an incorporation of rubber particles within cement based materials results in weak aggregate-paste bond structure. This poor bond structure leads to the pores interconnectivity, hence increasing the quantity porosity within the cement paste.

4.6. Chapter summary

Testing of material properties of concrete mortars were carried out and summary of the main findings is discussed in this section. In addition, the age at cracking and intensity of cracking (crack area) were also determined using the ring tests.

It was observed in both initial and main testing phase that the replacement of natural aggregates by rubber particles results in reduction in compressive strength and tensile strength. The trends from free shrinkage testing results showed that incorporation of rubber particles has less or no influence on free shrinkage capacity of 0.60:R0 and CRM:R0 mixes. When comparing the degree of free shrinkage for rubberized mortars and control mixes, it can be seen that the incorporation of rubber

particles only had little influence on shrinkage of 0.80 w/b ratio mix. The increased shrinkage in this mix may be because of the higher void content introduced by incorporation of rubber particles.

In spite the reduction in tensile strength and little increase in free shrinkage in mortars. It was observed, from initial and main experimental ring testing results, that incorporation of rubber particles result in delayed time of cracking. It was also observed that rubberized mortar mixes exhibit less crack widening, compared to their respective control mortar mixes. Most of the rubberized mortar specimens developed only one continuous crack, for specimens that developed 2 cracks, both cracks ran through the entire height of the ring specimens. The crack growth trends were mainly due to the evolution of the opening of the main crack. It was observed that the width of secondary crack stayed relatively the same since it developed thus having no effect in crack area growth. These 2 interesting observations made it conclusive that the crack area growth is the function of the crack width widening of the main crack only. It was seen from the main experimental phase test results that there is a positive synergetic effect on time of cracking and cracking intensity of mortar mixes when rubber particles are incorporated.

The relaxation test results indicate that an incorporation of rubber particles results in an increased margin of tensile relaxation. It is also observed that the margin of tensile relaxation decreases with an increase in age of testing. Specimens tested at the younger age seem to undergo higher margin of relaxation than the specimens tested at the older age. This observation is consistent with the findings by Masuku (2009) and Chilwesa (2012). Masuku (2009) commented that due to higher degree of hydration in later age, specimens seem to undergo lower relaxation because of higher strength they have gained.

It was also observed that an incorporation of rubber particles results in the reduction of elastic modulus of mortar mixes. This effect can be rationalized by the coherent fact that the elastic modulus of any concrete mix is governed by the elasticity of its constituents, characteristics of constituents interface and their volumetric content (Goulias & Ali, 1997). There incorporation of a more elastic material (rubber particles) in a concrete mix will result in reduction of elastic modulus.

CHAPTER FIVE

CONCLUSIONS AND RECOMMENDATIONS

5.1. Introduction

All concrete structures deteriorate over time due to their exposure to harsh environmental conditions. Deteriorations often lead to the concrete structures reaching unserviceable state before their design end of service life. It is at this state that rehabilitation becomes necessary to retain the good structural functionalities. Often, concrete overlays are used in rehabilitation of concrete structures.

After repair placement, differential shrinkage is often experienced by the concrete overlays due to drying shrinkage. Differential shrinkage results in development of tensile stresses within concrete overlays. These tensile stresses may lead to cracking if they exceed the tensile strength of the concrete overlay. But this cracking problem could be avoided or delayed by increasing concrete overlays' tensile strength, reducing shrinkage, reducing elastic modulus or by increasing the tensile relaxation of concrete overlay.

Incorporation of recycled tyre rubber particles is a relatively new technology used in concrete and concrete mortars. The studies concerning this technology involve incorporation of rubber particles to in concrete mortars in order to change the material properties of mortars for an intended use. However, no research has been conducted on the effects of optimizing rubber particle gradation and content on cracking resistance of concrete mortars. The current research therefore focused on investigating how the incorporation of the rubber particles influences material properties that affect cracking resistance of concrete mortars. The positive or negative effects were analyzed.

The most observable positive effect of incorporating rubber particles in concrete mortars to improve their cracking resistance was the reduction in elastic moduli of rubberized mortars. In addition to the reduced elastic moduli, incorporation of rubber particles resulted in an increased tensile relaxation capacity. The higher tensile relaxation capacity decreases development of stresses with concrete mortars by allowing tensile stresses to be released. This effect has potential to delay cracking or reduce the likelihood of cracking. Both these effects improve the strain capacity of cementitious materials, meaning that higher tensile stresses could be sustained with less risk of cracking.

Although a little increase in free shrinkage and reduction of tensile strength observed on rubberized concrete mortar specimens, ring test results showed that rubberized mortar ring specimens were all characterized by the delayed cracking age. It was also observed from the initial testing phase that crack area growth reduces with increasing the content of rubber particle.

5.2. General conclusions

The incorporation of rubber particles influenced the cracking performance of mortar mixes both positively and negatively. The variation of rubber particles content (5%, 10% and 20%) and gradation (G1, G2, & G3) of rubber particles influenced various material properties of concrete mortars in different ways. The significance and influence of rubber particles incorporation on various mortar mixes are summarized in this section and concluding remarks are given. These concluding remarks were drawn from the analysis of research results from both initial and main experimental testing phases, as discussed in Chapter 4.

5.2.1. Initial experimental phase conclusions

The influence of rubber particles incorporation was investigated on compressive strength, splitting tensile strength and ring tests. The compressive strength and splitting tensile strength test results indicated that an increase in rubber particle content results in a reduction of strength and slower strength development. These influences are more prominent on mortar specimens with a lower w/b ratio (0.45 w/b) or rather the specimens with higher strength properties.

The incorporation of rubber particles influences the degree of restrained shrinkage (ring test) significantly. From both mortars mixes with 0.45 w/b and 0.60 w/b ratios, the results showed that increasing rubber particle content improves the cracking performance of ring specimens under restrained condition. Age of 1st crack development on all mortar specimens was prolonged when the content of rubber particles was increased. An increase the content of rubber particles also reduces the chances and intensity of crack widening.

The results obtained in the current research agree with the results obtained by Ho & Turatsinze (2009); Turatsinze *et al*. (2005) and Turatsinze *et al*. (2007) which state that; strength reduces with increasing rubber particle content and that age of cracking gets delayed with increasing the content of rubber particles. Most importantly, using the rubber particles with gradation that is similar to that of the natural aggregates being replaced results in a minimal strength reduction and it delays the

occurrence of cracks. The 20% content of gradation 3 rubber particles was found to be the sample that performed in resisting cracking (optimum content and gradation).

5.2.2. Main experimental phase conclusions

Incorporation of optimum rubber particle content and gradation enhanced cracking resistance of the mortar mixes. It resulted in the increased tensile relaxation, reduced elastic modulus, prolonged age of cracking and reduction in crack area. However, it was observed that incorporation of optimum gradation and content of rubber particles also resulted in a little increase in the rate of drying free shrinkage that occurs at early ages after the casting of the overlay. It was also observed that incorporation of rubber particles results in reduced OPI values and increased WSI values of the concrete mortars. These observations indicate that the permeability of the mortar mixes increases when rubber particles are incorporated.

5.2.3. Analytical modeling conclusions

The analytical model results showed that incorporations of rubber particles in concrete mortars results in the delay of their cracking age. For control concrete mortars, the model predicted the cracking age within reasonably accurate range when comparing them with the cracking age observed from the experimental results. However, the model seemed to underestimate the age of cracking for rubberized mortars.

5.3. General recommendations

The results from the current research showed that incorporation of rubber particles in concrete mortars could potentially enhance some of the properties that influence cracking resistance. It was observed that most of the positive effects become more observable in concrete mortars of higher w/b ratio (0.8 w/b). It was also observed that increasing rubber particle content affects strength development detrimentally; however optimization of rubber particle content and gradation improves the overall cracking resistance performance.

The outcomes on this research are limited to the scope and objectives of the study. Although the influence of rubber particles on material properties that affect cracking resistance of concrete mortars were identified, it is recommended that the following aspects be considered for deeper understanding:

- The sampling of the initial experimental phase of the current research involved incorporation of 3 different rubber particle gradations and 3 different contents. The total of 18 rubberized concrete mortars were tested and their 2 respective control mortars. Due to this large number of mixes, the effects of rubber particles on were only tested in 2 different concrete mortars (0.45 w/b ratio and 0.60 w/b ratio mixes). Therefore, it is proposed that further research and testing be performed on a wide variety of concrete mortars of different w/b ratios.
- The main experimental phase involved the testing of only 1 commercially available polymer modified repair mortar (CRM) and other 2 laboratory made concrete mortars. Further research should be done in order to determine the influence of incorporating rubber particles on a wide variety of common commercial repair mortars.
- In both initial and main experimental phase, only 1 curing regime was considered. It is therefore recommended that further research focusing on different curing regimes be done to investigate any benefits of incorporating rubber particles in concrete mortars in conjunction to various curing regimes.
- The ring test and free shrinkage specimens were exposed to uncontrolled, open laboratory space during the entire duration of the inspection and testing. The daily temperature data recorded using HygroLog HL20 data logger showed that there were changes in temperature and RH during the time of inspection. It is therefore recommended that when a similar research is conducted, ring test specimens and free shrinkage specimens be kept in fully controlled laboratory conditions for the duration of inspection. This will help to limit uncertainties and overestimations of shrinkage reading that may result in fluctuating conditions at the early age of testing.
- The strength tests conducted (compressive, splitting tensile and direct tensile strength) showed that incorporation of rubber particles affects strength development detrimentally. It is therefore recommended that the research focusing on mitigating and minimizing the strength reduction be conducted to investigate further benefits of incorporating rubber particles in concrete mortars.

REFERENCES

Ahmed, I., & Lovell, C.W. 1992. Use of Waste Materials in Highway Construction: State of the Practice and Evaluation of Shredded Waste Products. *Transportation Research Board*. Washington DC.1-9.

American Concrete Institute (ACI) 1999, ACI 318 (1999). "Building Code Requirements for Structural Concrete (ACI 318-99) and Commentary (ACI 318R-99)", Farmington Hills, Michigan, USA

Alexander, M.G. 1994. Deformation properties of blended cement concretes containing blast furnace slag and condensed silica fume. *Advances in cement research*. 6(22):73-81.

Alexander, M.G. 2001. Deformation and volume change of hardened concrete. In Fulton's Concrete Technology. G. Owens, Ed. 8th ed. Midrand, South Africa: Cement and Concrete Institute.

Alexander, M.G. & Mackechnie, J.R. 2001. Use of durability indexes to achieve durable cover concrete in reinforced concrete structures. *In Materials Science of Concrete*. J.P. Skalny and S. Mindess, Ed. Westerville: American Ceramic Society. 483-511.

Alexander, M.G. & Beushausen, H. 2008. The South African durability index test in an international comparison. *Journal of the South African institution of civil engineering*. 50 (1):25-31.

Allen, R.T.L. & Edwards, S.C. 1987. The Repair of Concrete Structures. Glasgow & London: Blackie.

Ali, N.A., Amos, A.D. & Roberts, M.1993. Use of Ground Rubber Tyres in Portland Cement Concrete. *Proc. Int. Conf*. University of Dundee, UK: Concrete 2000.379-390.

Asad, M., Baluch, M.H. & Al-Ghadib, A. H. 1997. Drying shrinkage stresses in concrete patch repair systems. *Magazine of Concrete Research*. 49(181):283–293.

ASTM C 1581-04. 2004. Standard test method for determining age at cracking and induced tensile stress characteristics of mortar and concrete under restrained shrinkage. Book of standards ASTM committee C09 on concrete and concrete aggregates C09.68.

Atis, C.D. 2003. High-volume fly ash concrete with high strength and low drying shrinkage. *Journal of Materials in Civil Engineering.15* (2):153–156.

Ballim, Y. & Alexander, M.G. 2005. Towards a performance based specification for concrete durability. *African concrete code symposium*. 206-209.

Ballim, Y., Beushausen, H. & Alexander, M. 2009. Durability of concrete. In Owens, G. (ed). *Fulton's concrete technology.* 9th ed. Midrand, South Africa: Cement & Concrete Institute. 155-188.

Ballim, Y. & Graham, P.C. 2009. The effects of supplementary cementing materials in modifying the heat of hydration of concrete. *Materials and structures*. 42:803-811.

Banthia, N., & Gupta, R. 2006. Repairing with fiber reinforced concrete repairs. *ACI Concrete International*. 28(11):36–40.

Banthia, N. & Gupta, R. 2008. Plastic shrinkage cracking in cementitious repairs and overlays. *Materials and Structures*. 42(5):567-579.

Beushausen, H. 2005. Performance of bonded concrete overlays subjected to differential shrinkage. *Doctoral Thesis*. University of Cape Town.

Beushausen, H. & Alexander, M.G. 2006. Localized strain and stress in bonded concrete overlays subjected to differential shrinkage. *Materials and Structures*. 40(2):189-199.

Beushausen, H. & Alexander, M. 2009. Concrete repair. In Owens, G. (ed). *Fulton's concrete technology.* 9th ed. Midrand, South Africa: Cement & Concrete Institute. 393-412.

Beushausen, H., Masuku, C. & Moyo, P. 2012. Relaxation characteristics of cement mortar subjected to tensile strain. *Materials and Structures*. 45(8):1181-1188.

Care, S. & Nicolle, O. 2005. Characterization des gradients de microstructure des materiaux cimentaires induits par les couplages hydratation-transfert d'eau: application aux structures de beton arme reparees. 17th congresfrancais de mecanique,troyes.

Carlson,R.W. & Reading, T.J. 1988. Model of studying shrinkage cracking in concrete building walls. *ACI Structural Journal*. 85(4):395–404.

Carlswärd, J. 2006. Shrinkage cracking of steel fibre reinforced self-compacting concrete overlays; Test methods and theoretical modelling. *Doctoral Thesis*. Luleå University of Technology: Luleå, Sweden.

Caron, I., Fiori, F., Mesmacque, G., Pirling, T. & Su, M. 2004. Expanded hole method for arresting crack propagation: residual stress determination using neutron diffraction. *Physica B: Condensed Matter B*. 350:503–504.

Chilwesa, M. 2012. Assessing the age at cracking of concrete repair mortars/overlays subjected to restrained drying shrinkage. Cape Town: University of Cape Town. MSc Thesis.

Durability Index Testing Procedure Manual (2010)

Eldin, N.N. & Senouci, A.B. 1993. Rubber-tyre particles as concrete aggregate. *Journal of Materials in Civil Engineering*. 5(2):478-496.

Fatuhi, N.I., & Clark, N.A. 1996. Cement-based materials containing tyre rubber. *Construction Building Materials*. 10(4):229-236.

Gadkar, Shubhada. 2013. Freeze-thaw durability of portland cement concrete due to addition of crumb rubber aggregates. South Carolina. Clemson University. PhD Thesis.

Ganjian, E., Khorami, M., & Maghsoudi, A.A. 2009. Scrap-tyre-rubber replacement for aggregate and filler in concrete. *Construction and Building Materials*. 23:1828–1836.

Ghali, A, Favre, R & Eldbadry, M. 2006. Concrete Structures: Stresses and deformations. *Third edition e-copy ed*. London: Taylor & Francis e-library.

Geiker, M.R., Bentz, D.P. and Jensen, O.M. 2004. Mitigating autogenous shrinkage by internal curing: High performance structural lightweight concrete, SP-218. In Ries J.P., and Holm, T. A. (eds.) *American Concrete Institute*. Farmington Hills: Mich. 143-154.

Goulias, D.G., & Ali, A.H. 1997. Non-destructive evaluation of rubber modified concrete. *Proceedings, Special Conference*. New York: ASCE. 111-120.

Goulias, D.G. & Ali, A.H. 1998. Evaluation of rubber filled concrete and correlation between destructive and non-destructive testing results. *Cement, Concrete and Aggregates*. 20(1):140–144.

Grieve, G. 2009. Aggregates of concrete. InOwens, G. (ed). *Fulton's concrete technology*.9th ed. Midrand, South Africa: Cement & Concrete Institute. 25-61.

Grieve, G. 2009. Cementitious materials. In Owens, G. (ed).*Fulton's concrete technology*.9th ed. Midrand, South Africa: Cement & Concrete Institute. 1-16.

Ho, A.C., Turatsinze, A. & Vu, D.C. 2008. Innovative materials and influences of material composition: On the potential of rubber aggregates obtained by grinding end-of-life tyres to improve the strain capacity of concrete. In Alexander, M.G., Beushausen, H., Dehn, F., & Moyo, P. (eds.). *Concrete Repair, Rehabilitation and Retrofitting II*. London: Taylor & Francis Group. 123-129.

Ho, A., & Turatsinze A., Hameed, R. & Vu, D.C. 2012. Effects of rubber aggregates from grinded used tyres on the concrete resistance to cracking. *Journal of Cleaner Production*. 23:209-215.

Hobbs, D.W. & FInst, P. 1971.The dependence of the bulk modulus, Young's modulus, creep, shrinkage and thermal expansion of concrete upon aggregate volume concentration. *Matériauxet Construction*. 4(20):107–114.

Khatib, Z.K. & Bayomy, F.M. 1999. Rubberized Portland cement concrete. *Journal of Materials in Civil Engineering*. 11:206-213.

Kellerman, J. & Crosswell, J. 2009. Properties of fresh concrete. In Owens, G. (ed). *Fulton's concrete technology*.9th ed. Midrand, South Africa: Cement& Concrete Institute. 83-95.

Mangat, P. & O'Flaherty, F. 2000. Influence of elastic modulus on stress redistribution and cracking in repair patches. *Cement and Concrete Research*. 30(1):125-136.

Masuku, C. 2009. Tensile relaxation of bonded concrete overlays. Cape Town: University of Cape Town. MSc Thesis.

Meadows.W.R. 2014.Concrete Restoration. Available: http://www.wrmeadows.com/concrete-restoration. 09 March 2014.

Mehta, K.P. & Monteiro, PJ.M. 2006a. Dimension Stability. *In Concrete: Microstructure, Properties, and Materials*. Third ed. United States of America: McGraw-Hill Companies. 85.

Mindess. S. Young, J.F. & Darwin, D. 2003. Concrete. *Second edition.* New Jersey: Prentice-Hall, Pearson Ed.

Naik, T.R., Ramme, B.W., & Tews, J.H. 1995. Pavement construction with high-volume class C and class F fly-ash concrete. *ACI Material Journal*. 92(2):200–210.

Nehdi, M. & Khan, A. 2001.Cementitious composites containing recycled tyre rubber: An overview of engineering properties and potential applications. *Cement, Concrete, and Aggregates, CCAGDP*. 23(1):3–10.

Nguyen T.-H., Toumi, A., Turatsinze, A. & Tazi, F. 2012. Restrained shrinkage cracking in steel fibre reinforced and rubberized cement-based mortars. *Materials and Structures.* 45:899–904.

Owen, K.C. 1998. Scrap Tyres: A Pricing Strategy for a Recycling Industry. *Corporate Environmental Strategy*. 5(2): 42-50.

Oikonomou, N. & Mavridou, S. 2009. Improvement of chloride ion penetration resistance in cement mortars modified with rubber from worn automobile tyres. *Cem Concr Compos.* 31:403–407.

Pearlman, S.L. & Porbaha, A. 2006. Design and monitoring of an embankment on controlled modulus columns. *Transportation Research Record.* 1975:96–103.

Pelisser, F., Zavarise, N., Longo, T.A., & Bernardin, A.M. 2011. Concrete made with recycled tyre rubber: effect of alkaline activation and silica fume addition. *Journal of Cleaner Production*. 19(7) 757-763.

Perrie, B. 2009. Strength of hardened concrete. In Owens, G. (ed). *Fulton's concrete technology.*9th ed. Midrand, South Africa: *Cement & Concrete Institute*. 97-110.

Raghavan, D., Huynh, H. & Ferraris, C.F. 1998. Workability, Mechanical Properties, and Chemical Stability of a Recycled Tyre Rubber-Filled Cementitious Composite. *Journal of Materials Science*. 33(7):1745–1752.

SANS 5863. 2006. Concrete tests - Compressive strength of hardened concrete. Pretoria: South African Bureau of Standards.

SANS 5865: 1994. Concrete tests - The drilling, preparation, and testing for compressive strength of cores taken from hardened concrete. Pretoria: South African Bureau of Standards.

SANS 6253. 2006. Concrete tests - tensile splitting strength of concrete. Pretoria: South African Bureau of Standards.

Savas, B.Z., Ahmad, S. & Fedroff, D. 1996. Freeze-thaw durability of concrete with ground waste tyre rubber. *Transportation Research.* 1574: 80-88.

See, H.T., Attigole, E.K. & Miltenberger, A. 2003. Shrinkage cracking characteristics of concrete using ring specimens. *ACI Materials Journal*. 100(3):239–245.

Segre, N. & Joekes, I. 2000. Use of tyre rubber particles as addition to cement paste. *Cement and Concrete Research.* 30:1421-1425.

Shazali, M.A., Rahman, M.K. & Baluch M.H. 2012. Shrinkage stress damage effect in concrete patch repair. *Concrete Repair, Rehabilitation and Retrofitting III .*In Alexander, M.G., Beushausen, H., Dehn, F. & Moyo, P. (eds.). London: Taylor & Francis Group. 1071-1076.

Shkarayev, S. 2003. Theoretical modelling of crack arrest by inserting interference fit fasteners. *International Journal of Fatigue.* 25(4):317–324.

Subramaniam, K. 2005. Influence of ultrafine fly ash on the early age response and the shrinkage cracking potential of concrete. *Journal of Materials in Civil Engineering*. 17(1):45–53.

Tantala, M.W., Lepore, J.A. & Zandi, I. 1996. Quasi-elastic behavior of rubber included concrete. *Proceedings 12th International Conference on Solid Waste Technology and Management*. Philadelphia.

Toumi, A., Nguyen, T.-H. & Turatsinze, A. 2013. Debonding of thin rubberised and fibre-reinforced cement-based repairs: Analytical and experimental study. *Materials and Design*. 49:90–95.

Toutanji, H.A. 1996. The use of rubber tyre particles in concrete to replace mineral aggregates. *Cement and Concrete Composites*. 18:135–139.

Topcu, I.B. & Avcular, N. 1997. Collision behavior of rubberized concrete. *Cement and Concrete Research*. 27(12):1893-1898.

Topcu, I. B. & Demir, A. 2007. Durability of Rubberized Mortar and Concrete. *Journal of Materials In Civil Engineering.* 19(2):173–178.

Tritsch, N., Darwin, D. & Browning, J. 2005. Evaluating shrinkage and cracking behavior of concrete using restrained ring and free shrinkage tests. Kansas: The University of Kansas Center for Research.

Troxell, G.E., Davis, H.E. & Kelly, 1.W. 1968. Influence of shrinkage and creep on concrete cracking. *In Composition and Properties of Concrete*. New York: McGraw-Hill. 342.

Turatsinze, A., Bonnet, S. & Granju, J.L. 2003. Cement-based materials incorporating rubber aggregates shrinkage length changes. In: Brandt, A.M., Li, V.C., Marshall, I.H., (eds). *Proceedings of the sixth international symposium on brittle matrix composites BMC7.* Warsaw: Woodhead Publishing Ltd. 259–368.

Turatsinze, A., Bonnet, S. & Granju, J.L. 2005. Mechanical characterization of cement based mortar incorporating rubber aggregates from recycled worn tyres. *Building and Environment.* 40:221–226.

Turatsinze, A., Bonnet, S. & Granju, J.L. 2006. Positive synergy between steel-fibres and rubber aggregates: effect on the resistance of cement-based mortars to shrinkage cracking. *Cement and Concrete Research.* 36:1692–1697.

Turatsinze, A., Bonnet, S. & Granju, J.L. 2007. Potential of rubber aggregates to modify properties of cement based-mortars: improvement in cracking shrinkage resistance. *Construction and Building Materials.* 21:176–181.

Turki, M., Bretagne, E., Rouis, M.J. & Quéneudec, M. 2009. Microstructure, physical and mechanical properties of mortar-rubber aggregates mixtures. *Constr Build Mater.* 23:2715-2722.

Uygunoglu, T. & Topco, J.B. 2010. The role of scrap rubber particles on the drying shrinkage and mechanical properties of self-consolidating mortar. *Constr Build Mater.* 24(7): 1141-1150.

Vaysburd, A.M., Emmons, P.H., McDonald, J.E., Poston, R.W. & Kesner, K.E. 2000. Selecting durable repair materials: performance criteria – field studies. *Concrete International*. 2000.39-45

Vaysburd, A.M., Emmons, P.H. & Bissonnette, B. 2012. Concrete repair as an engineering task: An approximate solution to an exact problem. *Concrete Repair, Rehabilitation and Retrofitting III.* In Alexander, M.G., Beushausen, H., Dehn, F. & Moyo, P. (eds.). London: Taylor & Francis Group. 862-869.

Weiss, W.J., & Shah, S.P. 2002. Restrained shrinkage cracking: The role of shrinkage reducing admixtures and specimen geometry. *Materials and structures*. 34(246):85-91.

Weiss, W.J., Yang. W., & Shah, S.P. 1998. Shrinkage Cracking of Restrained Concrete Slabs. *Journal of engineering mechanics*. July: 765-774.

Zhang, Y., Wei, S. and Shengxia, C. 2006. Study on Properties of Rubber Included Concrete under Wet-dry Cycling Measuring. *Monitoring and Modeling Concrete Properties*. 395-401.

APPENDICES

Appendix A: Average temperatures and relative humidity for open laboratory section

Date	Temp [^{0}C]	RH [%]
2014/08/05	18.49	60.91
2014/08/06	18.36	60.97
2014/08/07	18.30	62.31
2014/08/08	18.47	59.92
2014/08/09	18.77	67.57
2014/08/10	18.88	64.84
2014/08/11	18.91	63.88
2014/08/12	19.25	64.21
2014/08/13	19.52	63.42
2014/08/14	19.25	64.40
2014/08/15	18.77	60.86
2014/08/16	18.79	60.68
2014/08/17	19.01	56.12
2014/08/18	19.08	59.63
2014/08/19	18.95	64.21
2014/08/20	18.87	61.58
2014/08/21	18.30	54.22
2014/08/29	17.95	55.83
2014/08/30	18.01	55.70
2014/08/31	18.48	54.54
2014/09/01	18.88	55.48
2014/09/02	19.23	54.11
2014/09/03	18.99	56.81
2014/09/04	19.02	57.23
2014/09/05	19.01	58.86
2014/09/05	18.98	59.74
2014/09/06	18.87	63.76
2014/09/07	18.85	59.52
2014/09/08	18.77	62.47
2014/09/09	18.68	61.86
2014/09/10	18.56	61.55
2014/09/11	18.58	63.73
2014/09/17	19.06	64.26
2014/09/18	18.84	57.57
2014/09/19	18.83	55.50
2014/09/20	18.56	54.15

Appendix B: Tables of laboratory test results from initial testing phase

B.1: Compressive strength for 0.45 w/b mixes [GPa]

3 days results			
	Batch 1: Gradation 1	Batch 2: Gradation 2	Batch 3: Gradation 3
Control mix: 0%	27.6	27.6	27.6
Rubber particles: 5%	20.8	19.4	21.8
Rubber particles: 10%	15.3	14.9	17.4
Rubber particles: 20%	14.7	11.7	15.0

7 days results			
	Batch 1: Gradation 1	Batch 2: Gradation 2	Batch 3: Gradation 3
Control mix: 0%	32.9	32.9	32.9
Rubber particles: 5%	27.5	27.0	27.7
Rubber particles: 10%	24.9	21.6	26.9
Rubber particles: 20%	21.6	15.2	25.4

14 days results			
	Batch 1: Gradation 1	Batch 2: Gradation 2	Batch 3: Gradation 3
Control mix: 0%	39.3	39.3	39.3
Rubber particles: 5%	34.1	32.1	37.8
Rubber particles: 10%	27.8	25.6	28.8
Rubber particles: 20%	24.1	22.9	27.1

B.2: Compressive strength for 0.60 w/b mixes [GPa]

3 days results			
	Batch 1: Gradation 1	Batch 2: Gradation 2	Batch 3: Gradation 3
Control mix: 0%	23.6	23.6	23.6
Rubber particles: 5%	14.3	12.2	15.2
Rubber particles: 10%	12.9	11.1	14.2
Rubber particles: 20%	10.1	6.9	10.9

7 days results			
	Batch 1: Gradation 1	Batch 2: Gradation 2	Batch 3: Gradation 3
Control mix: 0%	26.5	26.5	26.5
Rubber particles: 5%	20.7	15.7	21.6
Rubber particles: 10%	17.0	13.3	19.7
Rubber particles: 20%	16.2	12.5	16.3

14 days results			
	Batch 1: Gradation 1	Batch 2: Gradation 2	Batch 3: Gradation 3
Control mix: 0%	32.4	32.4	32.4
Rubber particles: 5%	24.9	21.2	25.9
Rubber particles: 10%	23.5	19.1	23.7
Rubber particles: 20%	21.5	18.0	21.9

B.3: Splitting tensile strength for 0.45 w/b mixes [GPa]

3 days results			
	Batch 1: Gradation 1	Batch 2: Gradation 2	Batch 3: Gradation 3
Control mix: 0%	2.7	2.7	2.7
Rubber particles: 5%	2.0	2.0	2.2
Rubber particles: 10%	1.9	1.9	2.0
Rubber particles: 20%	1.5	1.4	1.7

7 days results			
	Batch 1: Gradation 1	Batch 2: Gradation 2	Batch 3: Gradation 3
Control mix: 0%	3.2	3.2	3.2
Rubber particles: 5%	2.6	2.7	3.1
Rubber particles: 10%	2.5	2.6	2.9
Rubber particles: 20%	2.1	2.0	2.1

14 days results			
	Batch 1: Gradation 1	Batch 2: Gradation 2	Batch 3: Gradation 3
Control mix: 0%	4.4	4.4	4.4
Rubber particles: 5%	3.3	2.9	4.3
Rubber particles: 10%	2.8	2.1	3.6
Rubber particles: 20%	2.3	1.8	2.9

B.4: Compressive strength for 0.60 w/b mixes [GPa]

3 days results			
	Batch 1: Gradation 1	Batch 2: Gradation 2	Batch 3: Gradation 3
Control mix: 0%	2.7	2.7	2.7
Rubber particles: 5%	1.7	1.5	1.8
Rubber particles: 10%	1.6	1.3	1.7
Rubber particles: 20%	1.3	0.8	1.3

7 days results			
	Batch 1: Gradation 1	Batch 2: Gradation 2	Batch 3: Gradation 3
Control mix: 0%	3.6	3.6	3.6
Rubber particles: 5%	2.2	2.0	2.6
Rubber particles: 10%	1.9	1.8	2.2
Rubber particles: 20%	1.6	1.5	2.0

14 days results			
	Batch 1: Gradation 1	Batch 2: Gradation 2	Batch 3: Gradation 3
Control mix: 0%	3.6	3.6	3.6
Rubber particles: 5%	2.9	2.5	3.1
Rubber particles: 10%	2.6	2.1	2.7
Rubber particles: 20%	2.4	2.4	2.5

Appendix C: Tables of laboratory test results from main testing phase

C.1: Compressive strength

3 days compressive strength test results

Mix ID	Rubberized Mix [GPa]	Control Mix [GPa]
0.80 w/b Mixes	6.2	9.2
0.60 w/b Mixes	14.0	23.4
CRM Mixes	12.1	18.7

7 days compressive strength test results

Mix ID	Rubberized Mix [GPa]	Control Mix [GPa]
0.80 w/b Mixes	9.2	13.3
0.60 w/b Mixes	16.2	27.5
CRM Mixes	14.3	26.6

14 days compressive strength test results

Mix ID	Rubberized Mix [GPa]	Control Mix [GPa]
0.80 w/b Mixes	13.5	16.7
0.60 w/b Mixes	19.5	32.2
CRM Mixes	15.3	28.9

C.2: Tensile strength

3 day tensile strength test results

Mix ID	Rubberized Mix [GPa]	Control Mix [GPa]
0.80 w/b Mixes	1.2	1.23
0.60 w/b Mixes	1.7	1.8
CRM Mixes	1.8	1.9

7 day tensile strength test results

Mix ID	Rubberized Mix [GPa]	Control Mix [GPa]
0.80 w/b Mixes	1.4	1.9
0.60 w/b Mixes	1.6	2.3
CRM Mixes	1.9	2.3

14 day tensile strength test results

Mix ID	Rubberized Mix [GPa]	Control Mix [GPa]
0.80 w/b Mixes	2.1	1.6
0.60 w/b Mixes	1.7	2.3
CRM Mixes	2.0	2.4

C.3: Elastic modulus

7 days elastic modulus test results

Mix ID	Rubberized Mix [GPa]	Control Mix [GPa]
0.80 w/b Mixes	7.1	8.8
0.60 w/b Mixes	9.5	11.2
CRM Mixes	16.2	17.6

14 day elastic modulus test results

Mix ID	Rubberized Mix [GPa]	Control Mix [GPa]
0.80 w/b Mixes	13.9	16.6
0.60 w/b Mixes	15.4	17.9
CRM Mixes	21.6	23.4

28 day elastic modulus test results

Mix ID	Rubberized Mix [GPa]	Control Mix [GPa]
0.80 w/b Mixes	17.1	19.9
0.60 w/b Mixes	19.1	22.0
CRM Mixes	25.6	27.6

C.4: Free shrinkage

Free shrinkage strains						
Mix ID	0.60:R0	0.60:R20G3	0.80:R0	0.80:R20G3	CRM:R0	CRM:R20G3
AGE (days)	Average (10^{-6} m)	Average (10^{-6} m)	Average (10^{-6} m)	Average (10^{-6} m)	Average (10^{-6} m)	Average (10^{-6} m)
3.0	0.0	0.0	0.0	0.0	0.0	0.0
4.0	10.8	16.7	8.3	130.0	20.0	10.0
5.0	32.5	35.0	41.7	231.7	51.7	28.3
6.0	64.2	83.3	58.3	291.7	61.7	63.3
7.0	110.8	146.7	88.3	418.3	93.3	110.0
8.0	170.8	215.0	145.0	458.3	133.3	161.7
9.0	275.8	286.7	231.7	498.3	150.0	186.7
10.0	324.2	373.3	231.7	531.7	170.0	223.3
11.0	404.2	440.0	361.7	586.7	180.0	233.3
12.0	459.2	508.3	355.0	626.7	216.7	266.7
13.0	519.2	558.3	355.0	665.0	256.7	273.3
14.0	547.5	606.7	518.3	700.0	276.7	286.7
15.0	617.5	668.3	546.7	721.7	300.0	286.7
16.0	655.8	720.0	578.3	773.3	305.0	370.0
17.0	724.2	768.3	611.7	815.0	326.7	408.3
18.0	757.5	803.3	631.7	846.7	326.7	423.3
19.0	785.8	818.3	648.3	878.3	453.3	483.3
20.0	800.8	865.0	675.0	935.0	463.3	486.7
21.0	809.2	865.0	688.3	970.0	488.3	510.0
22.0	842.5	956.7	718.3	840.0	518.3	523.3
23.0	842.5	978.3	741.7	876.7	521.7	538.3
24.0	980.8	1055.0	760.0	891.7	550.0	553.3
25.0	1004.2	1055.0	776.7	955.0	563.3	563.3
26.0	1009.2	1071.7	790.0	993.3	576.7	596.7
27.0	1039.2	1103.3	810.0	1003.3	590.0	616.7
28.0	1050.8	1118.3	813.3	1033.3	595.0	640.0
29.0	1079.2	1116.7	835.0	1066.7	600.0	660.0
30.0	1085.8	1116.7	846.7	1093.3	605.0	690.0

Appendix D: Material properties regression graphs

D.1: Tensile strength

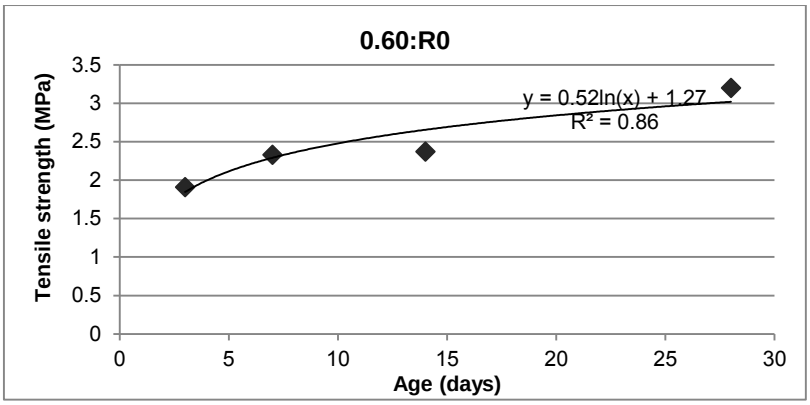

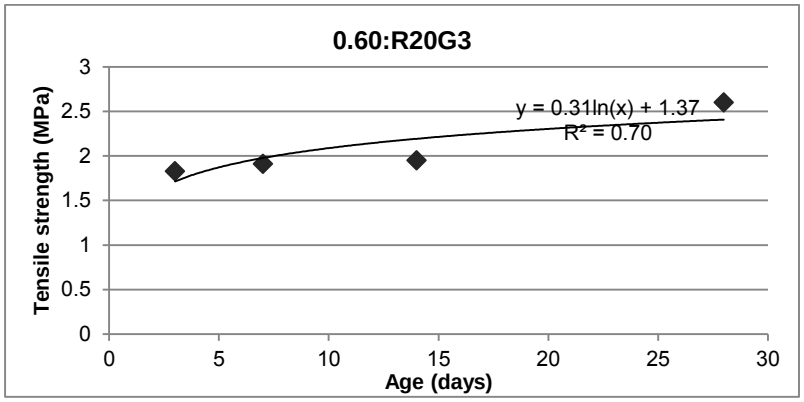

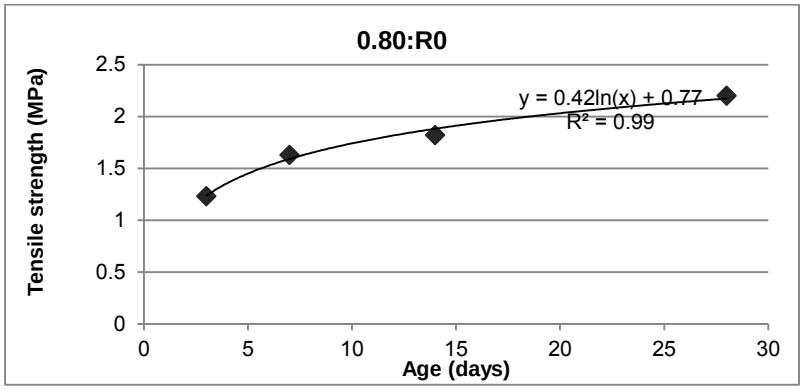

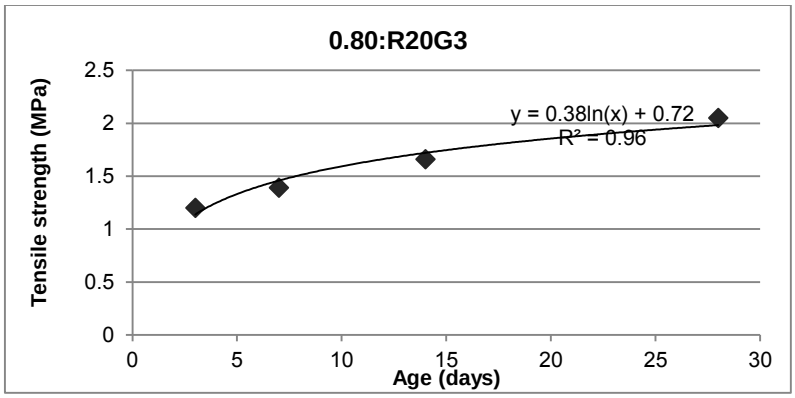
0.80:R20G3
Tensile strength (MPa)
y = 0.38ln(x) + 0.72
R² = 0.96
Age (days)

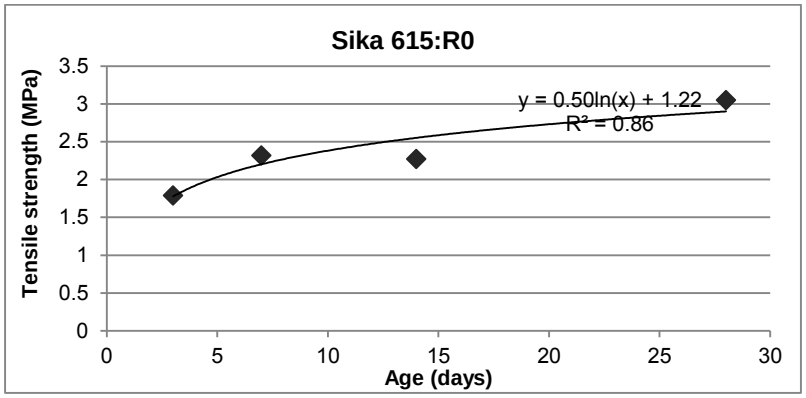
Sika 615:R0
Tensile strength (MPa)
y = 0.50ln(x) + 1.22
R² = 0.86
Age (days)

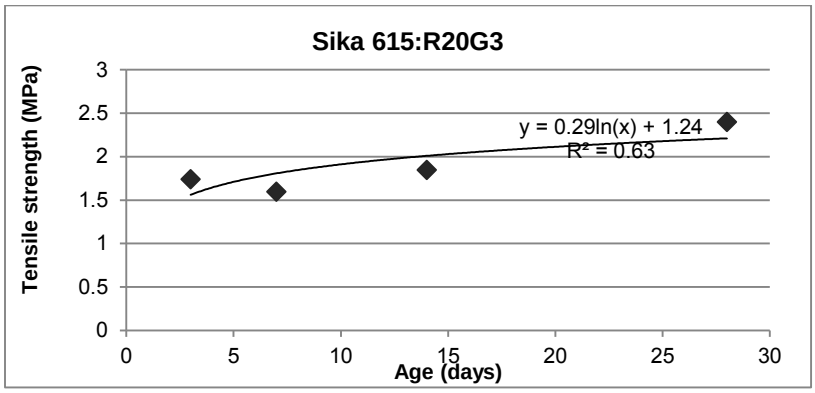
Sika 615:R20G3
Tensile strength (MPa)
y = 0.29ln(x) + 1.24
R² = 0.63
Age (days)

D.2: Elastic modulus

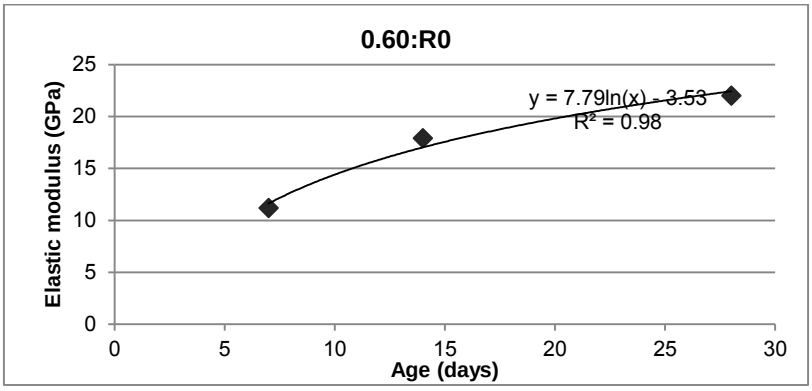

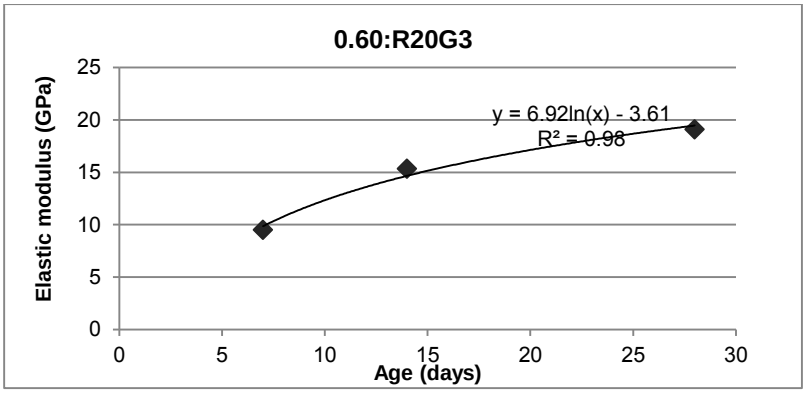

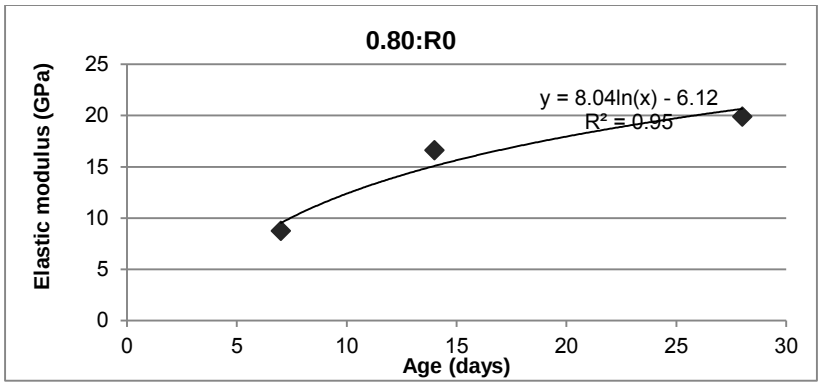

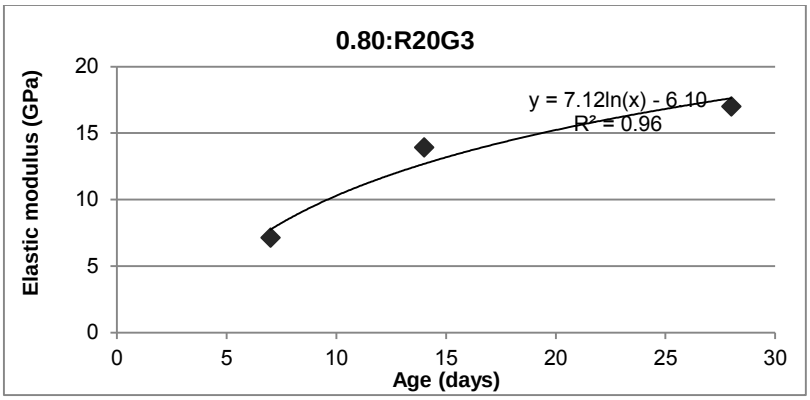
0.80:R20G3
Elastic modulus (GPa)
Age (days)
y = 7.12ln(x) - 6.10
R² = 0.96
0
5
10
15
20
25
30

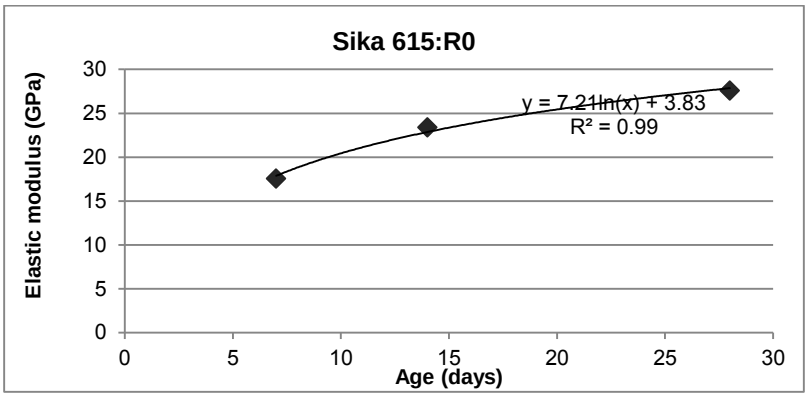
Sika 615:R0
Elastic modulus (GPa)
Age (days)
y = 7.21ln(x) + 3.83
R² = 0.99
0
5
10
15
20
25
30

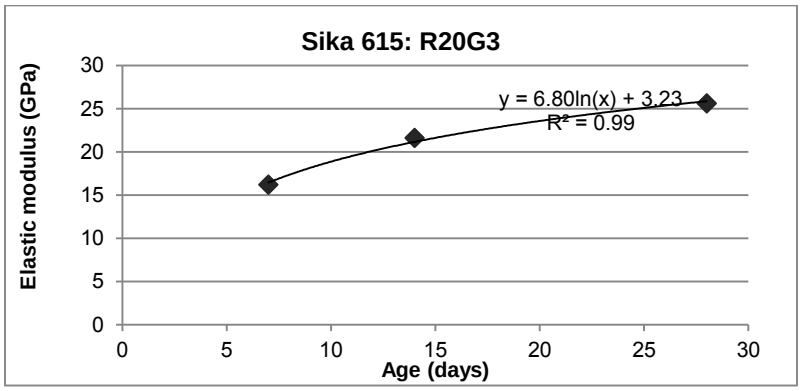
Sika 615: R20G3
Elastic modulus (GPa)
Age (days)
y = 6.80ln(x) + 3.23
R² = 0.99
0
5
10
15
20
25
30

D.3: Tensile relaxation

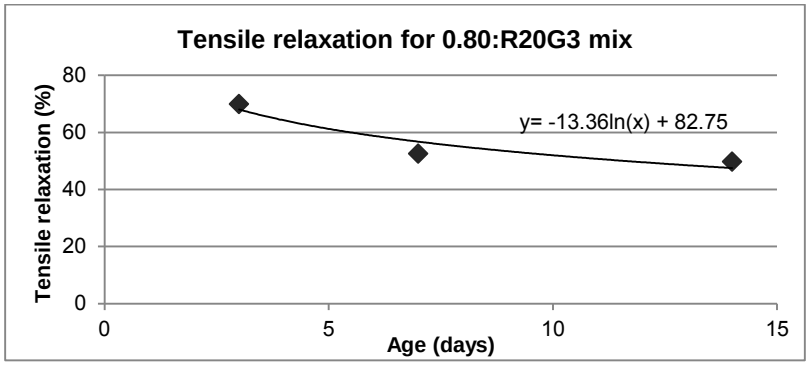

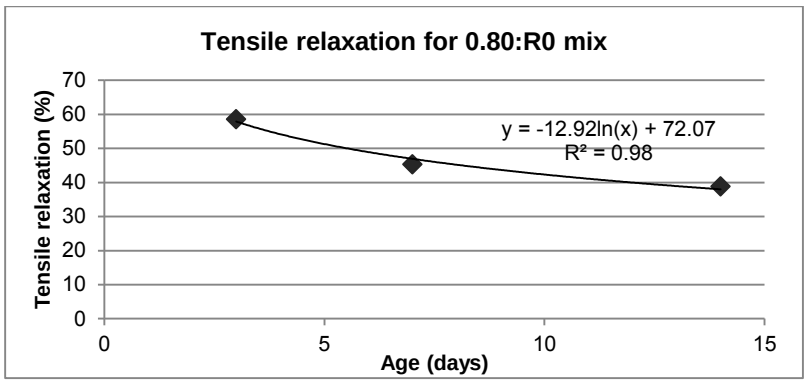

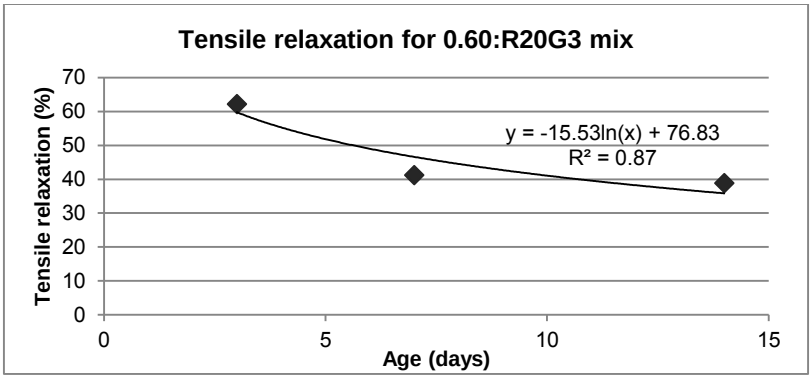

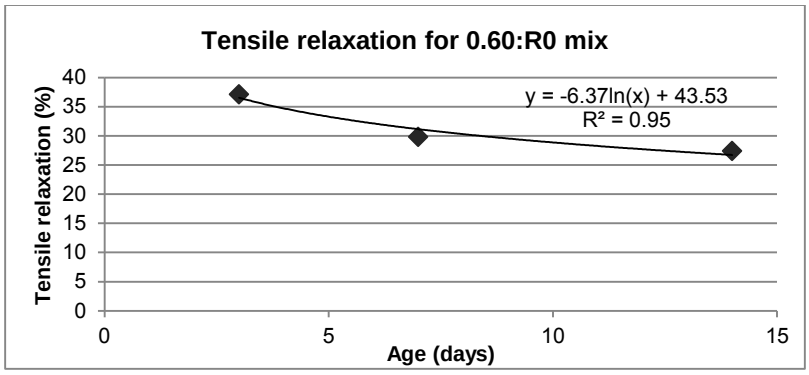
Tensile relaxation for 0.60:R0 mix
y = -6.37ln(x) + 43.53
R² = 0.95
Tensile relaxation (%)
Age (days)
0
5
10
15
20
25
30
35
40

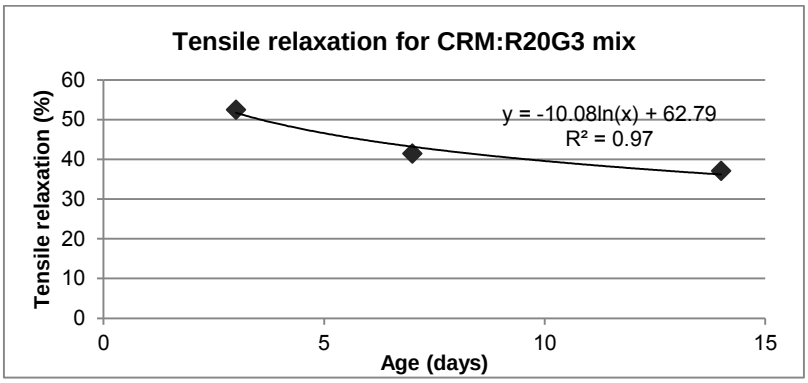
Tensile relaxation for CRM:R20G3 mix
y = -10.08ln(x) + 62.79
R² = 0.97
Tensile relaxation (%)
Age (days)
0
5
10
15
20
30
40
50
60

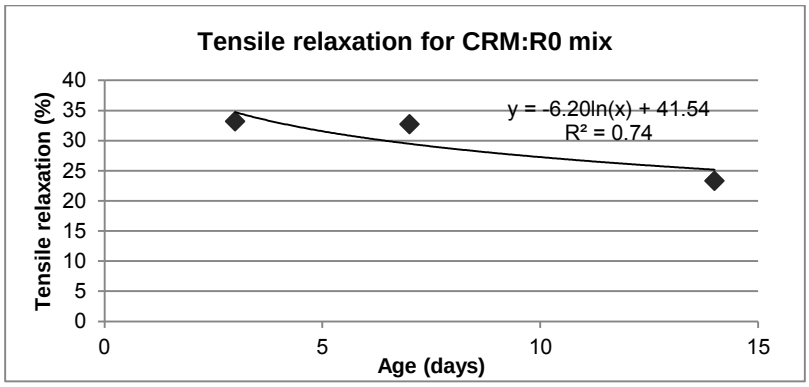
Tensile relaxation for CRM:R0 mix
y = -6.20ln(x) + 41.54
R² = 0.74
Tensile relaxation (%)
Age (days)
0
5
10
15
20
25
30
35
40